Covalent Organic Frameworks based on Schiff-base Chemistry. Synthesis, Properties and Potential Applications

José L. Segura,*[a] María J. Mancheño[a] and Félix Zamora*[b,c]

Covalent organic-frameworks (COFs) are an emerging class of porous and ordered materials formed by condensation reactions of organic molecules. Recently, the Schiff-base chemistry or dynamic imine-chemistry has been widely explored for the synthesis of COFs. The main reason of this new tendency is based on their high chemical stability, porosity and crystallinity in comparison to previously reported COFs. This critical review article summarizes the current state-of-the-art on the design principles and synthetic strategies toward COFs based on Schiff-base chemistry, collects and rationalizes their physicochemical properties, as well as aims to provide perspectives of potential applications which are at the forefront of research in materials science.

1. Introduction

Covalent organic frameworks (COFs) comprise an emerging class of materials based on the atomically precise organization of organic subunits into two- or three-dimensional porous crystalline structures connected by strong covalent bonds with predictable control over composition, topology and porosity.[1-6,7] Although they have been first explored for applications related with gas adsorption and storage,[1, 3, 5, 6, 8-12] the suitable incorporation of new functional building blocks has opened up new potential uses as advanced materials including their application in catalysis, as ultrasensitive sensors, in the fabrication of solar energy collectors and optoelectronic devices, and in clean energy applications.[2, 4, 11, 13-16]

Most of the interesting applications found for COFs are associated to their internal order, which is a rather unusual feature in comparison to that found in classical covalent polymers, in which the linkage between the organic subunits is due to irreversible covalent bonds that tend to form polymeric structures with a short-range structural order.[17] Synthesis of COFs relies on reversible covalent-bond-forming reactions, such as condensations that furnish boroxines or imines. It seems that only the reversible reactions are appropriate for the assembly of crystalline COF structures. Therefore, the concept of dynamic covalent chemistry of imine bonds is a useful approach. However, reversibility does not guarantee structural order. In other to avoid the formation of amorphous structures, other general features such as the rigidity in structure and the symmetric multi-connectivity meet the requirement for constructing the regular pores of the COF materials. The match of both shapes and angles of the building units should be taken into account for the reversible formation of covalent bonds. Finally, finding suitable synthetic conditions for the COF synthesis is by no means a trivial issue.[18] Thus, energetic synthetic reaction conditions and/or long reaction times seem to favour the thermodynamic control of the COF formation and allow the error correction and crystallization. However, the control of concentration of the reactants, water and catalyst is also crucial.

Thus, an important challenge in the production of COFs deals with the selection of suitable reactions that permit the regulation of the thermodynamic equilibrium during bond formation thus allowing self-correction and formation of thermodynamically stable crystalline architectures. The building blocks should contain reactive groups that trigger dynamic covalent bond formation. In addition, the building blocks should be conformationally rigid with the bond formation direction being discrete. Furthermore, special conditions such as, for example, solvothermal reaction conditions (see below) are very often required in order to obtain crystalline materials.

The majority of the COFs synthesized to date are based on condensation reactions.[19] Among them, the self-condensation reactions of boronic acids and their condensation with catechols to form boronate esters have been largely explored. Although they are thermally robust, this type of COFs are susceptible to attack and are even hydrolysed in basic and acidic conditions and sometimes even by water vapour in air.[20]

[a] *Departamento de Química Orgánica. Facultad de Química. Universidad Complutense de Madrid. Avenida Complutense s/n 28040 Madrid (Spain). E-mail: segura@ucm.es.*

[b] *Departamento de Química Inorgánica and Condensed Matter Physics Center (IFMAC). Universidad Autónoma de Madrid. 28049 Madrid (Spain). E-mail: felix.zamora@uam.es.*

[c] *Instituto Madrileño de Estudios Avanzados en Nanociencia (IMDEA Nanociencia), Cantoblanco, 28049 Madrid, Spain.*

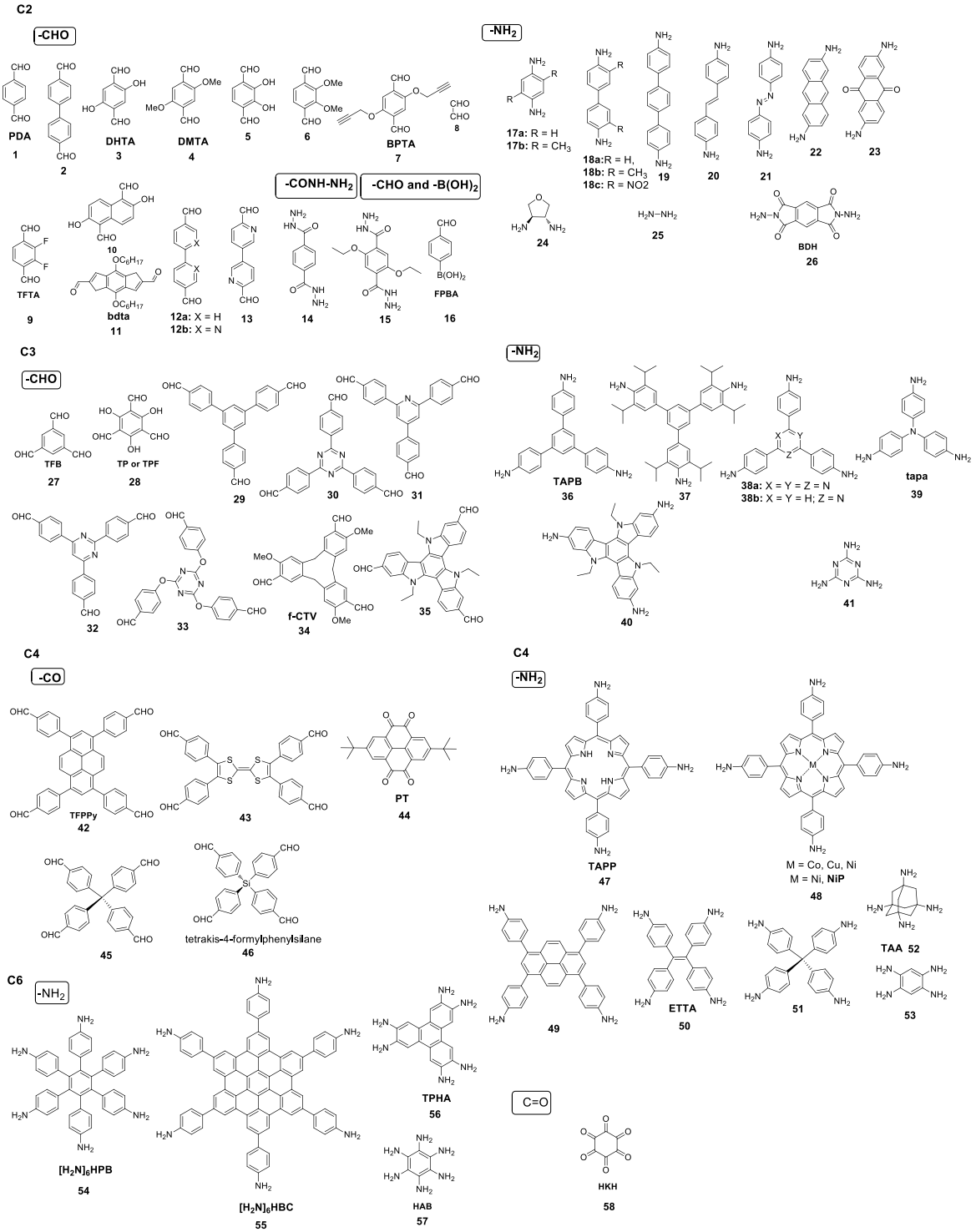

Fig. 1 Building blocks used for the synthesis of COFs *via* Schiff-base Chemistry categorized into geometries and reactive groups.

In general, the number of reactions that fulfil the above mentioned criteria for the formation of thermodynamically stable crystalline architectures is still very limited. Very recently, the use of Schiff-base chemistry or dynamic imine-chemistry has been profusely used for the synthesis of covalent organic-frameworks (COFs). The literature collected in this review article shows that COFs based on Schiff-base chemistry present the following features: i) they have been prepared in a variety of experimental conditions, including reactions carried out at room temperature; ii) there are a large variety of molecular precursors that have been successfully used (Figure 1); iii) they can be processed and deposited on several substrates; iv) these materials show enhanced chemical stability among other COFs; and v) they have already showed a large variety of interesting physico-chemical properties and potential applications.

The aim of this review is to provide an in-depth understanding of the different synthetic strategies successfully used for the production of COFs based on Schiff-base chemistry, providing key aspects to improve their crystallinity and porosity, as well as to summarize the different ways to incorporate selected functional groups in their structure, and the studies of their properties and potential used in different areas.

At this stage it is worth pointing out that Figure 1 will be used to guide the reader throughout the text in which the different COFs reviewed will be related to the constituting building blocks used for their synthesis and collected in this Figure.

2 Synthetic methods

COFs based in Schiff base-type linkages have emerged as a new type of materials with multiple applications, mainly due to their stability in different media.[21, 22] They are pre-designable in terms of the molecular building blocks employed.

To date, a significant amount of stable two-dimensional (2D) COFs and a few 3D COFs with different topologies have been synthesized. In 2D-COF the stability originates from two factors: the bonding strength between components of the 2D layers and the interlayer force. Although many building blocks and synthetic methods have been used, finding suitable synthetic conditions for the COF synthesis is not an easy matter. Usually, the solvothermal synthesis is the method most extensively used for the production of stable, crystalline COFs. Nevertheless, other methods have also recently been explored including mechanochemical and microwave-assisted reaction conditions as well as methods for growing COFs onto surfaces. Herein it is summarized the progress in the synthesis of this specific type of COFs (Scheme 1).

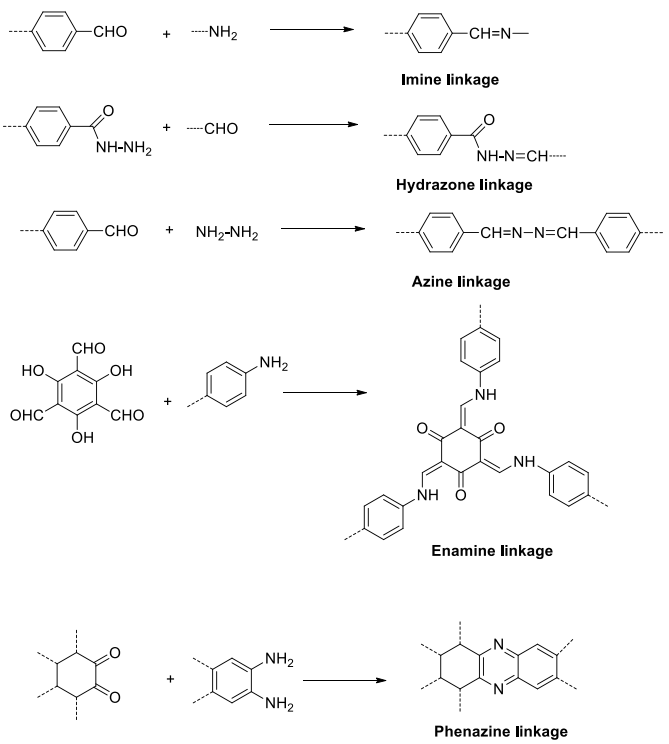

Scheme 1 Schematic representation of the dynamic chemical reactions used for the preparation of COFs *via* Schiff-base chemistry.

2.1 Solvothermal reaction conditions

The vast majority of COFs obtained *via* Schiff-base Chemistry have been prepared by using solvothermal reactions which involve harsh experimental conditions such as reaction in a sealed Pyrex tube under an inert atmosphere and long reaction times. It often takes several days and requires heating at high temperature (usually 120 °C). Finding the appropriate temperature is one of the key parameters in order to ensure the reversibility of the reaction. Generally, COFs obtained *via* Schiff-base Chemistry have been prepared at temperatures ranging between 85 and 120 °C. However, the pressure inside the sealed vessel is only indicated in a few cases (autogenous pressure). In addition, solvent combinations and ratios chosen for the condensation reactions seem to be crucial in order to obtain COFs with enhanced crystallinity. Usually, a battery of solvents are initially tested to optimize the reaction conditions. We will summarize below the solvothermal reaction conditions used for the different types of Schiff-base linkages formed so far.

2.1.1 Imine linkages

Imine-based COFs constitute the largest amount of COFs based on Schiff-base chemistry. In general, they are quite stable in

most organic solvents and insensitive to water, acidic and basic conditions. The nitrogen atoms within the framework may be coordinated with a series of metal ions. These features provide the imine-based COFs with high potential in further development, especially for diverse applications, as we will review in the second part of this article. For imine condensation reactions, mixtures of mesytilene/dioxane/AcOH are profusely used as the most suitable combination of solvents. Other mixtures such as dioxane–aqueous acetic acid, *n*-BuOH/*o*-DCB/3M AcOH have also been employed extensively. The catalyst, typically AcOH, plays a central role in the formation process.

In order to enhance the chemical stability and crystallinity in 2D-COFs, some authors protect the inner part of the COF by introducing -OH functionalities adjacent to the Schiff-base centres (C=N), creating an intramolecular O-H----N=C hydrogen bond. Thus, stability, crystallinity and porosity can be tuned by using this modification.[23, 24]

The H-bonding interactions also play an important role in the construction of the layered framework in 2D-COFs. Thus, due to these complementary forces, in the synthesis of [C_4+C_2] COFs such as **DhaTph** (Figure 2), the torsion of the edge units are suppressed and the tetragonal 2D sheets are locked in a planar conformation, enhancing the interlayers interactions. These intramolecular hydrogen bonds, along with the *trans* -C=N bond, reduces structural defects, and enhances structural rigidity, leading to an improved crystallinity of the COF.[25]

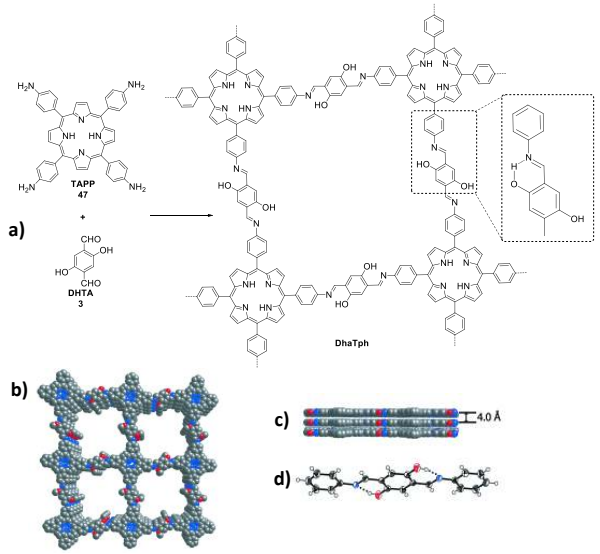

Figure 2 a) Syntheses of **DhaTph** by the condensation of square planar **TAPP** (**47**) building unit and linear **DHTA** (3) building **DhaTph** unit. b) Graphical view of the porous framework of COF **DhaTph** in a stacking form. c) Eclipsed stacking model of COF. d) ORTEP diagram of **DhaTph** linker unit shows the presence of the intramolecular hydrogen bond; all atoms are in one plane. Figure extracted from ref. [25]. Reproduced with permission of Wiley-VCH.

Thus, the chemically stable hollow spherical COF (**DhaTab**) has been synthesized from 2,5-dihydroxy-terephthalaldehyde (**DHTA**, **3**) and 5,10,15,20-tetrakis(4-aminophenyl)-21H,23H-porphyrin (**TAPP**, **47**) *via* self-templated synthesis, making use of H-bonding interactions too. The high crystallinity of the COF formed is due, again, to the presence of intramolecular hydrogen bonding interactions between the hydroxyl and imine functional groups, which locks the phenyl rings in one plane and improves the stacking interaction between the adjacent COF layers.[26]

In addition to H-bonding, the integration of other forces, such as π–π or van der Waals interactions might provide control over porosity, stability and crystallinity of COFs, although π-π interactions seem not to be necessary to obtain crystalline materials, as it is reported in triptycene based COFs.[27] Thus, Jiang and col. described imine-linked porphyrine COFs with fluoro-substituted arenes integrated into the edge units at different molar ratio, as a way of managing interlayer interactions based on self-complementary π-forces.[28] The same authors have also developed a strategy to soften the polarization influence of the C=N bond in the destabilization of the layered structure in hexagonal 2D-COFs based in imine reactions.[29] In imine-linked COFs, the C=N bond is polarized to yield partially positively charged carbon and negatively charged nitrogen. Thus, in a hexagonal 2D-COF, each macrocycle consists of 12 polarized C=N segments; the aggregation of a large number of charged groups causes electrostatic repulsion and destabilizes the layered structure, as predicted theoretically.[30] Therefore, in this case, crystallinity and stability were enhanced by incorporating methoxy groups in the pore walls of **COFs**. Introducing the two electron donating methoxy groups to each phenyl edge delocalizes the two lone pairs from the oxygen atoms over the central phenyl ring, which reinforces the interlayer interactions and so stabilizes the COF and aids in its crystallization (Scheme 2).

On the other hand, the use of macrocyclic host derivatives with a shallow rigid cavity as triformylcyclotrianisylene (**f-CTV**, **34**), a derivative of the well-known cyclotriveratrylene (**CTV**), seems to stabilize the perfect eclipsed stack model rather than COFs based on planar motifs. The columnar stacking of crown CTV motifs avoid sliding between layers in **CTV-COFs**.[31]

Regarding the size and shape of pores in 2D-COFs, it is known that they can be well tailored by changing the structures of monomers.[4, 5, 20, 32] In general, COFs with hexagonal and tetragonal topologies are by far the most extensively investigated. However, modifications of these topologies can induce structural changes in the COFs. Hence, COFs with a trigonal topology have been rationally designed by using C_6-symmetrical vertices as hexaphenylbenzene (**HPB**) and hexabenzocoronene (**HBC**), thus providing small pores sizes and high π-columns densities.[33]

A very challenging task involves the introduction of different kinds of pores into a COF, as it is extremely hard to simultaneously control the formation of two pores bearing different sizes. Furthermore, polymorphism might arise, which usually results in several topological structures at the same time. To address this challenge, delicate design of monomers is required. In this respect, Zhao *et al* have recently synthesized a novel COF which bears two different kinds of ordered pores with controllable sizes: one with microporous range (7.1 Å) and the other in mesoporous range (27 Å) *via* one-step synthesis. The dual-pore 2D-COF has been designed by combination of a

D_{2h} symmetric and a C_2 symmetric monomers, resulting in a single structure due to thermodynamic control (Scheme 3).[34]

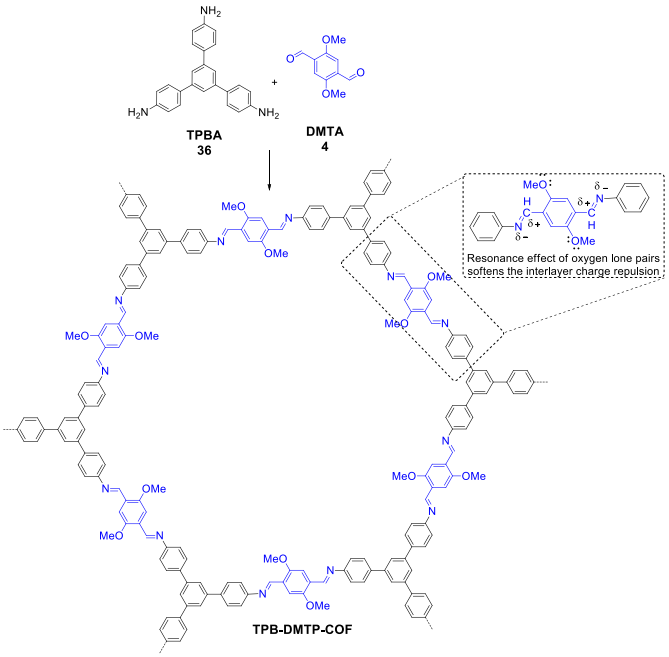

Scheme 2 Synthesis of **TPB-DMTP-COF** through the condensation of **DMTA** (**4**, blue) and **TPBA** (**36**, black). Inset: The structure of the edge units of **TPB-DMTP-COF** and the resonance effect of oxygen lone pairs that weaken the polarization of the C=N bonds and soften the interlayer repulsion in the COF.

Finally, although many examples of 2D imine based COFs have been described, the development of three-dimensional (3D) analogues is still in its infancy. In 2009, Yaghi *et al* described the first crystalline permanent porous 3D framework material with a diamond-like structure by condensation reaction between tetra-(4-anilyl)methane (**51**) and terephthaldehyde (**1**).[10] Interestingly, 3D-COFs obtained by reaction between tetra-(4-anilyl)methane (**51**) and 4,4'-biphenyldialdehyde (**12a**) have allowed the determination of their crystal structure by using the rotation electron diffraction (RED) method for data collection.[35] More recently, two new 3D microporous based functionalized COF_S have been obtained by combining a tetrahedral alkylamine (1,3,5,7-tetraaminoadamantane (**TAA, 52**) with triangular aldehyde reaction partners (1,3,5-triformylbenzene, **TFB**, (**27**) or triformylphloroglucinol (**28**)) under solvothermal reaction conditions.[36] These contributions pave the way for the development of new 3D-COFs by their rational design with pores and windows of different sizes.

An outstanding 3D COF have been recently reported by Yaghi *et al*.[37] (Fig. 3) consisting of helical organic threads, designed to be mutually weaving at regular intervals. The preparation was carried out by imine condensation reactions of aldehyde functionalized copper(I)-bisphenanthroline tetrafluoroborate, $Cu(PDB)_2(BF_4)$, and benzidine. The copper centres are topologically independent of the weaving within the COF structure and serve as templates for bringing the threads into a woven pattern, rather than the more commonly observed parallel arrangement. The Cu(I) ions can be reversibly removed, by heating the material in KCN methanol-water solution, and added without loss of the COF structure, for which a tenfold increase in elasticity accompanies its demetallation. Interestingly, the threads in **COF-505** have many degrees of freedom for huge deviations to take place between them, throughout the material, without undoing the interlacing of the overall structure.

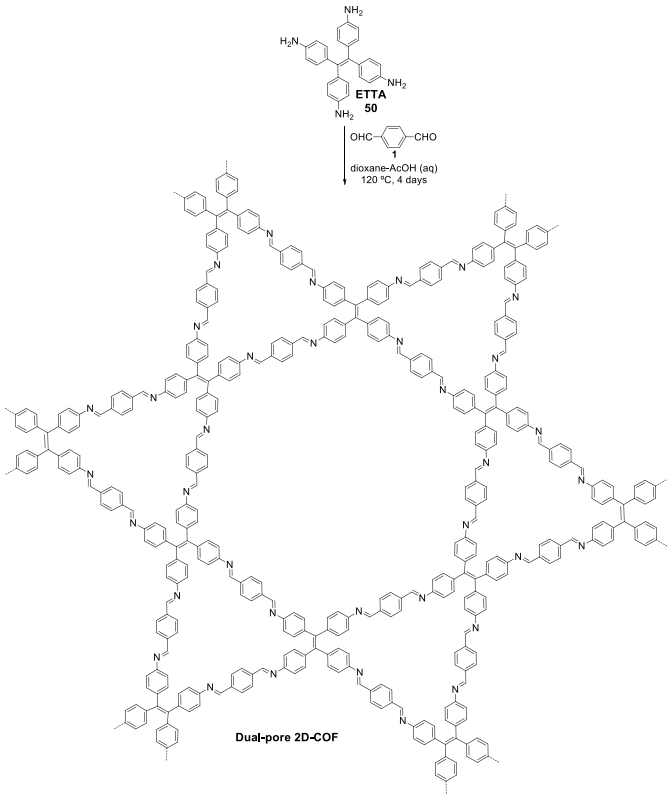

Scheme 3 Synthesis and structure of a Dual-pore 2D-COF.

Very recently, a first study on the mechanism of imine-linked 2D-COF formation has shown that the crystallinity of a simple COF formed by condensation between **TAPB** (**36**) and **PDA** (**1**) in 4:1 dioxane:mestiylene at 70 °C for 3 days strongly depends on the water and glacial acetic acid concentrations. Thus, the network crystallizes to the 2D-COF under conditions that allow imine exchange, and does not require the presence of additional imine or aldehyde monomers. The ability of imine networks to undergo this transformation highlights the importance of maximizing imine exchange and providing the system with sufficient reaction time. This seminal study points out the importance to gain knowledge in the understanding of COFs formation processes.[18]

2.1.2 Hydrazone linkages

In 2011, with the aim of widening the range of possible materials that could be achieved through any kind of linkage, Yaghi *et al* reported a pioneering work aimed to the synthesis of COFs with hydrazone groups as strong organic linkages.[38] Easily accessible hydrazine (2,5-diethoxyterephthalohydrazide) (**15**) and functionalized aldehyde building blocks (1,3,5-triformylbenzene, **27** or 1,3,5-tris(4-formylphenyl)benzene, **29**) give hydrazone-linked structures, whose crystallinity is

controlled by the well-known pH-dependent reversibility of hydrazone linkages.[39] Interestingly, Yaghi *et al* also reported that nonsubstituted terephthalohydrazides do not yield permanently porous materials, probably due to their poor solubility in organic solvents that leads to blockage of the pore network by unreacted starting material. Thus, it is necessary to increase the solubility of the terephthalohydrazide moiety component in order to facilitate activation and allow the isolation of crystalline and permanently porous structures.

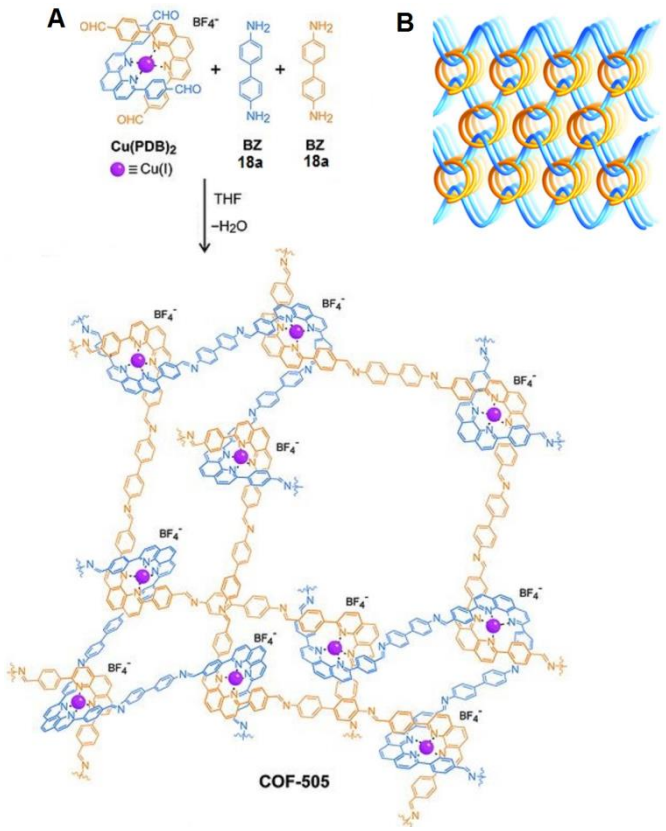

Fig. 3 a) Scheme of the synthesis of **COF-505** built from organic threads using copper(I) as a template to make an extended weaving structure, which can be subsequently demetalated and remetalated; b) Illustration of weaving of threads in three dimensions. From *Science* 2016, 351, 365-369. Reprinted with permission from AAAS.

Hydrazones are typically much less prone to hydrolysis than imines and are generally formed by the acetic acid catalysed reversible condensation of the building blocks in dioxane/mesitylene (1:2 v/v) at 120°C in a sealed pressure vial under argon atmosphere for 72 h. In fact, acylhydrazones as linkages in 2D-COFs, offer improved hydrolytic and oxidative stability. Besides, the incorporation of novel polar and hydrogen-bonding units into the pore surface can lead to new applications of these materials.

It is worth mentioning that hydrazone based COFs such as **TFPT** (Scheme 4) can also be synthesized by *in situ* acetal deprotection to generate aldehyde-containing building blocks which condensate with 2,5-diethoxy-terephthalohydrazide (**15**) in a one-pot procedure. This protocol opens the door to a new variety of acetal-protected building blocks and at the same time enhances the solubility of otherwise insoluble building blocks due to the aliphatic protection group.[40]

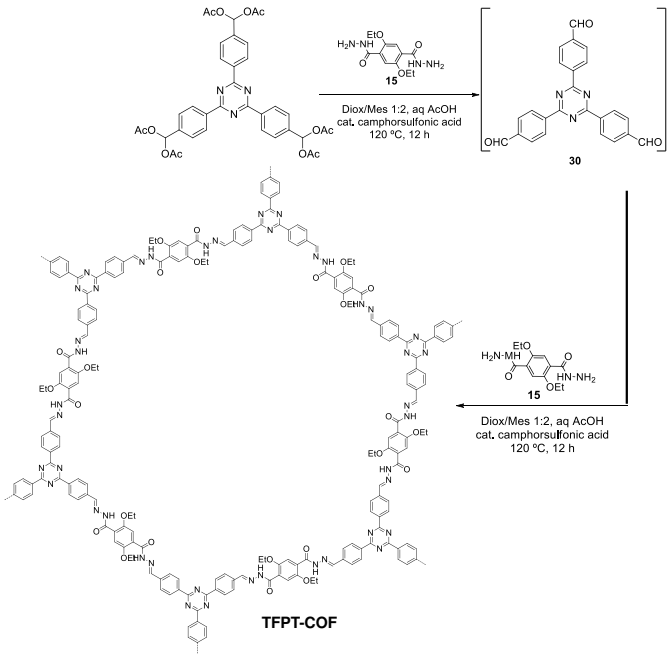

Scheme 4 Scheme showing the one-pot acetal deprotection and subsequent condensation to furnish the **TFPT-COF**.

2.1.3 Azine linkages

In order to explore a robust linkage for the synthesis of COFs that meet the requirements in crystallinity, porosity, and stability, Jiang *et al* reported in 2013 the syntheses of a COF based on the azine linkage by condensation between hydrazine and 1,3,6,8-tetrakis(4-formylphenyl)pyrene, **TFPPy** (**42**) (Scheme 5).[41]

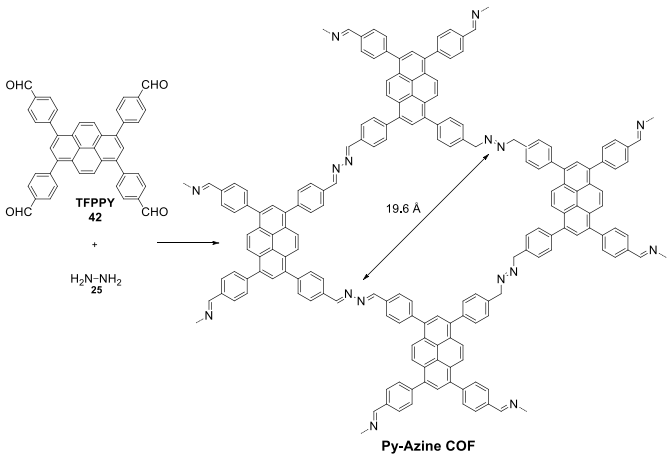

Scheme 5 Synthesis of the Azine-Linked COF (**Py-Azine COF**).

Condensation of hydrazine with aldehydes is a thermodynamically controlled reaction that leads to the formation of azine derivatives and water as by-product. Following this seminal work, the syntheses of several COFs based on the azine linkage have been carried out by condensation between hydrazine and suitable co-monomers containing multiple aldehyde functionalities. These COFs exhibit high crystallinity, high porosity, and robust chemical stability. Solvents such as *o*-dichlorobenzene (*o*-DCB), *o*-DCB/*n*-BuOH

(1.9/0.1 by vol), mesitylene/dioxane (1/3 by vol), and *o*-DCB/dioxane (3/1 by vol) in the presence of AcOH catalyst (6 M) have been used to obtain crystalline polymers.[41-44]

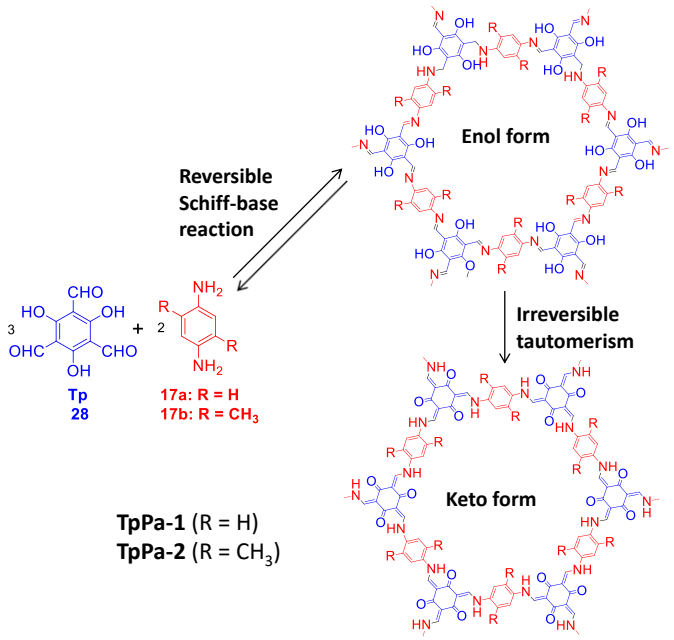

Scheme 6 Schematic representation of the synthesis of **TpPa-1** and **TpPa-2** by the combined reversible and irreversible reaction of 1,3,5-triformylphloroglucinol (**28**) with *p*-phenylenediamine (**17a**) and 2,5-dimethyl-*p*-phenylenediamine (**17b**), respectively. The total reaction proceeds in two steps: (1) reversible Schiff-base reaction and (2) irreversible enol-to ketotautomerism.

The azine linkage could be widely extended to the large variety of aldehydes included in Fig. 2 and many others which allows not only structural predesign, but also functional exploration based on the robust frameworks.

In the last couple of years, this strategy have been a common procedure in order to develop COFs for practical applications, including sensors and catalysts as it will be shown in the second part of this review.

It is also worth mentioning that by template-assisted replication of nanometer sized ZnO-nanorods, hollow and tubular **TpPa-COF** structures have been synthesized.[45] The hollow **TpPa** structures were synthesized by a two-step protocol. The first step involves the synthesis of hybrid structures with ZnO-nanorods as cores and **TpPa COFs** as shells (**ZnO@TpPa**). They were obtained by reaction between 1,3,5-triformylphloroglucinol (**28**) and *p*-phenylenediamine (**17a**) in 1:1 mesitylene–dioxane solvent in the presence of pre-synthesized and well dispersed ZnO-nanorods (Fig. 4), using acetic acid in a catalytic amount.

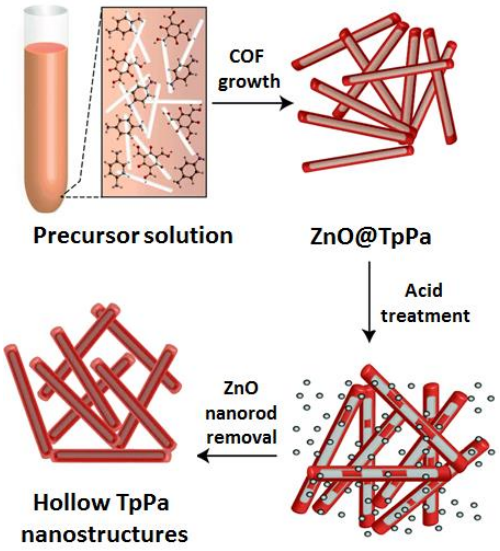

Fig. 4 Scheme of synthesis of highly stable and hollow COF structures *via* a templating strategy by in *situ* solvothermal reaction of 1,3,5-triformylphloroglucinol (**Tp, 28**) and *p*-phenylenediamine (**Pa, 17a**), in the presence of ZnO-nanorods. Adapted from Ref. [45] with permission from The Royal Society of Chemistry.

2.1.4 β-ketoenamine or keto-enol linkages

Banerjee *et al* have introduced a new protocol for the synthesis of highly acid- and base-stable crystalline covalent organic frameworks by a combination of reversible and irreversible organic reactions.[46-48] Usually triformylphloroglucinol (C_3, **28**) and different diamines (C_2) are employed in the design of [C_3+C_2] COFs. The total reaction can be divided into two steps (Scheme 6): In the first step, a reversible Schiff base reaction leads to the formation of a crystalline framework. The second step is an irreversible enol to-keto tautomerization, which enhances the chemical stability. The irreversible nature of the tautomerism does not affect the crystallinity of the COF, since the transformation involves only shifting of bonds while keeping the atomic positions almost unaltered. Moreover, the COFs backbone can be further functionalized suitably due to the presence of new functional groups. For these reactions, mixtures of solvents such as dioxane:mesytilene (1:1) and dimethylacetamide (DMA): *o*-dichlorobenzene (1:1) have given satisfactory results. This keto-type COFs are highly stable; however, it has only been described a loss of crystallinity under strong alkaline conditions (6 M NaOH,) because of the backward keto-to-enol conversion.[49]

The second step involves selective removal of ZnO-templates after treatment with dilute acid solution to yield the hollow nanostructures. The as synthesized nanostructures composed of microporous **TpPa** shells have high surface area and are highly stable in aqueous as well as in acidic environments.

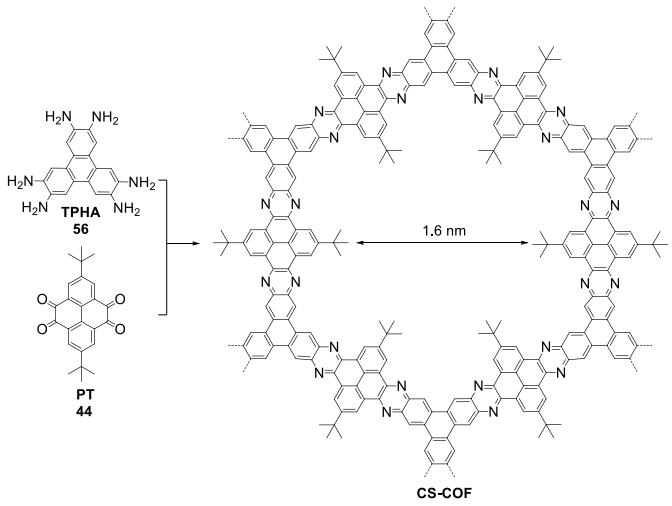

Scheme 7 Schematic representation of the synthesis of the **CS-COF**. The dotted blue lines on the periphery imply the extension of periodic structures.

2.1.5. Phenazine linkages

In the search of new linkages and properties in the synthesis of COFs, Jiang *et al* reported a phenazine-linked COF (**CS-COF**, Scheme 7), using C_3-symmetric triphenylene hexamine (**TPHA**, **56**) and C_2-symmetric *tert*-butylpirene tetraone (**PT**, **44**) as building blocks for the topological ring fusion reaction under solvothermal conditions.[50] Bulky side groups in the *tert*-butylpireno tetraone (**PT**, **44**) monomer were employed for enhancing the solubility of monomer. The topologically designed COF with phenazine linkages allows generating wire frameworks and open nanochannels, in which the π-conjugation spans into the two-dimensional sheets. This framework permits inborn periodic ordering of conjugated chains in all three dimensions and exhibits a striking combination of properties: chemical stability, extended π-delocalization, ability to host guest molecules and hole mobility.[50]

2.1.6 Orthogonal reaction strategy: COFs based on imine group and boroxine ring linkages

The vast majority of successful methods for the construction of COFs are limited to reactions based on only one type of covalent bond formation. However, the exploration of new judicious synthetic strategies has revealed as a crucial and emergent task for the development of this field. An interesting approach developed by Zhao *et al* in 2015 involves a new orthogonal reaction strategy to construct COFs by reversible formation of two types of covalent bonds.[51] In the reported case, the obtained COFs (**NTU-COF-1**, **NTU-COF-2**, Scheme 8) consist of the formation of imine group and boroxine ring through multicomponent reactions and is based on the utilization of building blocks containing ditopic groups of boronate and aldehyde such as **BFPBA (16)**, (Scheme 8). Thus, this building block can be readily converted to boroxine ring under high temperature or easily generate an imine group in the presence of an amino group. For example, **NTU-COF-1** can be synthesized by solvothermal reaction of **TAPB** (**36**) and **FPBA** (**16**). On the other hand, to evaluate the adaptability of the strategy to complicated reaction systems, the novel three-component COF (**NTU-COF-2**) could be synthesized also under solvothermal conditions from three building blocks such as **FPBA** (**16**), **TAPB** (**36**) and **HHTP** (**59**) through the formation of imine group and C_2O_2B boronate ring (Scheme 8). To examine the stepwise method to prepare the above mentioned COFs, the same authors attempted to use the boronic acid derivative **IM-1** (Scheme 8) to construct **NTU-COF-1** as well as **IM-1** and **IM-2** (Scheme 8) to construct **NTU-COF-2**. In these last cases, it was observed mainly the formation of amorphous solids. In order to rationalize this behaviour, exploration of the kinetics of COF growth was carried out.

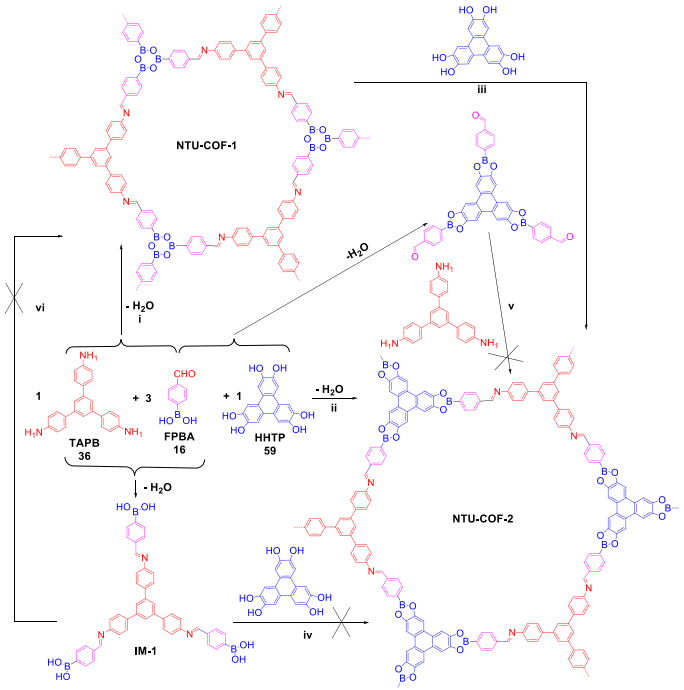

Scheme 8 Syntheses of (i) **NTU-COF-1** and (ii) **NTU-COF-2** involving the formation of two types of covalent bonds from orthogonal reactions.

This study indicates that the relative consumption rates of the building blocks are close to stoichiometric ratios which suggest that the formation of **NTU-COF-1** and **NTU-COF-2** are a parallel mechanism, instead of a tandem process. Concerning with the generation of amorphous solids from **IM-1** and **IM-2**, the parallel formations of imine and boronate/boroxine groups have to be concurrently accompanied by the crystallization of COFs, followed by irreversible aggregations of crystallites. Thus, the proposed mechanism can be used to interpret the unsuccessful constructions of **NTU-COF-1** and **NTU-COF-2** from intermediate compounds via the step-by-step procedure. However, this strategy can be considered as a general protocol applicable to construct not only binary COFs but also more complicated systems for which regular synthetic methods do not work.

2.2 Microwave-assisted solvothermal reaction conditions

Microwave heating, which allows a considerable reduction of the reaction time, has been used in organic chemistry for several decades.[52] As it is shown in Scheme 6, the **TpPa-COF-1**,

with β-ketoenamine-linkage , was synthesized by condensation reaction between *p*-phenylenediamine (**17a**) and 1,3,5-triformylphloroglucinol (**28**) under standard solvothermal conditions.[46] A long time (2–3 d) and high temperature (120 °C) are required to obtain **TpPa-COF-1** with high crystallinity in high yield (60–80%) with the conventional solvothermal method. In 2015, Wei, Zang *et al* have synthesized **TpPa-COF-1** under microwave heating conditions by preparing a 3 : 2 molar ratio solution of *p*-phenylenediamine (**17a**) and 1,3,5-triformylphloroglucinol (**28**) in a 20 mL glass microwave tube and heated by microwave irradiation at 100 °C with stirring for only 60 min.[53] After the work-up, the **TpPa-COF-1** is obtained in 83% yield based on the starting materials and exhibit similar characteristics in comparison with the COF obtained through standard solvothermal synthesis.

In order to obtain a COF with good performances, it is important to adjust every synthetic parameter, which should be based on many experiments and a lot of experience. Therefore, the development of the microwave-assisted solvothermal reaction conditions provides a rapid and efficient method for the synthesis of stable COFs thus facilitating the optimization task and opening the way for industrial production.

2.3 Synthetic procedures carried out at room-temperature without solvothermal conditions

Engineering COFs with good morphology and stability *via* rapid and easy synthetic methods under mild conditions is still challenging, but of great importance for the broad potential applications of COFs. Two different approaches have been developed in this respect. The first one is related with *synthetic procedures carried out by mechanochemical (MC) grinding.* A second and important approach involves the synthesis of COFs carried out in solution at room temperature and in air.

2.3.1 Synthetic procedures carried out by mechanochemical (MC) grinding

Solvent-free mechanochemical synthesis of porous solids has gained importance as an alternative synthetic route compared to conventional solution-based synthesis, as the process is quick, environmentally friendly and potentially scalable.[54] So far, this methodology has not been very successful in the synthesis of many COFs based in Schiff reactions. However, triformylphloroglucinol (**28**) based COFs (Fig. 5) have been obtained by manual grinding in a mortar and pestle at room temperature in a rapid, solvent-free, room-temperature MC synthesis.[47]

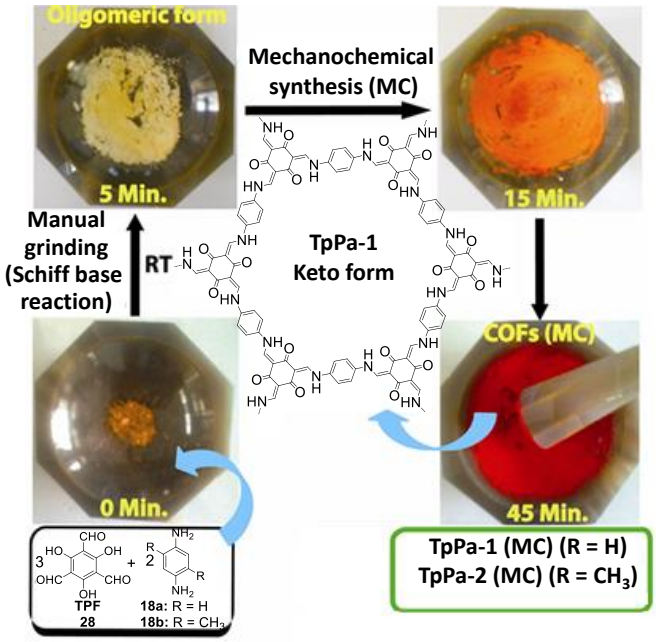

Fig. 5 Schematic representation of the MC synthesis of **TpPa-1** and **TpPa-2** through simple Schiff base reactions performed via MC grinding using a mortar and pestle. Adapted with permission from *J. Am. Chem. Soc.* 2013, 135, 5328-5331. Copyright (2013) American Chemical Society.

2.3.2 Synthetic procedures carried out at room-temperature in solution

We have recently shown that the Schiff reaction between two trigonal building blocks, 1,3,5-tris(4-aminophenyl)benzene (**36**) and 1,3,5-benzenetricarbaldehyde (**27**) (Fig. 6) rapidly occurs at room temperature and in air, leading to the formation of a COF (**RT-COF-1**) which is crystalline, showing a laminar hexagonal structure, stable up to 450 °C and porous to both N_2 and CO_2.[55] **RT-COF-1** can be easily synthesized by adding 0.1 mL of acetic acid to 1 mL of **36** and **27** (1:1 molar ratio; 0,028 M) in either *m*-cresol or DMSO under gentle stirring at room temperature. After 1 min, a characteristic yellow gel is formed, which after the work-up provides crystalline **RT-COF-1** as a yellow solid. It is especially remarkable that this approach enables the fabrication and position of low-cost micro- and sub-micropatterns of the RT-COF on several surfaces by using lithographically controlled wetting and conventional ink-jet printing.

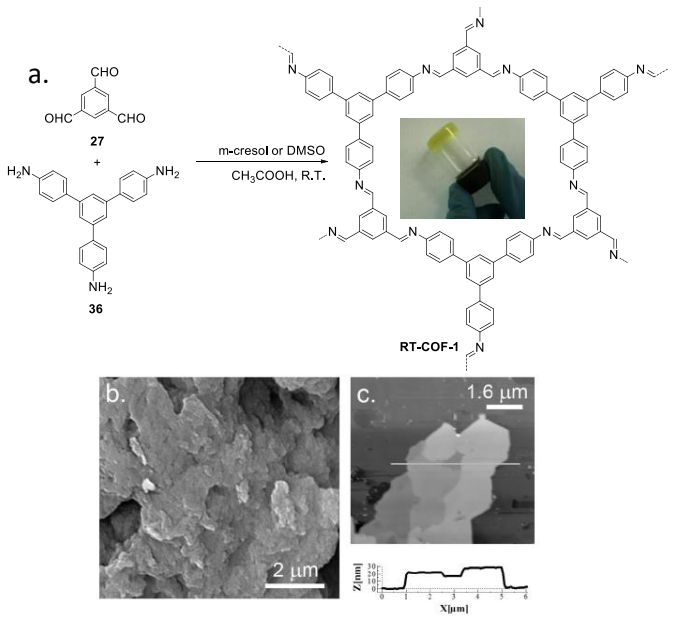

Fig. 6 a) Schematic illustration of the room-temperature polyimine condensation to form **RT-COF-1**. Instantaneous formation of the gel is shown in the image in the inset of the COF structure. b) Representative FE-SEM image of **RT-COF-1**. c) Representative AFM topographic image of isolated flakes of **RT-COF-1** on SiO_2 (top) and the corresponding height profile (bottom). Figure extracted from ref. [55]. Reproduced with permission of Wiley-VCH.

Yan *et al* have also reported a solution-phase approach at room temperature which has been used for the fabrication of spherical COF **TpBD** (a COF synthesized from 1,3,5-triformylphloroglucinol (**Tp**, **28**) and benzidine (**BD**, **18a**, R = H) with good solvent and thermal stability.[56] The synthesis of **TpBD** can be simply achieved by stirring an ethanolic solution of **Tp** and **BD** at room temperature. Although this method for the synthesis of **TpBD** is faster than the conventional solvothermal method (120 °C for 72 h), yields obtained are poorer and the obtained COF shows moderate crystallinity in comparison with the already mentioned methods. However, the Brunauer-Emmett-Teller (BET) surface area seems to be superior.

Interestingly, the wet-chemical reaction between hexaaminobenzene (**HAB**, **57**) trihydrochloride and hexaketocyclohexane (**HKH**, **58**) octahydrate leads to layered 2D crystals, named as **C_2N-*h*2D** (Fig. 7).[57] The functional moieties have to be directly included in the designed building units prior to the COF synthesis. The formation of the phenazine linkages takes place by simply mixing **HAB** and **HKH** in *N*-methyl-2-pyrrolidone in the presence of a few drops of sulphuric acid or in trifluoromethanesulfonic acid.

The tremendous potential energy gained by aromatization is responsible for the spontaneous polycondensation between the **HAB** and **HKH** and leads to the formation of a layered crystalline 2D network structure with uniform holes and nitrogen atoms and a C_2N stoichiometry in its basal plane. The resultant dark-black graphite-like solid has a layered and highly crystalline structure, as proved by the powder X-ray diffraction (XRD) pattern. Like the XRD pattern of graphite, the pattern of this crystal also shows a sharp 002 diffraction peak at 27.12 Å whose position corresponds to an interlayer distance (d-spacing) of 0.328 nm.

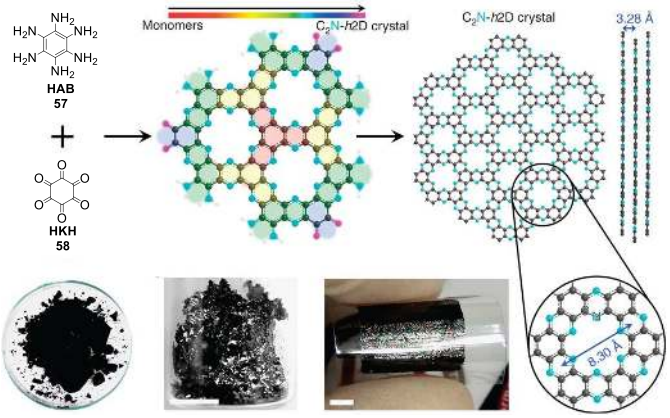

Fig. 7 Preparation and structure. a) Schematic representation of the reaction between hexaaminobenzene (**HAB**) trihydrochloride and hexaketocyclohexane (**HKH**) octahydrate to produce the **C_2N-h2D** crystal. The inset in the image of **HAB** is a polarized optical microscopy image of the **HAB** single crystal. Digital photographs: b) as-prepared **C_2N-h2D** crystal; c) solution-cast **C_2N-h2D** crystal on a SiO_2 surface after heat-treatment at 700 C; d) a **C_2N-h2D** crystal film (thickness: approximately 330 nm) transferred onto a PET substrate. The shiny metallic reflection of the sample indicates that it is highly crystalline. Figure extracted from ref. [57]. Reproduced with permission of the Nature Pub. Group.

More recently, Nakashima *et al*.[58] have reported on the room-temperature synthesis of a COF obtained by direct reaction between benzene-1,3,5-tricarbaldehyde and 1,4-phenylenediamine. The COF has a high surface area and high thermal stability due to its high crystallinity compared to that of the COF synthesized by a conventional solvothermal synthetic method using the same monomer combination.

Although these examples show the feasibility of obtaining COFs under mild conditions, the generalization of these synthetic routes remains still as a challenge in order to broaden the potential applications of COFs.

2.4 Towards 2D-polymers based on COFs

2D-polymers (atomic thickness) is an emerging research field of high current interest.[59] The past decade has witnessed an extraordinary increase in research progress on ultrathin two-dimensional (2D) nanomaterials in the fields of condensed matter physics, materials science, and chemistry after the exfoliation of graphene from graphite in 2004. This unique class of nanomaterials has shown many unprecedented properties and thus is being explored for numerous promising applications.[60] Therefore, the development of facile, feasible, and reliable methods for preparation of ultrathin 2D nanomaterials is of great importance for the exploration of their properties, function, and applications. There are several approaches aiming to produce purely bidimensional materials (few layers thickness), including the use of covalent and coordination bonds.[59, 61, 62] Layered COFs have been selected as a potential source for the production of 2D-polymers. Indeed, the integration of 2D-COFs on different surfaces is currently receiving a great deal of interest as it provides a unique opportunity of obtaining both atomic thick sheets or thin films,

with covalently bonded organic building units with unique properties associated with reduced dimensionality, well-defined in-plane structure, and tuneable functionalities.

A straightforward way to obtain single or few layer COFs involves the exfoliation of bulk COFs.[63, 64] Thus, in 2013, Bunck and Dichtel reported that 2D hydrazone-linked COFs can be exfoliated into 2D-polymers that assemble organic subunits into covalently linked, high-aspect-ratio networks with long-range order.[65]

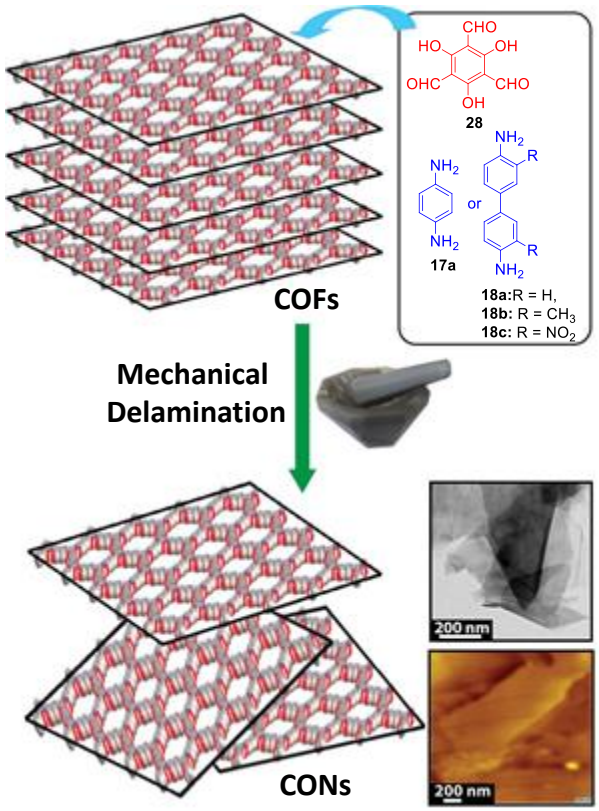

Fig. 8 Schematic representation of the formation of covalent organic nanosheets (CONs) from as-synthesized COFs *via* mechanical grinding. TEM and AFM images of CONs are shown at the right bottom. Adapted with permission from *J. Am. Chem. Soc.* 2013, 135, 17853-17861. Copyright (2013) American Chemical Society.

In order to avoid the high energy consuming ultrasonication process and the use of ultrapure and absolutely dry solvents, Banerjee *et al* have employed mechanical grinding as a simple, safe, eco-friendly, and energy efficient process for COFs exfoliation.[48] With this aim, they use a library of eight crystalline porous COFs. The monomers used for the syntheses of these COFs are depicted in Fig. 8.

The laminar structure of the materials (CONs) obtained by mechanical grinding of as-synthesized COFs was assessed by AFM measurements in order to obtain precise information about the existence of single-/few-layer materials. These CONs show flat nanosheet like structures with lengths and widths of several micrometers and thicknesses ranging from 3 to 10 nm, which corresponds to the existence of only ~10–30 COF layers. As far as the chemical stability is concerned, it has been found that these CONs retain their structural integrity throughout the delamination process and also remain stable in aqueous, acidic (3–9 N HCl) and basic (3 N NaOH) media like the parent COFs, which is confirmed by PXRD and IR analyses.

Considering the scalability and energy efficiency of this method, this "top-down" strategy can be envisaged as a cost-effective and scalable approach for the preparation of a variety of bulk 2D-layered structures. However, due to the tendency to multilayer formation and mechanical damage a lot of effort has been devoted to develop alternative procedures.

Well-defined surfaces can offer an ideal interface to template polymerization reactions in 2D. We will now review the different approaches followed in this direction.

The area of surface chemistry has been the subject of different review articles[66, 67] highlighting the significance of this relatively new, but increasingly influential, branch of nanotechnology research. In 2012, Greenwood and Baddeley used scanning tunnelling microscopy to investigate the Schiff-base condensation reaction between melamine (**41**) and terephthaldehyde (**1**) on Au/mica following deposition from solution in ambient conditions.[68] They could demonstrate that the reaction can proceed at room temperature to produce oligomers containing imine linkages.

Shortly afterwards, Kunitake *et al* reported that 2D π-conjugated metal porphyrin covalent organic frameworks can be produced on an iodine-modified Au (111) surface using a soft solution method.[69] The self-assembly of the sophisticated covalent nanostructures on well-defined surfaces in aqueous solution can be achieved by reversible equilibrium "on-site" polymerization at the solid–liquid interface, whereby aromatic building blocks spontaneously and selectively form linkages consisting of metal-free porphyrin and bifunctional aromatic linkage molecules. Scanning tunnelling microscopy (STM) studies confirm the capacity of this strategy to generate solid-supported 2D π-conjugated porphyrine-based COFs.

Tian, Lei *et al* have recently reported the *in situ* reaction of 1,3,5-tricarbaldehyde (C_3, **27**) with different aromatic diamines (C_2) on highly oriented pyrolytic graphite (HOPG) surface. The COF is formed at the solid-liquid interface at room temperature or in low vacuum with moderate heating. 2D honeycomb structures can be obtained with almost complete surface coverage.[70] The on-surface coupling at the liquid/HOPG interface represents the simplest preparation procedure, which involves only dissolving the monomers in octanoic acid and then drop-casting onto a HOPG surface at room temperature. An extended surface COF can be obtained at the liquid/HOPG interface spontaneously. On the other hand, the on-surface condensation *via* mild heating under low vacuum exhibits wider adaptability to a variety of monomers. The higher reaction reversibility and diffusion rate at elevated temperature enable formation of surface COFs with high uniformity and crystallinity. The single crystalline domain can extend to more than 1μm^2.

A self-limiting solid–vapour interface reaction method has also been reported as a suitable strategy to grow large-scale highly ordered bicomponent 2D-COFs such as **SCOF-LZU1** (obtained from 1,3,5-triformyl-benzene (**TFB**, **27**) and *p*-phenylenediamine (**17a**).[71] One precursor (**A**) is first preloaded

onto the substrate through drop-casting and then the other one (**B**) is introduced, and the whole system is thereafter sealed up in a closed reactor with the presence of a thermodynamic regulation agent. By heating the reactor to a specific temperature, precursor **B** will vaporise and then land on the surface covered with precursor **A** (Fig. 9). The coupling of the reactive groups separately carried out by precursors **A** and **B** results in nucleation for the SCOF. Since the rate at which precursor **B** reaches the surface and reacts is very low, the freshly vaporized precursor **B** or the freshly formed small oligomer, can diffuse on the surface and attach to the available SCOF nuclei, resulting in the growth of the SCOF. The monomer introduction is determined by the vapour pressure of the precursors. Accordingly, the covalent bond can form at the solid–vapour interface, leading to the growth of high quality COFs. In this way, different large-scale high-quality networks and topologies can be fabricated on highly oriented pyrolytic graphite (HOPG) using imine linkages.

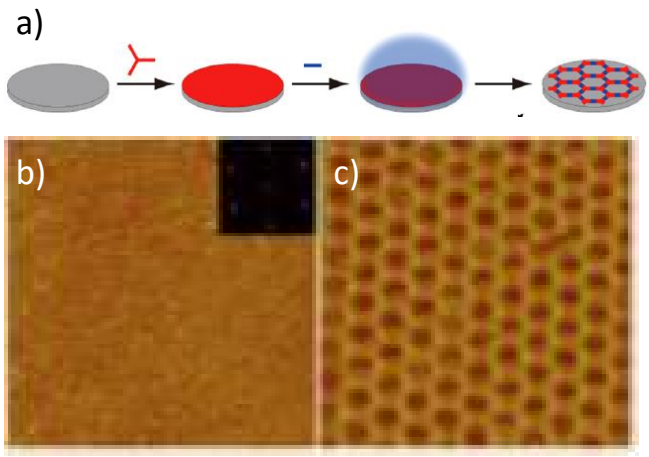

Fig. 9 a) Scheme diagram for solid–vapor interface reaction. b) Large-scale STM image (100 × 100 nm^2) of **SCOF-LZU1** with the inset depicting the corresponding FFT spectrum of the STM image. c) High resolution STM image (20 × 20 nm^2) of **SCOF-LZU1**. Adapted with permission from *J. Am. Chem. Soc.* 2013, 135, 10470-10474. Copyright (2013) American Chemical Society.

Similarly, two isomeric based single-layered covalent organic frameworks (sCOFs) with non-aromatic linkages have been prepared on HOPG surface with 6-fold symmetry, using an autoclave and $CuSO_4.5H_2O$ as a chemical equilibrium control agent.[72] It has been found that, compared to systems with rigid aromatic linkages, the use of ditopic monomers without aromatic rings as building blocks (hydrazine (**25**) or glyoxal (**8**)) contributes to the formation of more disordered networks.

A method to synthesize a 2D extended aromatic Schiff base surface COF with single atomic thickness on single-layer graphene grown on copper foil (SLG-copper) by CDV has been recently reported, providing information at the molecular-level of the on-surface condensation on graphene.[73] An extended adlayer of π-conjugated surface **COFBTA-PDA** was observed by STM several minutes after applying one droplet of the mixture of the two precursors (benzene-1,3,5-tricarbaldehyde, **PDA** (**27**) and *p*-phenylenediamine (**17a**)) to the graphene surface). The surface of the COF extends all over the graphene surface and the final structure is unperturbed by steps of the underlying copper foil. The well-developed transfer techniques for graphene make it possible to transfer the G-surface-COF composite to various substrates and to investigate its properties as a true 2D material.

The possibility of generating single-layered covalent organic frameworks (sCOFs) on surfaces, paves the way to true bottom-up assembly of a vast array of solid-supported, designed supramolecular nanoarchitectures towards different applications. Furthermore, they can serve as surface templates for subsequent growth of extended 3D architectures. On the other hand, in addition to the synthesis of COFs, there is also an increasing interest towards the development of methods for the preparation of 2D-COF films on surface.

In this respect, Lei *et al* have recently reported a non-covalent way to modify three-dimensional graphene (3DG) with anthraquinone moieties through on-surface synthesis of two-dimensional covalent organic frameworks.[74] The typical procedure for the synthesis of the composite material is the following: 2,6-diaminoanthraquinone (**DAAQ**, **23**) and benzene-1,3,5-tricarbaldehyde (**BTA**, **27**) are dissolved in dimethylacetamide. Simultaneously, 6% volume ratio of deionized water is added to the mixture. Then the resulting suspension is directly used to soak the 3DG. The composite was then heated and annealed under an argon atmosphere. This strategy allows the oriented growth of thin films of the COF on 3DG due to van der Waals epitaxy effect that facilitates the good conductive contact.

In 2015, Dichtel *et al* have reported the first oriented thin films of β-ketoenamine-linked 2D-COFs (**DAAQ-TFP**) on Au substrates (Fig. 10).[75] The films can be formed through the slow introduction (over 1 h) of the triformylphluroglucynol (**TP**, **28**) **TFP** monomer into a DMF solution at 90 °C containing 2,6-diaminoanthraquinone (**DAAQ**, **23**) under solvothermal conditions. Control of the resulting film thickness, from 60 to 560 nm, can be achieved by varying the initial concentrations of the monomers.

Bao *et al* have recently developed a method to fabricate thin films of a COF-based material compatible with transistor device fabrication. By reacting the monomers in a covered petri dish for 2 days in ambient conditions, a highly reflective film is formed at the solution/air interface. This film can be picked up from the surface of the solution with tweezers or substrates such as glass or silicon wafers and rinsed by transferring multiple times to petri dishes containing fresh DMF; films are held at the DMF/air interface by surface tension. Atomic force microscopy (AFM) showed that these films are composed of lace web-like structures roughly 50 nm thick.[76] The attempts at direct growth of the COF films on the substrates did not yield films good enough for this purpose. The synthesis of COF films onto amino functionalized silicon substrates has been performed as an alternative material for biosensors, by reaction of the substrates with the monomers in the presence of aqueous acetic acid as catalyst under 120 °C.[77] Oriented thin films of tetrathiafulvalene-based COF were also grown *in situ* from the liquid phase on Si/SiO_2 substrates and ITO-coated glass.[78]

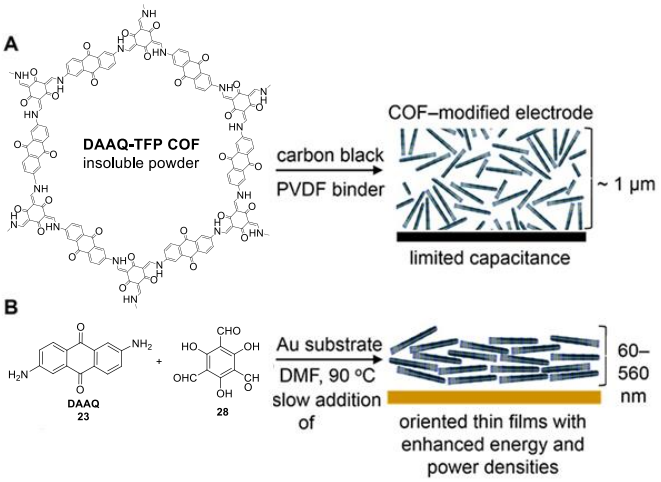

Fig. 10 a) Structure of the hexagonal subunit of the **DAAQ-TFP** COF, which forms as a 2D-layered microcrystalline powder. This material was previously prepared as a slurry, mixed with carbon black and a PVDF binder. b) Solvothermal growth of the **DAAQ-TFP** COF as an oriented thin film on Au electrodes. Adapted with permission from *ACS Nano* 2015, 9, 3178-3183. Copyright (2015) American Chemical Society.

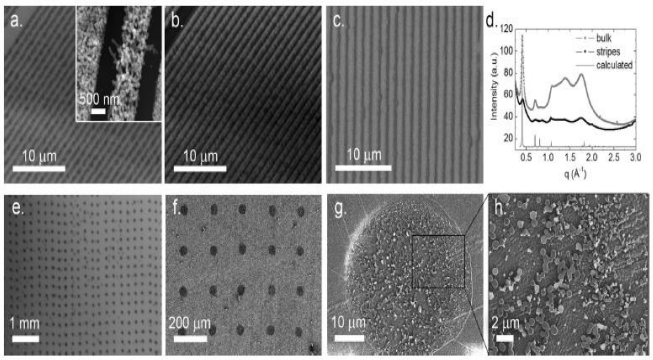

Fig. 11 a) Bright-field optical image of 1 mm wide **RT-COF-1** stripes fabricated by LCW. The inset shows a representative AFM image showing the formation of the characteristic **RT-COF-1** flakes. Z scale is 0–50 nm. b) Corresponding POM image. c) Representative FE-SEM image of 500 nm wide **RT-COF-1** stripes fabricated by LCW. d) Radial integration of the 2D-GIXRD image collected for the 1 mm wide **RT-COF-1** stripes (middle) compared to the one obtained in the synthesis of bulk **RT-COF-1** (top) and to the one derived from the theoretical structure (bottom). e) Representative optical image a 70 mm-in-diameter dot array of **RT-COF-1** on SiO_2 generated by an ink-jet printer. f) Representative FE-SEM image of a 40 mm-in-diameter dot array of **RT-COF-1** on flexible acetate paper generated by an ink-jet printer. g,h) Zoomed FE-SEM images of one of these dots, showing again the formation of the characteristic **RT-COF-1** flakes. Figure extracted from ref. [55]. Reproduced with permission of Wiley-VCH.

Finally, we have recently demonstrated that the room-temperature synthesis of **RT-COF-1** shown in Fig. 11 can be miniaturized on surfaces by using a soft-lithography technique and ink-jet printing. Both techniques have allowed the fabrication of micro/submicrometer patterns of **RT-COF-1** on solid and flexible supports (Fig. 11) that enable future applications.[55] Interestingly, the direct deposition allows the isolation of layers with a thickness of *ca*. 4 nm. Furthermore, the results using ink-jet printing are very interesting for automation and enables patterning with high resolution covering large areas in minutes, therefore being attractive for manufacturing.

2.5 Post-synthetic modification of COFs based on Schiff-base Chemistry

The possibility of post-synthetic modification of porous materials in general and COF systems, in particular, offers an effective route to incorporate functional groups or metallic species in the pores and thus tailor the structural and chemical environment of the pores. We will review now the different strategies developed to date for the post-synthetic modification of COFs.

2.5.1 Functional group interconversion by post-synthetic modification

COFs with highly functionalized pore wall structures are difficult to obtain *via* direct polycondensation reactions. Click reactions constitute an excellent tool for systematic functionalization of COFs with different purposes.[79] Therefore, conventional COFs incorporating alkynyl functionalized building blocks are active platforms for post-synthetic channel-wall functionalization. Reaction of 2,5-bis(2-propynyloxy)terephthalaldehyde (**BPTA**, **7**) and 2,5-dimethoxyterephthalaldehyde (**DMTA**, **4**) at different molar ratios with nickel 5,10,15,20-tetrakis(4'-tetraphenylamino) porphyrin (**NiP**, **48**) under solvothermal conditions yielded **NiPCOF**, with ethynyl units on the COF walls) (Scheme 9).

The ethynyl groups undergo click reaction with 4-azido-2,2,6,6-tetramethyl-1-piperidinyloxy in a smooth and clean manner to yield TEMPO functionalized COFs (**[TEMPO]100%-NiPCOF**) (Scheme 9).[29] Similarly, quantitative click reactions between the ethynyl units and azide compounds were performed to anchor a variety of functional groups, including ethyl, acetate, hydroxyl, carboxylic acids, and amino groups;[80] these groups ranged from hydrophobic to hydrophilic and from basic to acidic enabling the tailor made covalent docking of the pore walls. Finally, chiral COFs have also been created by anchoring chiral centres ((S)-pyrrolidine) onto the channel walls after azide-ethynyl click reaction.[29]

Other strategy for channel-wall functionalization is the use of ring opening reaction with succinic anhydride, performed by phenol units on the pore walls of conventional imine-base COFs.[80] This method allows the incorporation of carboxylic acids groups, creating new versions of COFs with different properties. Notably, compared with click chemistry this type of reaction is free of metal catalyst, proceeds smoothly and cleanly, representing a promising way of channel-wall tuning.[80]

Medina, Bein *et al* have recently demonstrated for the first time a two-step post-synthetic modification in a COF.[81] The novel approach involves the synthesis of a β-ketoenamine COF bearing an amine functional group in the pores through a post-synthetic reduction reaction. For this purpose, they initially synthesized a chemically stable β-ketoenamine COF **TpBD(NO$_2$)$_2$** featuring nitro functionalities in the pores that serve as protective groups for the final desired amino groups. The nitro groups were then reduced to afford an amine functionalized COF, **TpBD(NH$_2$)$_2$** (Scheme 10).

The accessibility of the amino groups in the pores by a sequential post-synthetic modification step was demonstrated

through the aminolysis of acetic anhydride which was performed to obtain the amide functionalized COF, **TpBD(NHCOCH$_3$)$_2$**.

All these methods allow the incorporation of controlled amounts of different functionalities, creating new versions of COFs with different properties.

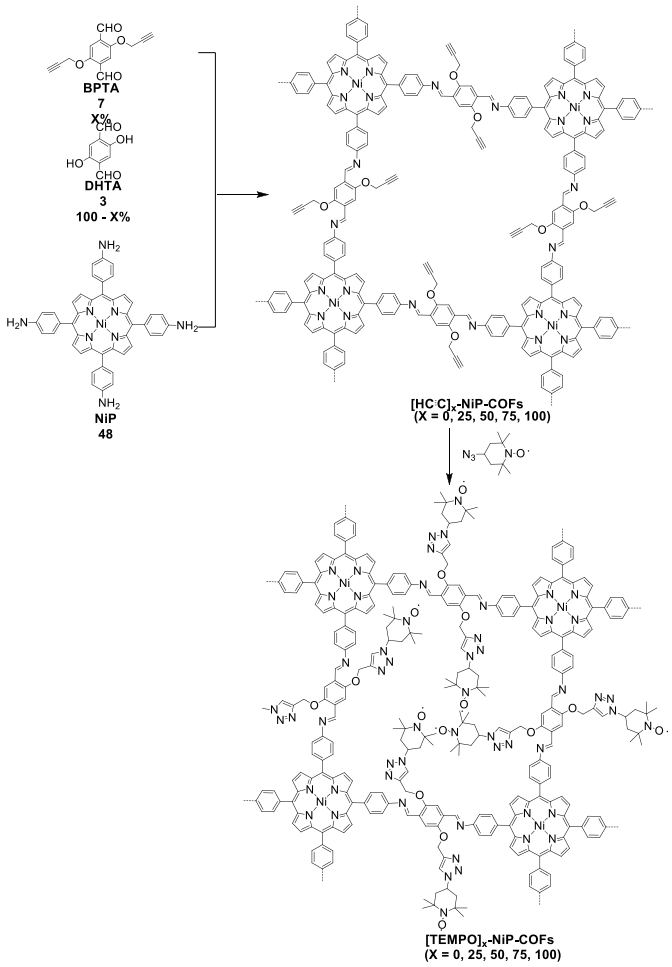

Scheme 9 Synthesis of radical **[TEMPO]$_n$-NIP-COF**.

2.5.2 Metal ions or complexes incorporated to COFs

As it has been demonstrated in coordination chemistry the imine type ligands are versatile in incorporating a variety of metal ions. As an example palladium(II) coordinated-COF material has been prepared by treatment of an imine based-COF with $Pd(OAc)_2$ at room temperature.[15] Otherwise, properly designed COFs can be further functionalized by coordination with the appropriate metal.

Thus, COFs designed with open docking sites on the channel walls have been metallated with vanadium(IV)-oxy acetonilacetonate $[VO(acac)_2]$.[79] Similarly, a molybdenum-doped COF, has been synthesized through a hydrazone linked COF, bearing the suitable ligands to coordinate with molybdenyl acetonylacetonate ($MoO_2(aca)_2$), *via* a bottom-up approach.[82]

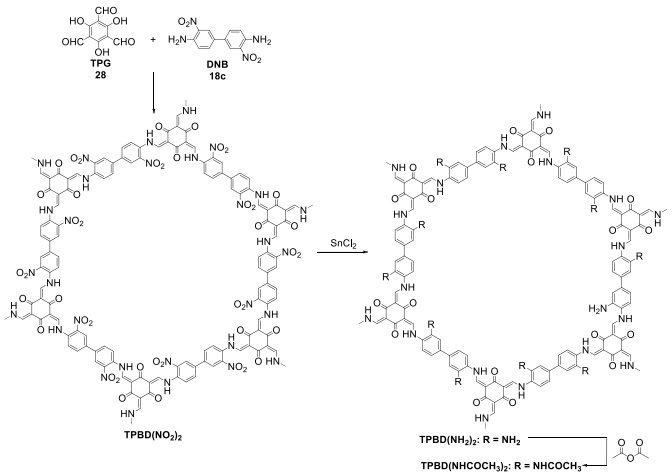

Scheme 10 Schematic representation of the synthesis of **TpBD(NO$_2$)$_2$** and post-synthetic modification to **TpBD(NH$_2$)$_2$** and **TpBD(NHCOCH$_3$)$_2$**.

2.5.3 Metal nanoparticles hybrids COFs

COFs based in β-ketoenamine linkages are attractive support matrix for anchoring active nanoparticles, and therefore improving their catalytic activity. Besides their stability, COFs based in β-ketoenamine linkages exhibit high surface area and porosity, extensive π–π conjugation along the layers, and heteroatoms in the framework to allow further functionalization. Thus, CdS nanoparticles can be deposited on a highly stable 2D-COF matrix, formed using this kind of linkage, producing a hybrid material.[83] COF support was observed to improve the photostability of the deposited CdS resulting in a remarkably high activity compared to that of bulk CdS.

Banerjee *et al* have recently reported a simple synthetic route to obtain highly stable, porous and crystalline hybrids based on Au nanoparticles supported on COF. The so called solution infiltration method that consists on mixing $HAuCl_4.3H_2O$ with an evacuated COF in methanol under vigorous stirring and further reduction with $NaBH_4$, allows to obtain the COF-based hybrid catalyst.[84]

3 Applications of COFs based on Schiff-base chemistry

Nanoporous frameworks such as zeolites, aluminophosphates (AlPOs) or metal–organic frameworks (MOFs) are attractive due to their well-defined crystalline nature combined with a great structural and compositional variety.

Many organic compounds can be efficiently produced and processed on a large scale and can be easily modified by the versatile tools of organic chemistry. [85, 86] The ability to design the desired material on a molecular basis permits fine tuning of different characteristics of the material such as the pore size, suitable functionalization, energy gap, the ionization potential, electron affinity and the light absorbance and emission of the semiconductor. These characteristics, together with the appreciable water, chemical and thermal stability of Schiff-based COF derivatives, have allowed the rapid development of applications for this new family of organic materials.

3.1 COF derivatives for gas storage applications

The so-called advanced porous materials[87, 88] such as metal–organic frameworks (MOFs), porous polymer networks, and zeolitic imidazolate frameworks have received attention for their use in gas storage,[89,90] and gas separations,[91] including CO_2 capture[92] and hydrocarbon and other liquid separations.[93,94] Among this type of porous materials, COFs have recently emerged as a realistic alternative for gas storage applications because they are lightweight, highly thermally stable, crystalline and exhibit permanent porosity.[21, 22] Much of the interest in these new classes of material arises from the utilization of reticular chemistry[95] in their design, facilitating modular assembly of materials with predictable topology and atomic-scale control over their internal surface chemistry. Thus, several theoretical studies have been carried out in order to rationalize the gas uptake of different COFs in terms of pore volume, pore size or isosteric heat.[96-99] One can use these principles to design COFs based on specific underlying topologies suitable to store specific adsorbates.

The first examples of COFs for gas storage applications were based on reversible B-O bonds. Though showing good gas storage ability, COFs based on boronates are very sensitive to aqueous environment, even humid air, because of the weak B-O bond.[15] Thus, it was obvious the need to find new COFs that allow increasing the hydrolytic stability but maintaining the outstanding gas storage capacity. In this respect, imine-linked 2D and 3D COFs have appreciable water, chemical and thermal stability[46] and display high potential in gas adsorption and storage. The interpenetration have been described in several crystalline 3D-COFs.[19] This is a phenomenon that affect to the surface area of the material therefore reducing its BET surface area. In principle, this is a structural problem less likely for 2D COFs that are the materials showing the highest surface area reported so far. We will briefly summarize the different COFs based on Shiff-base chemistry which have been designed for the uptake of different gases.

From a gas adsorption perspective, the on-board storage of H_2 and CH_4 fuels in automotive applications remains a considerable challenge and has to meet volumetric and gravimetric targets to be effective. On the other hand, specific attention has been paid to carbon dioxide capture and sequestration (CCS) as it is essential for a sustainable climate.[100] Carbon dioxide is one of the major components of greenhouse gases and its concentration level in the environment has risen with the increasing consumption of fossil fuel.[101]

Although Table 1 collects a summary of the most relevant adsorption data already reported on COFs based on Shiff-chemistry, in the following we will highlight some remarkable examples devoted with the specific design of the COF structure to improve gas sorption.

In 2013 El Kaderi *et al* reported the first example of an imine-linked COF (**ILCOF-1**, Fig. 12) for gas storage.[102]

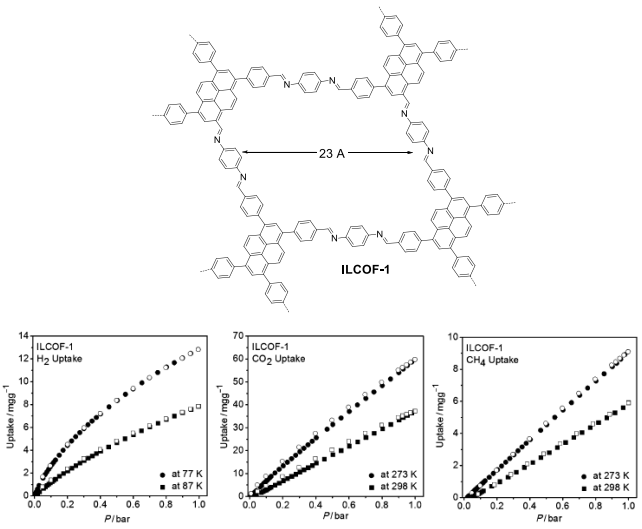

Fig. 12 Top: Chemical structure of **ILCOF-1**. **Bottom:** Hydrogen, carbon dioxide and methane sorption measurements for **ILCOF-1**. Figure extracted from ref. [102]. Reproduced with permission of Wiley-VCH.

This COF was synthesized by condensation of 1,3,6,8-tetrakis(*p*-formylphenyl)pyrene (**42**) with *p*-phenylenediamine (**17a**) under solvothermal conditions. A Brunauer–Emmett–Teller (BET) surface area of 2723 m^2g^{-1} was determined for **ILCOF-1** with a pore-size distribution of around 23 Å that is very similar to the calculated pore width of the model (24.3 Å) defined by the distance between the phenyl linkers. The total pore volume was found to be 1.21 cm^3g^{-1}. The calculated surface area and major pore-size distribution are considerably higher than those reported for previously reported crystalline imine-linked COFs probably as a consequence of the presence of the expanded pyrene building units. Thus, pyrene core was used in order to enhance porosity and therefore improve performance in high pressure storage.[103] At 1.0 bar, **ILCOF-1** stores moderate amounts of hydrogen (13 mgg^{-1}, 77 K), CH_4 (9 mgg^{-1}, 273 K), and CO_2 (60 mgg^{-1}, 273 K) (Fig. 12).

The US Department of Energy has set a target for on-board methane storage at 180 v/v at room temperature and 35 bar,[104] whereas the gravimetric density target for hydrogen are 5.5 wt.% (55 mgg^{-1}) for 2015.[105] Thus, high pressure (up to 40 bar) gas sorption measurements for H_2, CH_4 and CO_2 were also performed for **ILCOF-1.** The absolute gravimetric uptake for hydrogen at 77 K and 40 bar is 61 mgg^{-1} slightly above the target set by the DOE. On the other hand, the absolute adsorbed amount for CH_4 in volumetric units was estimated to be 129 LL^{-1} (92 gL^{-1}) at 298 K and 35 bar which is still lower than the DOE target for 2015. The volumetric CO_2 adsorption capacity at 298 K and 35 bar is 587 gL^{-1} (299 LL^{-1}), which is approximately eight times the density of carbon dioxide at the same temperature and pressure.

Table 1. Structural information and gas adsorption capacity of COFs based on Schiff-base chemistry.

Type	COF	Bulding units	Average pore size (Å)	BET surface area (m^2g^{-1})	Pore volume (V_p, $cm^3\ g^{-1}$)	H_2 uptake (wt%)[a]	CH_4 uptake (wt%)[b]	CO_2 uptake (wt%)	Ref.
Imine	ILCOF-1	42 + 17a	23	2723	1.21	1.3	0.9	6.0	[102]
Azine	ACOF-1	25+27	9.4	1176	0.91	0.99	1.15	17.7	[43]
Imine	CTV-COF-1	34+17a	14.8	1245	0.94	1.3	-	-	[31]
Imine	CTV-COF-2	34+18a	21.6	1170	1.07	0.75	-	49.1[d]	[31]
Imine	TAPB-TFPB	36+29	40	229	-	0.68	-	4	[106]
Imine	iPrTAPB-TFPB	37+28	50	391	-	0.43	-	3.1	[106]
Keto-enamine	TAPB-TFP	36+28	26	567	-	1.08	-	18	[106]
Keto-enamine	iPrTAPB-TFP	37+28	34	756	-	1.15	-	10.5	[106]
Imine	N-COF	38a+27	11	1700	0.84	-	-	120	[107]
Azine H bonded	COF-JLU2	28+27	9.6	415	0.56	1.6	3.8	21.7	[42]
Keto-enamine	TpPa-COF	17a+28	1.27	725	0.89	-	-	21.8	[53]
Imine	$[OH]_X$-H_2P-COF	1+3+47	25	1054-1284	0.78-1.02	-	-	46-63	[80]
Imine	$[HO_2C]_X$-H_2P-COF	From $[OH]_{X\%}$-H_2P-COF	14-22	364-786	0.43-0.66	-	-	96-174	[80]
Imine	$[C\equiv C]_X$-H_2P-COF	47+7+3	16-25	426-1474	0.28-0.75	-	-	39-72	[80]
Imine	$[Et]_X$-H_2P-COF	From $[C\equiv C]_X$-H_2P-COF	15-22	187-1326	0.18-0.55	-	-	38-55	[80]
Imine	$[MeOAc]_X$-H_2P-COF	From $[C\equiv C]_X$-H_2P-COF	11-21	156-1238	0.14-0.51	-	-	65-84	[80]
Imine	$[AcOH]_X$-H_2P-COF	From $[C\equiv C]_X$-H_2P-COF	13-22	186-1252	0.18-0.52	-	-	94-117	[80]
Imine	$[EtOH]_X$-H_2P-COF	From $[C\equiv C]_X$-H_2P-COF	14-22	214-1248	0.19-0.56	-	-	84-92	[80]
Imine	$[EtNH_2]_X$-H_2P-COF	From $[C\equiv C]_X$-H_2P-COF	13-22	382-1402	0.21-0.58	-	-	97-116	[80]

Based on previous research on polymers with intrinsic microporosity containing crown-shaped moieties, in 2014 Song et al. reported two new COFs based on cyclotriveratrylene (**CTV**).[31] The maximum hydrogen uptake for these COFs was 1.3 wt% at 1.1 bar and 1.23 wt% at 1 bar which is similar to that observed for **ILCOF-1**. The maximum uptake for CO_2 for these **CTV**-based COFs was of 49.1 wt%.

In 2015, a novel imine-based nitrogen-rich COF (**N-COF**) was synthesized *via* the Schiff base reactions of two triangular building units, namely 2,4,6-tris(4-aminophenyl)-1,3,5-triazine (**38a**) and 1,3,5-triformylbenzene (**27**) under solvothermal conditions.[107] The BET surface area of **N-COF** was calculated to be 1700 m^2g^{-1}, with a total pore volume of 0.84 cm^3g^{-1}. Its pore size distribution was calculated using DFT method, revealing a narrow distribution of pore size at 11 Å. The nitrogen-rich structure of the COF provides a volumetric CO_2 uptake capability as high as 61.2 cm^3g^{-1} (1 atm, 273 K) and 32.4 cm^3g^{-1} (1 atm, 298 K). On the other hand, the CH_4 uptake capability is 34.4 (1 atm, 273 K) and 11.4 cm^3g^{-1} (1 atm, 298 K). Finally, the N_2 uptake capability of **N-COF** is only 3.6 cm^3g^{-1} (1 atm, 273 K) which indicates its high adsorption selectivity toward CO_2 over N_2 under the same conditions.

Azine-linked COFs have been also used for gas storage applications. Azine-linked COFs are interesting because they not only possess exceptional chemical and thermal stability, but also can be easily predetermined to make smaller pore sizes originating from the short structural length of the azine unit. Thus, in 2014, Liu *et al* reported the synthesis of a new azine-linked covalent organic framework (**ACOF-1**, Scheme 5) by condensation of hydrazine (**25**) hydrate and 1,3,5-triformylbenzene (**27**) under solvothermal conditions. The BET surface area determined for this COF was 1176 $m^2\ g^{-1}$ with a pore size distribution of 9.4 Å and a total pore volume of 0.91 cm^3g^{-1}. The CO_2 isotherms of **ACOF-1** were measured at 298 and 273 K, which showed 17.7 wt % CO_2 uptake at 273 K and 1 bar. At 77 K and 1 bar, **ACOF-1** exhibits 0.99 wt % hydrogen uptake and at 273 K and 1 bar a methane uptake of 1.15 wt % was determined. In this work is also investigated the selective uptake of CO_2, CH_4 and N_2 to evaluate the potential application of this COF in the gas separation field. Adsorption selectivity of CO_2/N_2 and CO_2/CH_4 are of 40 and 37 at 273 K, respectively. Interestingly, the selectivity of CO_2/CH_4 surpasses imine-linked porous polymer frameworks[108] and electron-rich organonitridic frameworks.[109] The high selectivity of CO_2 over N_2 and CH_4 can be derived as in the previous **N-COF** from the abundant nitrogen atoms on the pore wall of the COF interacting more favourably with polarizable CO_2 molecules through dipole–quadrupole interactions. In order to increase the uptake capacity of COFs for small gas, a good strategy involves an increase in the surface area and pore volume, adjusting appropriate pore size. In addition, an effective strategy to improve the adsorption capacity for small gas is to introduce special active sites. In this context, Liu *et al* have prepared a modification of the above mentioned azine-based **ACOF-1** in which hydrazine (**25**) hydrate was reacted with 1,3,5-triformylphloroglucynol (**28**) instead of 1,3,5-triformylbenzene (**27**). This COF, named **COF-JLU2** presents a surface area of 415 m^2g^{-1} calculated using the BET model, a pore volume of 0.56 cm^3g^{-1} and a pore size distribution of 9.6 Å. This new crystalline framework not only possesses a relatively small pore size, but also has a large number of heteroatom active sites in the pore wall. These structural features function cooperatively, enhancing the uptake capacity of **COF-JLU2** in small gas storage. Thus, **COF-JLU2**, shows a CO_2 uptake value of 21.7 wt% at 273 K and 1 bar. The H_2 uptake of **COF-JLU2** at 77 K and 1 bar is 1.6 wt%. The CH_4 uptake reaches 3.8 wt% at 273 K and 1.0 bar, which is three-fold higher than similar crystalline **ACOF-1** (1.15 wt%). Finally, the estimated adsorption selectivity of CO_2/N_2 is 77. This value surpasses those of carbon-based materials,[110] **ACOF-1** (40)[43] or imine-linked porous polymers,[108] however it is lower than the high values of some microporous organic polymers (MOPs).[111] Furthermore, the CO_2 selectivity over CH_4 is 4.1 at 273 K and 3.2 at 298 K, respectively, which are also comparable to reported MOPs.[108]

Murugavel *et al* have prepared a series of imine or β-ketoenamine based COFs comprising less explored [3 + 3] motifs.[106] Reaction of 1,3,5-tris(4'- aminophenyl)benzene (**TAPB**, **36**) and 1,3,5-tris(4'-amino-3',5'-isopropylphenyl)benzene (***i*PrTAPB**, **37**) with 1,3,5-tris(4'-formylphenyl)benzene (**TFPB**, 29) and 1,3,5-triformylphluroglucinol (**TFP**, **28**) in dry dioxane and acetic acid (cat.) resulted in the formation of crystalline 2-D frameworks, **TAPB-TFPB**, ***i*PrTAPB-TFPB**, **TAPB-TFP** and ***i*PrTAPB-TFP** with pore size distribution of 40 Å, 50 Å, 26 Å and 34 Å respectively. BET surface areas between 229 and 756 m^2g^{-1} were determined for these series of COFs. The surface area of the four COFs follows the order: ***i*PrTAPB-TFP** > **TAPBTFP** >> ***i*PrTAPB-TFPB** > **TAPB-TFPB**. It is reasonably well understood that upon increasing the size of the building block(s), the chances of network entanglement increases leading to decrease in the surface area.[108] **TFPB** (**29**) building unit are much larger in size than **TFP (28)**, and therefore **TFPB** based COFs show surface areas which are only about 50% of the **TFP** based COFs. The difference in the surface areas of COFs constructed from ***i*PrTAPB (37)** and **TAPB** (**36**) is relatively small and is essentially dictated by the presence of bulky isopropyl groups. Isopropyl groups on the aromatic rings might hinder the process of network entanglement and therefore the surface area of ***i*PrTAPB** based COFs is higher than that of the **TAPB** based COFs.

To evaluate the CO_2 uptake capacities, the measurements were performed up to 1 bar at 273 K. The CO_2 uptake capacities were calculated to be 4 wt % (**TAPBTFPB**), 3.1 wt % (***i*PrTAPB-TFPB**), 18 wt % (**TAPB-TFP**) and 10.5 wt %, (***i*PrTAPB-TFP**) that follows the order ***i*PrTAPB-TFPB** < **TAPB-TFPB** < ***i*PrTAPB-TFP** < **TAPB-TFP**. The large difference in the uptake capacities of **TFP** COFs could be attributed to the steric hindrance caused by isopropyl groups. The best uptake values observed for the **TFP** derivatives may be due to the large number of heteroatom active sites in the pore wall due to the use of the 1,3,5-triformylphluroglucinol (**28**) building block. Furthermore, it is shown that by the virtue of triphenylbenzene as an inherently fluorescent platform, the COFs are endowed with fluorescence and fluorescence chemo-sensing ability for polynitroaromatic analytes. We will see it in detail in the following section dedicated to the sensing ability of COF derivatives.

The CO_2 uptake of a two-dimensional enamine-linked COF (**TpPa-COF**, Scheme 6) synthesized under microwave assisted solvothermal method have been recently reported.[53] The COF was obtained by reaction of *p*-phenylenediamine (**17a**) and 1,3,5-triformylphloroglucinol (**28**). The pore size distribution analysis of **TpPa-COF** results in pore size distributions of 1.1–1.5 nm, with peak maxima at 1.27 nm. The BET surface area of **TpPa-COF** synthesized under microwave conditions (**TpPa-COF (MW)**) was found to be 724.6 $m^2\ g^{-1}$, which is higher than that found for the COF obtained from the same starting materials under standard solvothermal conditions (**TpPa-COF (CE)**, 152.6 $m^2\ g^{-1}$).

The CO_2 sorption isotherm of **TpPa-COF (MW)** was measured at 273 K and 298 K, which shows a 21.8 wt% CO_2 uptake at 273 K and 1 bar. The relatively high CO_2 uptake capacity and binding by **TpPa-COF (MW)** can be derived from the combination of factors including porosity, the small pore size, high surface areas and the abundant N–H sites on the pore wall of **TpPa-COF(MW)**.

Very recently, imine-linked COFs have been synthesized to bear content-tuneable, accessible, and reactive groups on the walls of one-dimensional pores.[80, 112] These COFs have revealed as ideal platforms for pore-wall surface engineering aimed at anchoring diverse functional groups ranging from hydrophobic to hydrophilic units and from basic to acidic moieties with controllable loading contents. Jian *et al* have shown that this approach enables the development of various tailor-made COFs with systematically tuned porosities and functionalities while retaining the crystallinity. This strategy can be used to efficiently screen for suitable pore structures for gas adsorbents.

One approach developed by Jiang *et al* involved the synthesis of imine-linked COFs (COFs) bearing content-tuneable, accessible, and reactive ethynyl groups on the walls of one-dimensional pores.[80] With this aim, a three-component reaction system was developed consisting of 5,10,15,20-tetrakis(p-tetraphenylamino)porphyrin (**47**) and a mixture of 2,5-bis(2-propynyloxy)terephthalaldehyde (**BPTA**, **7**) and 2,5-dihydroxyterephthalaldehyde (**DHTA**, **3**) at various molar ratios (X = [**BPTA**]/([**BPTA**] + [**DHTA**]) × 100 = 0, 25, 50, 75, and 100) for the synthesis of four COFs with different ethynyl contents on their edges (Scheme 11, **$[HC{\equiv}C]_X$-H_2P-COFs**, X = 25, 50, 75, and 100).

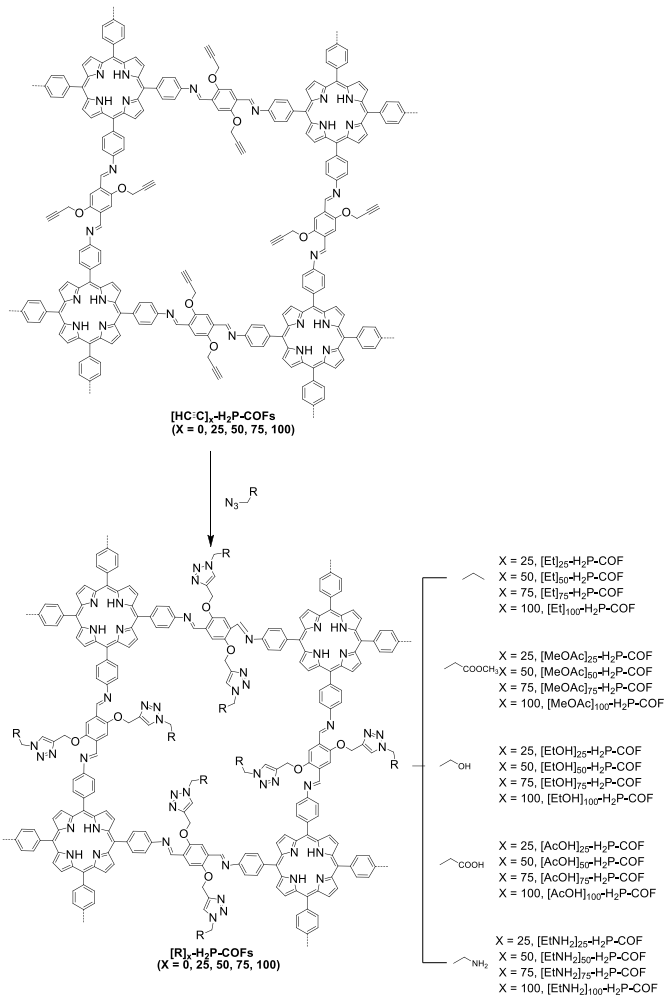

Scheme 11 Schematic of pore surface engineering of imine-linked COFs with various functional groups via Click reactions.

Subsequent quantitative click reactions between the ethynyl units and azide compounds were performed to anchor the desired groups onto the pore walls. By means of this strategy, 20 different COFs were obtained with pores functionalized with a variety of functional groups, including ethyl, acetate, hydroxyl, carboxylic acid, and amino groups; these groups ranged from hydrophobic to hydrophilic and from basic to acidic (**$[R]_X$-H_2PCOFs**, **$[Et]_X$-H_2P-COFs**, **$[MeOAc]_X$-H_2P-COFs**, **$[EtOH]_XH_2$P-COFs**, **$[AcOH]_X$-H_2P-COFs**, **$[EtNH_2]_X$-H_2P-COFs**).

The BET surface as well as the pore volume in the **$[HC{\equiv}C]_X$-H_2PCOFs** series decrease when the ethynyl content increases which indicates that the ethynyl groups occupies the pore space. By subsequent click functionalization of the COFs, the pore surface engineering steadily decreased the pore size from a mesopore to supermicropores, allowing the systematic tuning of the pore sizes from 2.2 to 1.9, 1.6, and 1.5 nm. Such fine adjustments of the pore size have not been achieved *via* direct polycondensation. The CO_2 uptake in these series of COFs was determined at 1 bar and 273 and 298 K. The best values was obtained for those COFs that can establish specific interactions with CO_2. For example, (i) derivatives endowed with polar ester units can interact with CO_2 *via* dipole interactions and thus

improve the affinity of the COF for CO_2; (ii) **[AcOH]$_X$-H$_2$P-COFs** and **[EtOH]$_X$-H$_2$P-COFs** can establish dipole and hydrogen bonding interactions of carboxylic and hydroxyl units with CO_2 and (iii) the amino groups can form acid−base pairs with CO_2. Interestingly, all these COFs (**[MeOAc]$_X$-H$_2$P-COFs**, **[AcOH]$_X$-H$_2$P-COFs**, **[EtOH]$_X$-H$_2$P-COFs**, and **[EtNH$_2$]$_X$-H$_2$P-COFs**) exhibit maximal capacities at X = 50. Among them, **[EtNH$_2$]$_{50}$-H$_2$P-COFs** exhibited an adsorption capacity of 157 mgg^{-1}, which is the highest adsorption capacity in the series. The dramatic change in the adsorption of CO_2 upon pore surface engineering is the result of a balance between the two contradictory effects of enhanced affinity and decreased porosity on adsorption.

Another approach for the pore-wall surface engineering strategy have been also developed by Jian *et al* that synthesized a conventional imine-linked 2D-COF (**[HO]$_{100\%}$-H$_2$P-COF**) as a scaffold with porphyrin at the vertices and phenol units on the pore walls;[112] this 2D-COF exhibits a low capacity for carbon dioxide adsorption. Nevertheless, the phenol groups undergo a quantitative ring opening reaction with succinic anhydride that decorates the channel walls with open carboxylic acid groups (**[HO$_2$C]100%-H$_2$PCOF**). The content of carboxylic acid units on the channel can be tuned by adjusting the content of phenol groups through a three-component condensation system with a mixture of 2,5-dihydroxyterephthalaldehyde (**DHTA**, **3**) and terephthaldehyde (**1**) as the wall components (**[HO]$_{X\%}$-H$_2$P-COFs**, X=[**DHTA**]/([**DHTA**]+[**PA**])). Using this method, it was possible to synthesize a series of **[HO$_2$C]$_{X\%}$-H$_2$P-COFs** with controlled carboxylic acid density that varied from 25 to 100 %. The BET surface area (SBET) decreased from 786 to 673, 482, and 364 m^2 g^{-1}, whereas the pore size decreased from 2.2 to 1.9, 1.7, and 1.4 nm, as the content of carboxylic groups was increased from 25 to 50, 75 and 100 %, respectively. The pore volume also decreased from 0.78 to 0.66, 0.54, and 0.43 cm^3 g^{-1}, as the content of carboxylic groups was increased. This reduction in porosity is indicative of space filling by the functional units appended to the channel walls.

The CO_2 adsorption by **[HO]$_{X\%}$-H$_2$P-COFs** at pressures up to 1 bar and at temperatures of 273 and 298 K was determined showing low capacities between 46 and 63 mgg^{-1} at 273 K and between 31 and 35 mgg^{-1} at 298 K. By contrast, the **[HO$_2$C]$_{X\%}$-H$_2$P-COFs** exhibited dramatically increased CO_2 adsorption capacities. For example, **[HO$_2$C]$_{100\%}$-H$_2$P-COF** exhibited a capacity of 180 and 76 mgg^{-1} at 273 K and 298 K, respectively. These capacities are 2.8- and 2.2-fold greater than those of **[HO]$_{100\%}$-H$_2$P-COFs**. Interestingly, the adsorption capacity of **[HO$_2$C]$_{X\%}$-H$_2$P-COFs** increased in proportion to their carboxylic acid content which clearly confirms the effectiveness of channel-wall functionalization in enhancing CO_2 adsorption.

These contributions above show the benefits of precise pore surface engineering as a key strategy for the selective capturing of gases with COFs.

3.2 COFs for large molecules uptake

Immobilization of enzymes into mesoporous materials is potentially useful for applications such as biosensors and biocatalysts because it can increase the recyclability of the costly enzyme and also improves the stability of enzymes under extreme conditions. However, the application of COFs is still mostly limited to the storage of gas molecules (see above), since most of the COFs synthesized are microporous in nature and their pores are not large enough to hold larger guests, such as enzymes. While examples of mesoporous boronic acid-based COFs have been reported in the literature[32, 113] their chemical instability prevents the usage of these materials for the storage of large molecules such as drugs and enzymes[20, 114] Banerjee *et al* have synthesized a chemically stable and mesoporous imino-based COF (**COF-DhaTab**), in order to study the adsorption and storage of the enzyme trypsin into the COF pores.[26]

Synthesis of **COF-DhaTab** was carried out by the Schiff base reaction between 2,5-dihydroxyterephthalaldehyde (**3**) and 1,3,5-tris(4-aminophenyl)benzene (**36**) under solvothermal conditions. The synthesized **COF-DhaTab** is highly crystalline, possesses high surface area of ~1500 m^{2}g^{-1} and has a pore size distribution of 3.7 nm. Since **COF-DhaTab** is mesoporous in nature and has chemical stability in phosphate buffer and water, it is suitable to perform protein adsorption studies in it. Trypsin is a globular protein having hydrodynamic size of ~3.8 nm, which is close to the **COF-DhaTab** pore size (3.7 Å). This close match in the relative size does not affect the trypsin adsorption in COF pores, since enzymes are soft molecules and can adjust their conformation to fit inside the COF pores. The maximum storage capacity of the trypsin for the COF was found to be 15.5 mmol g^{-1}. TEM images of the trypsin-loaded samples show that the hollow sphere morphology remains intact even after the loading process and remains ~60% of the activity of the free enzyme which is comparable to other literature-reported values.[26] Interestingly, the loading and release study of the anticancer drug doxorubicin (**DOX**) in the COF hollow system has been also tested. **DOX** loaded in COF was calculated to be 0.35 mg g^{-1} and the drug release profile shows a slow release of **DOX** (42%) after 7 d in phosphate (pH 5) buffer. This result paves the way for the future use of this type of COFs for the reversible binding and release of drug molecules.

As we mentioned in the description of the functionalization by post-polymerization methods, Medina, Bein *et al* have recently demonstrated for the first time a two-step post-synthetic modification in a COF and synthesized an amine functionalized COF, **TpBD(NH$_2$)$_2$** (Scheme 10).[81] They have used this functionalized COF to perform lactic acid adsorption experiments showing that the affinity for lactic acid can be successfully increased by post-synthetic modification of the functional side groups in the COF pores. While the demand for lactic acid is drastically increasing, separation from its sources is the main bottleneck limiting the further upscaling of the production process. Considering that new materials for selective adsorption of lactic acid are in great demand, this strategy for the functionalization of COFs can provide suitable materials for this purpose.

3.3 Sensors based on COFs

In addition to gas capture, chemo-sensing is another area of significant interest that has been explored for COFs. In 2013,

Jiang *et al* reported the synthesis of an azine-linked COF (**Py-Azine COF**) which is highly luminescent whereas the azine sites serve as docking sites to lock guest molecules.[41] (Scheme 5). The synergistic functions of vertices and edges endow the COF with unique chemosensing characteristics. As demonstrated in the vapour detection of 2,4,6-trinitrophenol (**TNP**) explosive, the COF exhibits high sensitivity and selectivity (Fig. 13). BET surface area of 1210 $m^2 g^{-1}$, pore volume of 0.72 $cm^3 g^{-1}$ and pore size distribution centred at 1.76 nm was determined for **Py-Azine COF**. Upon excitation at 470 nm, the **Py-Azine COF** emits a yellow luminescence with a red-shifted band centred at 522 nm. When acetonitrile solutions of **Py-Azine COF** are exposed to the **TNP** vapour, the characteristic COF fluorescence is quickly quenched. The fluorescence quenching degree reaches 69% when the concentration of **TNP** is as low as 70 ppm in acetonitrile which indicates that the COF is highly sensitive to TNP molecules. The chemosensing ability of this COF has been tested with a variety of nitrobenzene derivatives, including 2,4,6-trinitrophenol (**TNP**), 2,4-dinitrophenol (**DNP**), 2,4-dinitrotoluene (**DNT**), 2-nitrophenol (**NP**), and 2-nitrotoluene (**NT**), which are highly soluble in acetonitrile. Interestingly, when other nitrobenzene compounds are utilized under otherwise same condition, the COF does not show significant change. For example, the fluorescence quenching degrees are only 13, 5, 3, and 3% for **DNP**, **DNT**, **NP**, and **NT**, respectively. These remarkable results indicate that the **Py-Azine COF** offers a selective detection of **TNP** explosive among the above nitrobenzene compounds.

As we already mentioned in the previous section dedicated to the gas adsorption in COFs, Murugavel *et al* have prepared a series of imine or β-ketoenamine based COFs comprising [3 + 3] motifs **TAPB-TFPB**, ***i*PrTAPB-TFPB**, **TAPB-TFP** and ***i*PrTAPB-TFP**.[106] By the virtue of triphenylbenzene as an inherently fluorescent platform, the COFs are also endowed with fluorescence and fluorescence chemo-sensing ability for polynitro-aromatic analytes. Thus, the fluorescence is effectively quenched in the presence of various concentrations of different polynitro-aromatic compounds such as picric acid (**PA**), dinitrotoluene (**DNT**), *p*-dinitrobenzene (***p*-DNB**) and m-dinitrobenzene (***m*-DNB**). Notably, PA is the most efficient quencher among all the polynitro-aromatic compounds which could be because of the proton transfer from PA to the nitrogen atoms of the COFs.

Banerjee *et al* have also recently investigated the possibility of using chemical sensing of COFs for the detection of 2,4,6-trinitrophenol (**TNP**), over other nitroaromatic analytes such as 2,4,6-trinitrotoluene (**TNT**), **DNP**, **DNT**, and **NP**.[115] With this in mind, due to the well-known good photophysical properties of imides,[103] they synthesized two imide based COFs (**TpBDH** and **TfpBDH**), each possessing a two dimensional layered structure, that exhibit porosity, crystallinity and chemical stability. The new COFs were obtained by reaction between pyrromellitic-*N,N'*-bisaminoimide (**BDH**, **26**) and either 1,3,5-triformylfphloroglucinol (**Tp**, **28**) (for **TpBDH**) or 1,3,5-tris(4-formylphenyl)benzene (**TFp**, **29**) (for **TfpBDH**) under solvothermal conditions.

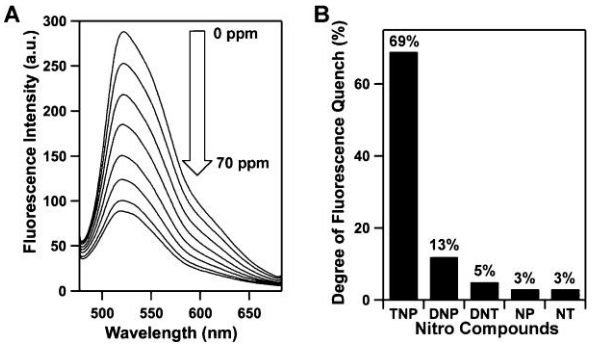

Fig 13. Fluorescence quenching of the Py-Azine COF (Scheme 5) upon addition of 2,4,6-trinitrophenol (TNP) (0–70 ppm) in acetonitrile. b) Degree of fluorescence quench upon addition of the nitro compounds (70 ppm). Reprinted with permission from *J. Am. Chem. Soc.* 2013, 135, 17310-17313. Copyright (2013) American Chemical Society.

In spite of the suitable photophysical characteristics of these COFs, the sensitivity and selectivity were found to be quite low for bulk COFs, due to the extensive aggregation of layers, which reduces the available electrons for analyte-COF interaction. Hence, an innovative strategy was developed that involved the exfoliation of these COFs into 2D covalent organic nanolayers (CONs) to minimize the aggregation and maximize the availability of electron density among the layers. By using one-step liquid phase exfoliation (LPE) undertaken in isopropyl alcohol (**IPA**) at room temperature it was possible to obtain thin 2D CONs composed of ~5–15 stacked COF layers. **TpBDH** and **TpBDH-CONs** do not show any PL activity, as in both **TpBDH** and **TpBDH-CONs** exist enol–keto tautomerization which leads to the disturbance in π-conjugation and "switches off" the fluorescence. On the other hand, it was observed that for **TfpBDH**, with increase in the sonication time, CONs exhibits a stronger PL peak almost ~ 90 times more intense than that observed for the bulk COF samples. Thus, **TfpBDH-CONs** show good selectivity and prominent, direct visual detection towards different nitroaromatic analytes. Quite interestingly, **TfpBDH-CONs** exhibit a superior "turn-on" detection capability for **TNP** in the solid state, but conversely, they also show a "turn-off" detection in the dispersion state. These findings describe a new approach towards developing an efficient, promising fluorescence chemosensor material for both visual and spectroscopic detection of nitroaromatic compounds with very low [10^{-5} (M)] analyte concentrations.

Triazatruxene based COFs have also been recently synthesized and shown a quick-response fluorescence-on and fluorescence-off nature towards electron rich and deficient arene vapours.[116] The triazatruxene-based COFs have a weak interaction with electron-rich arenes, so the fluorescence-on sensing of electron rich arenes can be reused conveniently.

Not only chemosensors but also biosensors have been developed based on COFs. Wang, Fang *et al* reported in 2014 the use of an imine-linked COF as biosensor for bovine serum albuminum (**BSA**) adsorption and probe DNA immobilization (Fig. 14).[77]

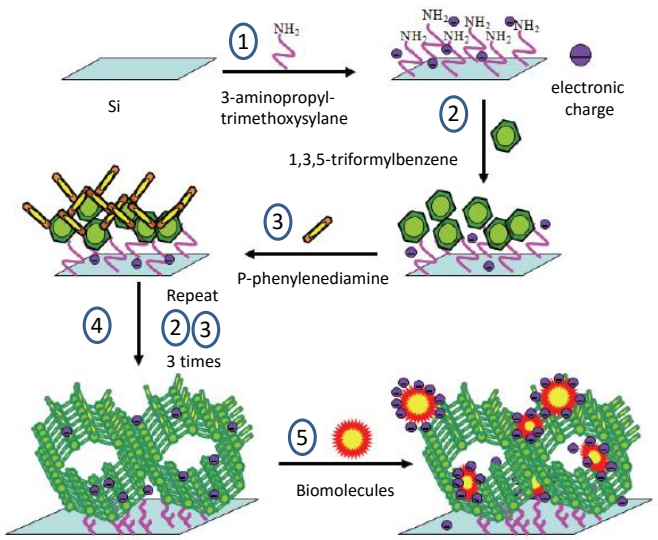

Fig. 14 Construction of imine-linked COF on surface for bio-molecular adsorption. Taken from ref. [77]. Reprinted with permission of Chin. J. Chem.

In this case, they do not use the bulky synthesis of a COF but the condensation of the building blocks onto an amino functionalized silicon substrate (denoted as Si-AMS). Thus, Si-AMS can be reacted with 1,3,5-triformylbenzene (**27**) in the presence of acid catalyst to yield **Si-AMS-CHO-1** which is subsequently reacted with *p*-phenylenediamine (**17a**) to afford **Si-AMS-NH$_2$**. Triformylbenzene and *p*-phenylenediamine are reacted with treated silicon wafer by turns for another 3 times to afford different materials denoted as **Si-AMS-CHO-2**, **Si-AMS-NH$_2$-2**, **Si-AMS-CHO-3**, **Si-AMSNH$_2$-3**, **Si-AMS-CHO-4**, and **Si-AMS-NH$_2$-4**, respectively. Since a large amount of amino groups were reserved in the functional COF films, it is very helpful for biomolecules to adhere on due to the strong electrostatic interactions. In this study, tentative experiments of biomolecules immobilization on the COF film were tested by electrochemical methods. Electron impedance spectroscopy was used to determine the DNA immobilization or BSA adsorption on the surface of **Si-AMS-NH$_2$-4**. It was clearly observed that the charge transfer resistance values of the composite electrodes decline, indicating that the adsorption of biomolecules onto COF films can strengthen the electrochemical activity of the functional film. This work represents a first example of how functionalized COFs can find use also as biosensors.

3.4 COF derivatives as catalysts

In comparison with amorphous porous materials, crystalline porous materials have great potential in catalysis because of their structural regularity.[117] Indeed, inorganic zeolites have been widely used as catalysts in refining and petrochemical industries.[118] Recent research has also demonstrated the possibility of employing MOF materials in catalysis.[119] In order to develop COF for catalysis applications, two basic but important issues had to be addressed. One is that the COF catalyst must show high stability to thermal treatments, water, and most of the organic solvents. Another is that the COF material should either have catalytic active sites or is able to incorporate catalytic species. As we have already seen COFs obtained by Schiff-base chemistry, being highly stable in water and most organic solvents, meet the first requirement as robust catalysts. Moreover, it has been well demonstrated[120] in coordination chemistry that the imine type (Schiff base) ligands are versatile in incorporating a variety of metal ions. This motivated different research groups to explore the possibility of using COFs based on Schiff-base chemistry for catalysis. Thus, in the last few years, COFs have revealed as excellent platforms to be used as catalyst in classical heterogeneous catalysis, photocatalyst and electrocatalyst.

3.4.1 Heterogeneous Catalyst

In 2011, Wang *et al* reported the first example of a COF based on Schiff-base chemistry for catalysis.[15] With this aim, they synthesized an imine-linked COF material (denoted as **COF-LZU1**) by reaction between 1,3,5-triformylbenzene (**27**) and *p*-phenylenediamine (**17a**) under solvothermal conditions. **COF-LZU1** possesses a two-dimensional eclipsed layered-sheet structure, making its incorporation with metal ions feasible. Thus, the palladium(II)-coordinated COF material (**Pd/COF-LZU1**) was synthesized *via* a simple treatment of **COF-LZU1** with $Pd(OAc)_2$ at room temperature.

The catalytic activity of **Pd/COF-LZU1** catalyst was examined in one of the representative Pd-catalysed reactions, i.e., the Suzuki-Miyaura coupling reaction (Table 2). The Suzuki-Miyaura coupling reaction has been widely applied in homogeneous media for the facile formation of C-C bonds.[121] In this study it is shown that **Pd/COF-LZU1** possesses high catalytic activity in catalysing the Suzuki-Miyaura coupling reaction.

Catalysed by 0.5 mol % of **Pd/COF-LZU1**, the substituted aryl iodides with either an electron-donating or an electron-withdrawing group afforded the cross coupling products in excellent yields (96-97%). Less active bromobenzenes also gave excellent yields (96-98%) within 2.5-4 h at 150 °C. Furthermore, when 0.1 mol % catalyst was used, the reaction also worked well but with a longer reaction time (5 h). Interestingly, in comparison with a Pd(II)-containing MOF,[122] **Pd/COF-LZU1** required less catalyst-loading and shorter reaction time and showed higher reaction yield.

The potential application of the Suzuki-Miyaura coupling reaction in industry is still limited due to the difficulty in separating and recycling the expensive Pd-catalysts from the product mixture. Using recyclable palladium catalysts is therefore a promising solution to these problems. Thus, the recycle use of **Pd/COF-LZU1** catalyst (1.0 mol %) was further examined in the reaction of *p*-nitrobromobenzene with phenylboronic acid. The results demonstrated that **Pd/COF-LZU1** catalyst could be reused at least for four times without loss of catalytic activity and selectivity.

Table 2. Reactions catalysed by COFs based on Schiff-base chemistry with indication of the catalytic system used.

Reaction	Catalyst	Reference
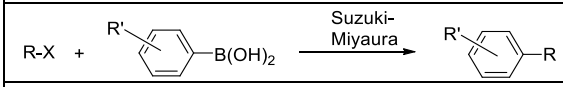	Pd/COF-LZU1 H_2P-Bph-COF	15 123
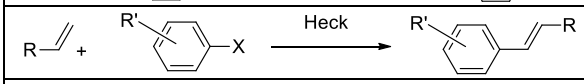	Pd(0)@TpPa-1	124
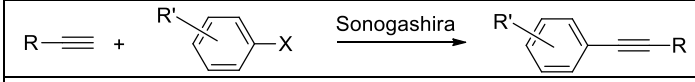	Pd(0)@TpPa-1	124
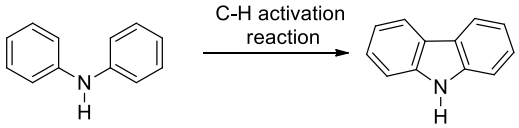	Pd(II)@TpPa-1	124
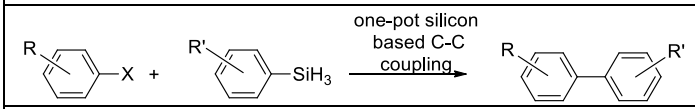	Pd(II)/COF-SDU1	125
	BF-COF1 BF-COF-2	126
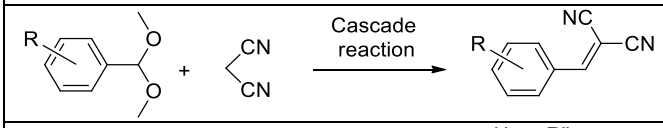	2,3-DhaTph 2,3-DmaTph	24
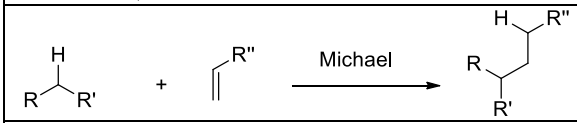	[Pyr]X-H2P-COFs	127
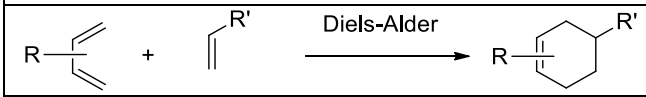	Py-An COF	128
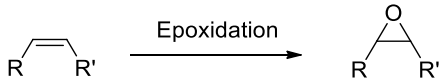	PMA@COF-300 Mo-COF	129 82
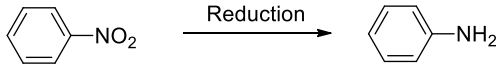	Au(0)@TpPa-1	84

More recently, Zhang *et al* have synthesized a metal-free porphyrin-based COF (**H_2P-Bph-COF**) which exhibit remarkable catalytic activity also toward the Suzuki-coupling reaction between bromoarenes and arylboronic acids under mild conditions with high yield of 97.1-98.5 %.[123] The COF was synthesized by reaction between 5,10,15,20-tetra(*p*-aminophenyl) porphyrine (**47**) and 4,4'-biphenyldialdehyde (**2**) under solvothermal reaction conditions. Due to the abundant and periodically distributed N atoms in this COF, it acts as good support to incorporate Pd ions in a very stable and uniformly disperse manner. Following the seminal approach toward the catalysis of Suzuki-Miyaura cross-coupling reactions, a variety of COFs based on Schiff-base chemistry has been used to catalyse different reactions. Thus, in 2014, Banerjee *et al* successfully immobilized not only Pd(II) complexes but also highly dispersed Pd(0) nanoparticles in a stable, crystalline and porous COF **TpPa-1**, obtained by reaction between *p*-phenylenediamine (**17a**) and 1,3,5-triformylphloroglucynol (**28**) (Scheme 6).[124] The successful incorporation of both Pd(0) nanoparticles and Pd(II) complex on the porous COF support was carried out at room temperature by a simple infiltration method.[47]

The most important aspect of these hybrids is their remarkable stability in water and under harsh conditions (e.g., strong basic or acidic conditions), which remains associated with the judicious selection of the **TpPa-1** framework enriched with nitrogen and oxygen atoms.

The COF skeleton imparted stability to the active metal centres and the strong interaction of loaded Pd(0) nanoparticles and Pd(II) complex with the nitrogen and oxygen atoms within the selected COF not only facilitates the catalysis in the absence of additional ligands but also provides extra strength. Thus, the described supported and highly dispersed Pd(0) nanoparticles exhibited excellent catalytic activity towards Cu free Sonogashira and Heck coupling reactions (Table 2) under basic conditions, and superior performance than the observed using commercially available Pd immobilized on activated charcoal. **Pd(0)@TpPa-1** catalyst was also efficient in one-pot sequential Heck/Sonogashira reactions. Moreover, the precursor Pd(II)-doped COF displayed competitive activity for the intramolecular oxidative bis-aryl synthesis under acidic conditions.

Other interesting carbon-carbon cross-coupling reaction which is receiving a lot of interest in recent years is the silicon-based cross-coupling reaction (Table 2).[130] In recent year, oxidation of organosilanes to fabricate silicon coupling reagents catalysed by transition metal has been rapidly developed.[131] This method was more green and facile over other conventional routes because the oxides in these reactions are water or alcohols and the only by-product is H_2Thus, Zhang *et al* have recently synthesized a novel COF material (**COF-SDU1**), containing both imine and triazine functional groups, by condensation reaction between *p*-phenylenediamine (**17a**) and nitrogen-rich triazine building block tri-(4-formacylphenoxy)-1,3,5-triazine (**33**).[132] This material can sturdily stabilize and regularly mono-disperse the palladium species due to the two dimensional eclipsed layer-sheet structure and nitrogen-rich content of to **COF-SDU1**. The **Pd(II)/COF-SDU1**, as a sustainable and green catalyst, exhibits excellent catalytic activity and selectivity towards the silicon-based one-pot cross-coupling reaction of silanes and aryl iodide. It is the first example of a COF derivative that combines the oxidation of silanes and the next cross coupling in a single catalytic system. In addition, the catalyst can be reused several times without obvious metal leaching, sintering behaviour and evident loss of catalytic activity.

COFs based on Schiff-base chemistry have been also used as catalysts in other important C-C bond-forming reactions in organic synthesis such as the Knoevenagel condensation reaction or the Michael nucleophilic addition reaction (Table 2). Interestingly, in these cases, it is not necessary additional metallic nanoparticles and the COF itself acts as the catalyst. Thus, in 2014 Yan *et al* reported the use of new 3D-microporous COFs as catalysts in Knoevenagel condensation reactions.[126] The new 3D microporous base functionalized COFs, termed **BF-COF1** and **BF-COF-2** were designed and synthesized by using a tetrahedral alkyl amine, 1,3,5,7- tetraaminoadamantane (**TAA**, **52**). As the aldehyde reaction partner, 1,3,5-triformylbenzene (**TFB**, **27**) or triformylphloroglucinol (**TFP**, **28**) were used to act as the planar triangular building unit. Condensation reactions between tetrahedral **TAA** (**52**) and triangular **TFB** (**27**) or **TFP** (**28**) give respectively **BF-COF1** and **BF-COF-2** as novel 3D porous functionalized COFs through imine-bond formation.

The catalytic properties of the **BF-COFs** were explored in the Knoevenagel condensation reaction, and both **BF-COFs** were shown to have excellent catalytic activity with high conversion (96% for **BF-COF-1** and 98% for **BF-COF-2**), highly efficient size selectivity, and good recyclability.

Nature's strategy of employing multistep cascade reaction for the synthesis of complex and bioactive organic molecules in living systems has been a source of inspiration for designing artificial catalysts. Most of the time, a multistep chemical process involves multisite catalysts. However, by performing the consecutive reaction steps in one pot, costly intermediate separations and purification processes will be avoided. Therefore, also from an energy savings point of view, the design of solid catalysts with well-defined multisites are of interest to achieve more-intensive chemical processes.[133] With this aim, in 2015, Banerjee *et al* have reported the use of a bifunctional COF with 2D organocatalytic micropores as catalysts for a cascade-type reaction that involves hydrolysis of a dimethylketal

followed by the reaction of the formed aldehyde with malononitrile trough a Knovenagel reaction (Table 2).[24]

The bifunctional COF used as the catalyst in cascade-type reactions, **2,3-DhaTph** (Figure 2), was synthesized by reversible Schiff-base reaction using 2,3-dihydroxyterephthalaldehyde (**3**) and a 5,10,15,20-tetrakis(4-aminophenyl)-21H,23H-porphirine unit (**47**) under solvothermal conditions. The **2,3-DhaTph COF** possesses separate antagonist catalytic sites in which catecholic –OH groups act as weak acidic sites, whereas porphyrin units and imine bonds act as basic sites, with high chemical stability in aqueous/acidic media along with high crystallinity and porosity. The catalytic activity of **2,3-DhaTph COF** toward acid–base catalysed one-pot cascade reactions[133] was analysed using a model reaction, wherein a number of substituted dimethyl acetal reactants reacts with malononitrile showing excellent conversion (80-96%). It is worth mentioning that the same reaction without the catalyst yielded less than 5 % of the products.

The pore surface engineering strategy has also revealed as an efficient tool for the construction of covalently linked and highly active organocatalytic COFs. Thus, Jiang *et al* have demonstrated this strategy by highlighting the controlled integration of organocatalytic sites into the pore walls of a fuctionalized COF to synthesize organocatalytic COFs that exhibit enhanced activity in asymmetric Michael addition reactions (Table 2) while retaining stereoselectivity.[127] A Michael addition is a typical organocatalytic reaction, is one of the basic C–C bond formation reactions and provides a powerful synthetic tool for the formation of synthons of many important natural and biologically active products.[134] For this purpose, it was used a mesoporous imine-linked porphyrin COF as a scaffold in which the porphyrin units are located at the vertices and the phenyl groups occupy the edges of tetragonal polygon frameworks.[28] The monomeric building blocks were functionalized such as they allow the synthesis of imine-linked COFs (COFs) bearing content-tuneable, accessible, and reactive ethynyl groups on the walls of one-dimensional pores edges (**[HC≡C]$_X$-H$_2$P-COFs**, X = 25, 50, 75, and 100 (X = 0: H$_2$P-COF), Scheme 11).[80] As it is shown in the previous section, these COFs have revealed as ideal platforms for pore-wall surface engineering aimed at anchoring diverse functional groups ranging from hydrophobic to hydrophilic units and from basic to acidic moieties with controllable loading contents. In this study, Jiang *et al* used the further click reaction of **[HC≡C]$_X$-H$_2$P-COFs** with pyrrolidine azide to quantitatively yield the corresponding **[Pyr]$_X$-H$_2$P-COFs** (Fig. 15). Pyrrolidine moieties were incorporated to the COFs as they are well-known organocatalysts for Michael addition reactions.[135] In comparison with the use of a small pyrrolidine derivative used as a control, it is shown that the organocatalytic COFs have significantly higher catalytic activity than the monomeric catalyst, while retaining the stereoselectivity. It is worth mentioning that the catalytic activity depends upon the density of the active sites on the pore walls. Highly dense pyrrolidine units in the pores cause a steric congestion and impede the mass transport through the channels.

The possibility of a continuous flow reaction using a columnar setup has been also tested by using a column consisting of a vertically mounted Teflon pipe loaded with silica gel at the bottom and **[Pyr]$_{25}$-H$_2$P-COF** atop the silica gel. It was found that the set up worked well at room temperature and yielded an optimal conversion when a solution of *trans*-4-chloro-β-nitrostyrene and propionaldehyde in a mixture of water–EtOH (1/1 v/v) was passed through at a flow rate of 18 μL min^{-1}. The column maintained a 100% conversion and its stereoselectivities (44% ee, 65/35 dr) for more than 48 h under flow conditions.[127]

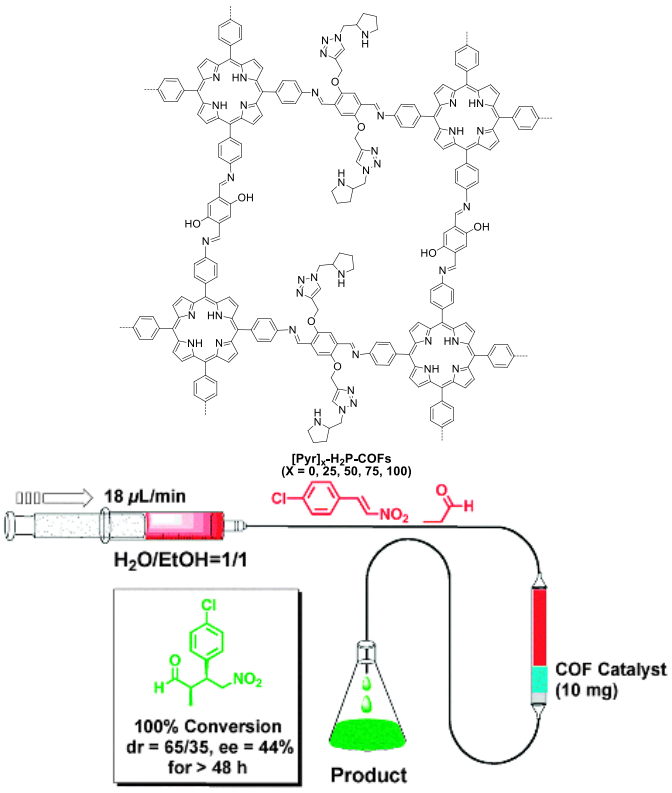

Fig. 15 Top: Schematic structure of pyrrolidine containing COFs **[Pyr]$_X$-H$_2$P-COFs**. **Bottom:** Representative chart for the flow reaction system based on the organocatalytic COF column fabricated with **[Pyr]$_{25}$-H$_2$P-COF**. Reproduced from Ref. [127] with permission from The Royal Society of Chemistry.

In 2015, Jiang *et al* converted achiral COF derivatives into chiral organocatalysts, with the high crystallinity and porosity retained, by appending chiral centres and catalytically active sites on its channel walls. The COFs thus prepared combine catalytic activity, enantioselectivity and recyclability and were shown to promote asymmetric C–C bond formation in water under ambient conditions.[29] For the synthesis of the novel structure developed, **[HC≡C]$_X$-TPB-DMTP-COF,** it was used a three component condensation system with 1,3,5-tris(4-aminophenyl)benzene (**TPB**, **36**), 2,5-bis(2-propynyloxy)terephthalaldehyde (**BPTA**, **7**) and 2,5-dimethoxyterephthalaldehyde (**DMTA**, **4**) as edge units. The **[HC≡C]$_X$-TPB-DMTP-COF**s were converted into chiral organocatalytic **[(S)-Py]$_x$-TPB-DMTP-COFs** ((S)-Py, (S)-pyrrolidine) in which chiral and catalytic (S)-Py sites were

anchored onto the channel walls through triazole rings formed quantitatively *via* click reaction in a random manner.

Typically, Michael reactions are conducted in organic solvents or in mixed organic–aqueous solutions; the use of neat water as a solvent is particularly attractive from the environmental and economic points of view. The high catalytic activity of **[(S)-Py]$_x$-TPB-DMTP-COFs** allows Michael reactions to be conducted in neat water at 25 °C and 1 bar. The insolubility of the **[(S)-Py]$_x$-TPB-DMTP-COFs** gives rise to heterogeneous systems that have outstanding catalytic activities.

The Michael reaction of cyclohexanone and β-nitrostyrene proceeds cleanly and smoothly and achieves 100 % conversion in 12 h with enantioselectivity (e.e.) and diastereoselectivity (d.r.) values of 92% and 90/10, respectively. When a molecular catalyst (S)-Py with the same catalytic structure is used as a control, a much longer reaction time of 22 h is required. Remarkably, **[(S)-Py]$_x$-TPB-DMTP-COFs** can be easily separated from the reaction mixture, and subsequently reused. Thus **[(S)-Py]$_{0.17}$-TPB-DMTP-COF** retained its activity, enantioselectivity and diastereoselectivity after five cycles.

Another important reaction which has been catalysed by COFs based on Schiff base chemistry is the Diels-Alder reaction (Table 2). The [4+2] cycloaddition reactions, known as Diels–Alder are some of the cornerstone transformations in modern organic chemistry and have been frequently used for the synthesis of biologically active compounds and natural products.[136] The COF used as catalytic beads for Diels-Alder reaction under ambient conditions was synthesized *via* condensation of 1,3,6,8-tetrakis(*p*-formylphenyl)pyrene (**42**) with 2,6-diaminoanthracene (**22**) under solvothermal conditions.[128] The π-electron rich COF (**Py-An COF**) is suited to create interactions between the pore walls and reagents suitable to form C–H···π interactions[137] thus promoting an accumulation of reactants within the pore walls reducing the entropy loss and activation energy of the reaction. Thus, to investigate the ability of **Py-An COF** to act as catalyst in Diels-Alder reaction, a variety of maleimide derivatives with different *N*-substituents, were used for the reaction with 9-hydroxymethylanthracene in neat water and under ambient conditions. In all cases, the **Py–An COF** catalysts significantly enhances the yields, compared to the controls without the COF catalyst and provides the highest catalytic activities among the heterogeneous catalysts reported to date, which work at elevated temperatures.[136]

COFs based on Schiff-base chemistry have been also used as catalysts in oxidation and reductions. Thus, Jia *et al* have reported an approach to obtain a COF-based catalyst for epoxidation reactions.[129] In this contribution a 3D structure COF material, named **COF-300**[10] was used as support to immobilize 12-phosphomolybdic acid (PMA) for getting novel hybrid PMA-based solid catalysts (**PMA@COF-300**). **COF-300** was obtained by reaction between terephthaldehyde (**1**) and tetra-(4-anilyl)-methane (**51**) under solvothermal conditions and the supported **PMA@COF-300** composites were prepared by wetness impregnation method. Different composites were prepared by changing the contents of PMA and the preparation temperatures. The catalytic properties of the **PMA@COF-300** composites were investigated in the epoxidation of cyclooctene, 1-octene and cyclododecene with t-BuOOH as oxidant. The studies show that the **PMA@COF-300** composites are all active and selective catalysts for the epoxidation of olefins. However, the catalytic activity is slightly lower than that of homogeneous PMA used for comparison purposes.

Jiang *et al* have developed an alternative and more efficient approach for the preparation of COF-based catalysts for epoxidation of olefins (Table 2). They have developed a bottom-up approach to engineer a molybdenum-doped covalent organic framework, henceforth denoted as **Mo-COF**, catalytic for selective oxidation reaction.[82] The synthetic strategy can be divided in two steps starting with the synthesis of the crystalline COF by reaction between 1,3,5-triformylphloroglucinol (**28**) and 1,4-dicarbonyl-phenyl-dihydrazide (**14**) under solvothermal conditions. The second step involves the introduction of a Mo resource into the porous network by treatment of a methanolic mixture of the COF with $MoO_2(acac)_2$ under reflux (Scheme 12). By means of this strategy, an efficient π-connected organomolybdenum catalyst with a high active site density (2.0 mmol g^{-1}) was successfully constructed. XPS studies indicate the strong coordination of Mo with the benzoyl salicylal hydrazine groups of COF; this group further withdrew electrons from Mo, which made the Mo species more electron-deficient.

To show that **Mo-COF** was catalytically active, the performance of **Mo-COF** as a nanochannel-reactor was evaluated in the context of the epoxidation of different olefin substrates of various molecular sizes using *tert*-butyl hydroperoxide (**TBHP**) as an oxidant. As a representative example, cyclohexane gave 99 % conversion and 71 % selectivity after 6 h which significantly improves the result of the same reaction when using homogeneous $Mo(HSY)_2$ as catalyst 29 % conversion and 68 % epoxidized selectivity). Upon the completion of the reaction, the catalyst could be easily recovered in almost quantitative yield by simple filtration and could be used repeatedly without significant degradation of the catalytic performance after four cycles.

Concerning with reduction reactions, COFs with gold[Au(0)] nanoparticles immobilized (**Au(0)@TpPa-1**) have shown superior catalytic activity for 4-nitrophenol (**4-NPh**) reduction to afford 4-aminophenol (**4-APh**).[84] Since 4-aminophenol is important due to its usage as a developer in black and white films and as an intermediate for the synthesis of drug paracetamol, for its synthesis a catalytic system with high associated product yield, selectivity and recyclability is desirable. **TpPa-1** (Scheme 6) was obtained by reaction between 1,3,5-triformylphloroglucinol (**28**) and *p*-phenylenediamine (**17a**) and the **Au(0)@TpPa-1** catalyst was synthesized by mixing $HAuCl_4{\cdot}3H_2O$ with evacuated **TpPa-1** in methanol under vigorous stirring. An uniform loading of 5 ± 3 nm sized Au nanoparticles on the **TpPa-1** matrix was observed under these conditions. The as-synthesised **Au(0)@TpPa-1** were tested for the catalytic reduction of 4-NPh in the presence of excess $NaBH_4$ in water as the solvent. The best performance was obtained when 1.2 wt% Au loaded **Au(0)@TpPa-1** catalyst was used as the catalyst, for which conversion of 4-NPh to 4-APh was completed within 13 min. The reaction did not occur when using only **TpPa-1** as the catalyst and proceeded

comparatively slower with $HAuCl_4 \cdot 3H_2O$ (conversion time: 20 min).

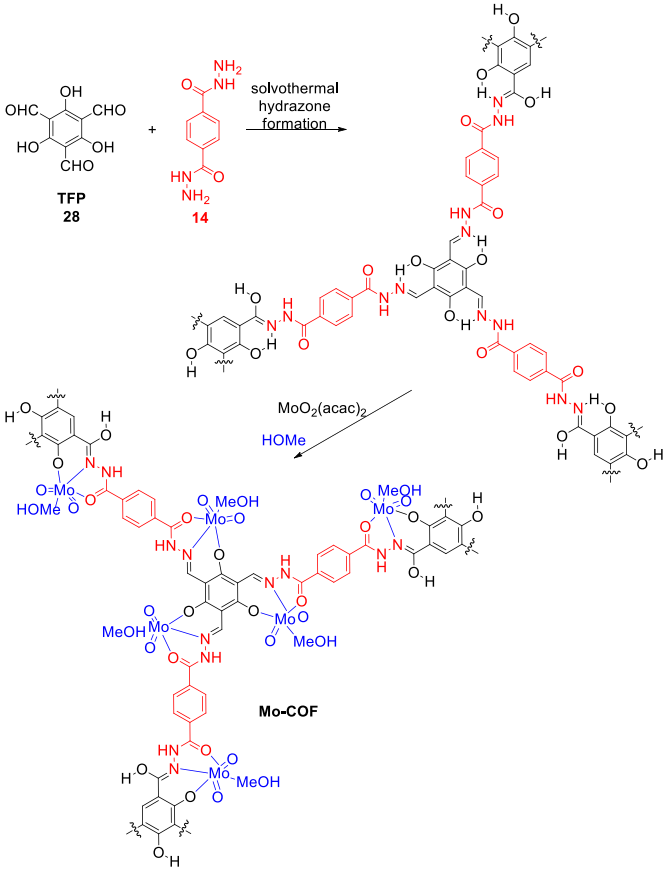

Scheme 12 Formation of the molecular building blocks of **Mo-COF**.

The probable reason of the momentous activity shown by **Au(0)@TpPa-1** may be the fine distribution of very tiny nanoparticles on the **TpPa-1** matrix, which lead to a very large surface area of the nanoparticles and high particle number per unit mass for the catalyst. The increased fraction of the atoms at the surface in **Au(0)@TpPa-1** leads to a significantly higher catalytic activity. Furthermore, the overall recyclability with almost unchanged reactivity for more than 6 cycles shown by the reported catalyst is promising towards the heterogenization of Au catalysts for commercially important transformation reactions.

3.4.2 Photocatalyst

Currently, a number of photocatalysts based on highly porous materials, such as MOFs,[138] carbon nitride sheets,[139] and polymers are employed as photosensitizers and support for the loading of active nanoparticles resulting in an improved catalytic activity. However, most of these materials show limited performance owing to the poor water stability, as in the case of MOFs and carbon nitride sheets, and poor crystallinity as in the case of polymers, which affects their photocatalytic activity.

As we have already seen, the remarkable stability in both acidic and basic mediums along with high surface area and porosity of several COFs based in Schiff-base chemistry together with their crystalline nature with high surface area and porosity make them an attractive support matrix for the loading of nanoparticles. Moreover, the 2D crystalline nature of some of these COFs is reported to enhance the charge mobility on its surface owing to the presence of π arrays in comparison to the 1D or 3D polymers.[140] Thus, Kurungot, Banerjee *et al* have employed a highly stable COF (**TpPa-2**, Scheme 6) as a support matrix for anchoring CdS nanoparticles and used these CdS@COF hybrids for photocatalytic H_2 production.[83] **TpPa-2** can be obtained by reaction between 1,3,5-triformylphloroglucinol (**28**) and 2,5-dimethylbenzene-1,4-diamine (**17b**) under solvothermal conditions. The **CdS@COF** hybrid was subsequently obtained by hydrothermal synthesis of CdS nanoparticles on the COF matrix (Fig. 16).

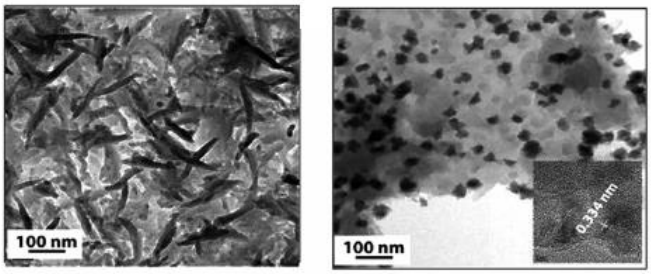

Fig. 16 TEM images of COF (left) and CdS-COF (90:10) hybrid (right); Inset: lattice fringes of CdS nanoparticles in CdS-COF (90:10) hybrid. Taken from ref. [83]. Reprinted with permission of Wiley-VCH.

To examine the photocatalytic behaviour of the **CdS@COF** hybrids, visible-light-driven H_2 evolution experiments were carried out using 0.5 wt% Pt as a co-catalyst, lactic acid as the sacrificial agent, and a 400 W xenon arc lamp with a UV cut-off filter ($\lambda \geq 420$ nm) as a visible light source. Under visible-light illumination, the as-synthesized bulk CdS showed a photocatalytic hydrogen production of 128 $\mu molh^{-1}g^{-1}$. Remarkably, upon addition of just 1 wt% of COF, a dramatic increase in the H_2 production with 1320 $\mu molh^{-1}g^{-1}$ was observed, which is about ten times higher than that of the bulk CdS. Furthermore, **CdS@COF** (90:10) was found to display the photocatalytic activity with 3678 $\mu molh^{-1}g^{-1}$ of H_2 production. The control experiments under dark conditions showed negligible H_2 production, which unambiguously confirmed that, the catalytic activity of the hybrid materials is triggered by light. The presence of a π-conjugated backbone, high surface area, and occurrence of abundant 2D hetero-interface highlight the usage of this COF as an effective support for stabilizing the generated photoelectrons, thereby resulting in an efficient and high photocatalytic activity. In addition, the TEM study confirmed that the **CdS@COF** hybrid is stable up to three consecutive cycles with CdS nanoparticles still dispersed on the COF matrix.

Lotsch *et al* have recently shown that a triphenylarene platform can readily be tuned for photocatalytic water reduction as a direct consequence of molecular engineering. Thus, they have reported triazine-based COF photocatalysts active for visible light induced hydrogen evolution.[40, 44] Triazine-based molecules

offer high electron mobilities, an electron withdrawing character and are hence widely used in synthetic chemistry and optoelectronics.[141] A progressive substitution of alternate carbons in the central aryl ring of the triphenylaryl platform (Fig. 17, green dots) by nitrogen atoms leads to a change in the electronic and steric properties of the central ring, that is, N = 0 (phenyl), N = 1 (pyridyl), N = 2 (pyrimidyl) and N = 3 (triazine). The substitution of the C–H moiety with nitrogen atoms produces a change in dihedral angle between the central aryl ring and the peripheral phenyl rings, which in turn leads to varied degrees of planarity in the platform. In addition, this results in a progressive decrease in electron density in the central aryl ring of the COF platform as the number of nitrogen atoms increase from 0 to 3. Thus, the synthesis of N_x–COFs (x =0, 1, 2 and 3) was carried out by an azine formation reaction of suitable aldehydes with hydrazine and the consequent influence on photocatalytic hydrogen production was explored.

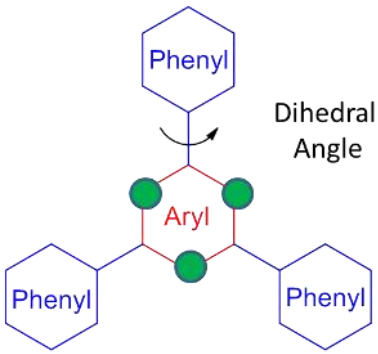

Fig. 17 A tunable triphenylarene platform for photocatalytic hydrogen evolution. Replacement of 'C–H' by 'nitrogen atoms' at the green dots changes the angle between central aryl and peripheral phenyl rings, which leads to varied planarity in the platform.

The hydrogen evolution experiments were performed by taking a suspension of the COFs in phosphate-buffered saline (PBS) at pH 7 and irradiating with visible light (≥420 nm) at 25 °C. Hexachloroplatinic acid was added for the *in situ* formation of the platinum (Pt) co-catalyst[142] to reduce the over-potential for hydrogen evolution, and triethanolamine (TEoA) was used as sacrificial electron donor.[98] All COFs evolve hydrogen in the test period of 8 h. Interestingly, though the N_x–COFs show about fourfold increase in hydrogen evolution with each substitution of C–H by N in the central aryl ring of the COF platform. Thus, at the end of 8 h the average amount of hydrogen produced by N_0, N_1, N_2 and N_3–COF was 23, 90, 438 and 1703 $\mu molh^{-1}g^{-1}$, respectively.

Theoretical calculations indicate an increase in stabilization of the radical anions in the most nitrogen-rich COFs which nicely correlates with the observed trend in hydrogen production. The stabilization of the anion radical likely enhances the charge separation, thereby increasing the probability of successful electron migration to a nearby Pt co-catalyst. The relevance of the anion radical for hydrogen evolution likewise shifts the focus to the sacrificial electron donor, whose interaction with the COF likely determines how quickly the hole can be quenched. Therefore, these results suggest that tuning the interfacial interactions between the COF and the electron donor may be a promising route to optimize the hydrogen evolution efficiencies further in such systems.

The amount of hydrogen evolved from the most active N_3–COF is competitive with carbon nitride photocatalysts and outperforms benchmark systems such as Pt-modified amorphous melon (720 $\mu molh^{-1}g^{-1}$)[139], g–C_3N_4 (840 $\mu molh^{-1}g^{-1}$)[143] or crystalline poly(triazine imide) (864 $\mu molh^{-1}g^{-1}$)[139]. This work demonstrates the potential of organic materials in solar energy conversion where a vast array of organic building blocks and bond-forming reactions provide an extensive toolbox for the systematic fine-tuning of their structural and physical properties thus making way for the application of COFs in photocatalytic water splitting.

The study of singlet molecular oxygen production and reactivity has emerged as a rich and diverse area with implications in fields ranging from polymer science to cancer therapy.[144] In this respect, Jiang *et al* have investigated the photocatalytic activity of COF derivatives for singlet oxygen generation.[23] With this aim, they synthesize a family of porphyrine-based 2D-COFs locked with intralayer hydrogen-bonding (H-bonding) interactions. The H-bonding interaction sites were located on the edge units of the imine-linked tetragonal copper porphyrin COF. For comparison purposes, analogous polymers were synthesized without H-bonding sites exhibiting an amorphous structure. The copper porphyrine based 2D-COF (**CuP-DHPh COF**, Fig. 18) with H-bonds was synthesized by reaction between dihydroxyterephthalaldehyde (**DHTA**, **3**) and the 5,10,15,20-tetrakis(4'-tetraphenylamino) porphyrin derivative (**CuP**, **48, M = Cu**). On the other hand, the amorphous polymer analogue (**CuP-Ph**, Fig. 18) was obtained by reaction between terephthaladehyde (**1**) and the 5,10,15,20-tetrakis(4'-tetraphenylamino) porphyrin derivative (CuP, **48, M = Cu**). The intralayer H-bonding interactions suppress the torsion of the edge units and lock the tetragonal sheets in a planar conformation. This planarization enhances the interlayer interactions and triggers extended π-cloud delocalization over the 2D sheets. Upon AA stacking, the resulting COFs with layered 2D sheets amplify these effects and strongly affect the physical properties of the material, including improving their crystallinity, enhancing their porosity, increasing their light-harvesting capability, reducing their band gap, and enhancing their photocatalytic activity toward the generation of singlet oxygen.

Thus, the photocatalytic activity of the COFs was examined by using 1,3-diphenylisobenzofuran (**DPBF**) as a label for the singlet oxygen generation monitored by time-dependent electronic absorption spectroscopy.[145] Indeed, the visible light irradiation of an oxygen-saturated DMF solution of **DPBF** in the presence of the **CuP-DHPh COF** triggered a steady conversion of molecular oxygen into singlet oxygen, as evidenced by the spectral change of DPBF, with clear isosbestic points. The **CuP-DHPh COF** is exceptionally active as a photocatalyst exhibiting a 10-20-fold enhancement in activity compared with those of other CuP derivatives. Control experiments carried out with the monomeric CuTPP as well as with the amorphous **CuP-Ph**

polymer without H-bonding sites on the edges exhibited low rate of reaction, thus demonstrating the remarkable effect of the supramolecular interactions in the structure of the material as well as in their physical properties.

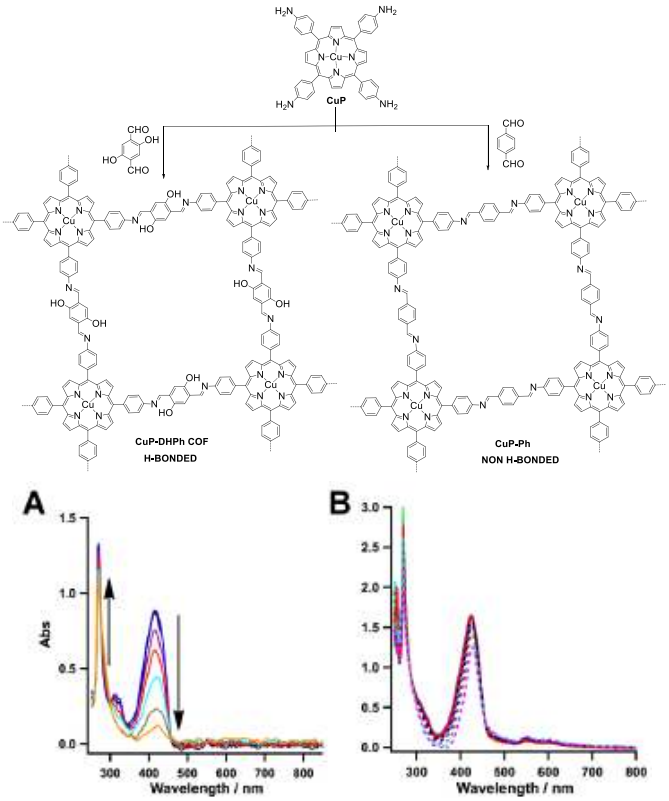

Fig. 18 Top: Chemical structure of the H-bonded **CuP-DHPh COF** and the non H-bonded amorphous **CuP-Ph**. **Bottom:** Absorption spectral changes of DPBF in the presence of a) the **CuP-DHPh COF** and b) the amorphous **CuP-Ph Polymer**, in an oxygen saturated DMF solution upon irradiation at 500 nm. Adapted with permission from *J. Am. Chem. Soc.* 2015, 137, 3241-3247. Copyright (2015) American Chemical Society.

3.4.3 Electrocatalyst

Mao *et al* have recently reported an approach to involve COF based materials in electrocatalysis.[146] They have demonstrated that cobalt-porphyrine-based COFs can be used as a new kind of Co,N-containing precursor to produce Co/N/C catalysts for oxygen reduction reaction (**ORR**). After the formation of the cobalt-porphyrine-based COFs, it is subsequently pyrolyzed under nitrogen atmosphere at 900 °C, resulting in the formation of a nanomaterial that exhibits an excellent electrocatalytic performance toward **ORR** in alkaline media, which is much comparable to the commercial 20% Pt/C catalyst. After pyrolysis at 900 °C, the characteristic diffraction peaks of the COF disappear with the generation of several new peaks in the PXRD pattern. Analysis of the new peaks suggests the formation of graphitic carbons upon pyrolysis. And the mechanism for the **ORR** catalysis remains unclear.

More interestingly, COF derivatives have been recently reported to act as catalysts for electrochemical reduction of CO_2. The sustainable reductive transformation of CO_2 to a value-added carbon product such as carbon monoxide (CO) receives currently broad interest as a consequence of the global energy demands and climate change. In this respect, electrolytic approaches benefit from using water as the reaction medium, as it is a cheap, abundant, and environmentally benign solvent that facilitates proton and electron transfer.[147] The charge carrier mobility of some COF derivatives (see below) derived from π-conjugation and π- π stacking, combined with their good thermal and chemical stability have prompted Yaghi, Chang *et al* to consider COF derivatives as suitable tuneable materials to be used as heterogeneous catalysts for electrochemical reduction.[125] They have shown that incorporation of catalytic cobalt porphyrin units into COFs, gives highly active, stable, and selective catalysts for electrochemical reduction of carbon dioxide to carbon monoxide in water. The model framework (**COF-366-Co**) was synthesized by the imine condensation of 5,10,15,20-tetrakis(4-aminophenyl)porphinato]cobalt [**Co(TAP)**, **48, M = Co**] with terephthaldehyde (**1**). For electrochemical experiments, the activated microcrystalline COF powders were deposited on porous, conductive carbon fabric. In controlled potential electrolyses performed in carbon dioxide–saturated aqueous bicarbonate buffer (pH = 7.3) under applied potentials between –0.57 and –0.97 V (*vs.* RHE), carbon monoxide was the major reduction product. Thus, at –0.67 V, **COF-366-Co** promoted carbon monoxide evolution at an initial current density of 5 mA per milligram of catalyst (*ca*. 80 mA per milligram of cobalt), with high selectivity over competing proton reduction [Faradaic efficiency for carbon monoxide (FECO) = 90 %]. The catalytic activity of the COF could be preserved for 24 h, accumulating more than 36 mL of carbon monoxide. To enhance this type of carbon dioxide catalyst platform, the synthesis of expanded derivatives with large pore size and the introduction of building block heterogeneity through a multivariate strategy[148] have been addressed providing different heterogeneous systems that promote carbon dioxide reduction to carbon monoxide with remarkably high activity and selectivity.[125]

The contributions reviewed in this section show that in comparison with other crystalline porous materials, the unique structure of these COFs provide efficient access to the catalytic sites and fast mass-transport of the reactant/products, thus providing good catalytic activities. It can be expected that the approaches outlined above will boost the research on employing COF materials for catalysis.

3. 5 Electrical conductivity and charge carrier mobility in COFs

Many organic compounds can efficiently be produced and processed on a large scale and can be easily modified by the versatile tools of organic chemistry.[85, 86] The ability to design the desired material on a molecular basis permits fine tuning of the energy gap and HOMO/LUMO levels of the semiconductor. However, important issues still need to be addressed for the fabrication of competitive electronic devices. For example, the devices often exhibit low stability and efficiencies that are lower than expected. The latter is often caused by low charge carrier mobilities and recombination, due to inefficient stacking of the conducting polymers or due to insufficient and disordered donor–acceptor interfaces.[149] Therefore it would be desirable

to have synthetic access to conducting materials with total control over their nanoscale structure and orientation.

By virtue of their three-dimensional orderings at the atomic scale, 2D-COFs have shown a great potential to perform core functions in organic electronics such as light emission,[2] charge transfer and separation,[103, 150] and semiconduction.[151, 152] However, typical COFs lack intra-sheet π-conjugation and chemical stability, which significantly limit their practical utility. To address this shortcoming, a chemically stable yet fully π-conjugated COF is highly desirable. Such a framework with three-dimensionally ordered chain alignment may provide a solution for the long-standing daunting challenges in semiconducting polymer technology.[153, 154] A conjugated polymer that combines permanent porosity and structural 3D ordering such as 2D-COFs is a suitable material to address these challenges.

While boronic acid condensation has been extensively used for the synthesis of COFs, such COFs do not possess in-plane conjugation. For incorporation into standard back-gate geometry field-effect transistors (FETs, the cornerstone device of organic-based electronics, commonly used to probe the electronic characteristics of new semiconducting materials),[155, 156] charge transport must occur in the plane of the film. Hence, while boronate ester-type COFs can possess out-of-plane charge transport properties,[2, 157] they would still have to assume an edge-on orientation with respect to the substrate to yield operational FETs, a configuration presenting considerable practical difficulty. Thus, a processable 2D material capable of in-plane charge transport could contribute both to the fabrication of nanoscale devices for practical applications and to furthering our understanding of the fundamental physics of 2D semiconducting materials. In this respect, COFs based on Schiff-base chemistry offer the possibility to develop fully conjugated 2D crystalline networks.

With this aim, in 2011, Yaghi *et al* reported the first charge carrier mobility study on imino-based 2D-COFs.[152] This COF (**COF-366**) was synthesized by reaction between tetra(*p*-aminophenyl)porphyrine (**47**) and *p*-phenylenediamine (**17a**) under solvothermal conditions. It has a BET surface area of 735 m^2g^{-1}, pore volume of 0.32 cm^3g^{-1} and pore size distributions of 17.6 Å. The electrical conductivity of **COF-366** across a gap of 2 µm between two Au electrodes was determined. It displayed almost linear I-V profiles in air at 25 °C and, for example, at 0.2 V bias voltage, the electric current of **COF-366** is 0.75 nA which proves that this COF is in fact conductive. In addition, the Time–of-flight (TOF) transient current integration measurements performed on 1.5-µm thick **COF-366** /poly(methylmethacrylate) films (60/40 in wt%) between Al and indium tin oxide electrodes reveal hole conduction. It transpires that **COF-366** is a *p*-type semiconductor with one-dimensional hole mobility (Σµ) of 8.1 $cm^2\ V^{-1}s^{-1}$. This mobility is extraordinarily high with the value being greater than that of inorganic amorphous silicon (~1 $cm^2\ V^{-1}s^{-1}$), and much higher than those of common conjugated polymers and highly ordered crystalline organic semiconductors.[15]

Different research groups have used the important electroactive TTF building block[158] as basic unit for the synthesis of semiconducting COFs. Thus, in 2014 Zhang, Liu *et al* synthesized the so-called **TTF-COF** by reaction between tetrathiafulvalene-tetrabenzaldehyde (**43**) and *p*-phenylenediamine (**17a**) under solvothermal conditions (Fig. 19). Thin films of **TTF-COF** with nominal thickness around 150 nm can be grown *in situ* from the liquid phase on Si/SiO_2 substrates and transparent ITO-coated glass.

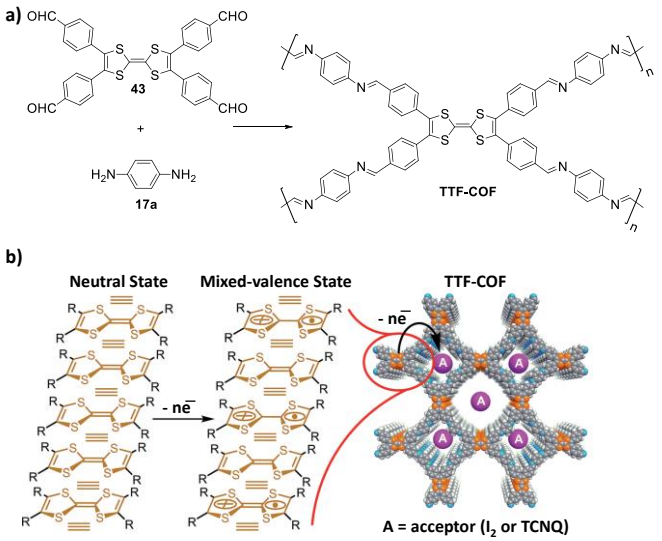

Fig. 19 a) Synthesis of **TTF-COF**. b) Illustration of the mixed-valence state in TTF-COF. The "≡" indicates inter-TTF-layer interactions. Reproduced from ref. [159] with permission from the Royal Society of Chemistry.

Grazing incidence wide angle X-ray scattering (GIWAXS) of the thin films indicates their polycrystalline nature with preferential orientation of the columns normal to the substrate. A conductivity of 1.2 x 10^{-6} S cm^{-1} was determined for these films. Exposure of the thin film to I_2 vapour in a closed chamber results in significant increase of electrical conductivity which reaches a maximum of 2.8 x 10^{-3} S cm^{-1}. This is due to the ability of TTF to form highly conductive charge-transfer salts with electron acceptors such as I_2 or tetracyanoquinodimethane (TCNQ) and the presence of open nanochannels within the 2D-COF that allow the incorporation of molecular dopants as a charge transfer partner (Fig. 19).[159] The conductivity changes are correlated with diagnostic signatures in UV-vis-NIR and EPR spectra, pointing to effective radical delocalization within mixed-valence TTF stacks. Thus, electron paramagnetic resonance (EPR) studies of the solid compounds further confirmed the effectiveness of chemical doping. A weak signal in the EPR spectrum of the pristine **TTF-COF** indicates the presence of very small amount of paramagnetic TTF^+, which corresponds to weakly doped TTF in as synthesized COF.

In 2014, Wang, Zhang *et al* reported the synthesis of **TTF-COF** by using the same starting materials.[161] In this work, cyclic voltammetry (CV) was used to investigate the electrochemical behaviour of **TTF-COF**. As **TTF-COF** is insoluble in common organic solvents, the working electrode for CV measurements has to be modified. With this purpose, **TTF-COF** and carbon black were grounded in an agate mortar, pestle, and the ground powder is then sonicated in CH_2Cl_2. Then the electrode was

prepared by drop-casting the CH_2Cl_2 suspension onto the tip of the Pt working electrode. With this setup it is possible to obtain a typical surface confined voltammetric profile with two reversible redox processes at 0.69 and 1.07 V, indicating the electron-donating character of **TTF-COF**. In this case, a maximum conductivity of 1.8 x 10^{-6} Scm^{-1} was obtained for **TTF-COF** after doping with iodine. Furthermore, the temperature dependence of the resistance in the range 0 to 40 °C reveals the semiconductor-like behaviour of **TTF-COF** after doping with iodine.

Jiang *et al* reported the synthesis also of **TTF-COF** from the same starting materials and, additionally, synthesized a new TTF-based COF (**TTF-Py-COF**) by reacting tetrathiafulvalene-tetrabenzaldehyde (**43**) and 2,3,6,7-tetra(4-aminophenyl)pyrene (**49**) under solvothermal conditions.[162]

Both TTF-based COFs constitute periodic TTF columns and ordered porous channels.**TTF-COF** has an interlayer distance of 3.71 Å for a slipped AA stacking mode, whereas **TTF-Py-COF** adopts a longer distance of 3.87 Å. Meanwhile, **TTF-COF** assumes an almost planar sheet conformation, whereas **TTF-Py-COF** displays a distorted conformation. These differences in layered structures originate from the difference of linkers between TTF units in the COFs. The phenyl linker in **TTF-COF** has a planar conformation, while the paddle shaped tetraphenylpyrene linker distorts the layer from a planar conformation and expands the interlayer distance. Interestingly, the charge carrier mobility of the COFs with periodically aligned TTF columns, was determined by using the electrodeless flash-photolysis time-resolved microwave conductivity (FP-TRMC) method providing values of 0.2 and 0.08 cm^2V^{-1} s^{-1} for **TTF-COF** and **TTF-Py-COF**, respectively. The high carrier mobility observed for **TTF-COF** is likely related to its tighter stacking layer structure, as was revealed by the crystalline structure. The mobilities of these TTF-based COFs are rather high, in comparison with the crystals of TTF derivatives that have mobilities of 10^{-5} to 1 cm^2V^{-1} s^{-1} with a majority under 10^{-2} cm^2V^{-1} s^{-1}.[163]

On the other hand, conductivity measurements were also performed for doped films of these TTF-based COFs showing values of 10^{-5} and 10^{-6} Scm^{-1} for **TTF-COF** and **TTF-Py-COF**, respectively. This study allows to conclude that the linker unit play an important role in perturbing the layered lattice and thus the conductivity. These results provide a step towards organic metals with pre-designable lattice architectures.

In 2015, Bao *et al* demonstrated the synthesis and device incorporation of a processable, in-plane conjugated 2D polymer (polyTB) that can be formed as a thin film over large areas.[76] Reacting triamine **tapa** (**39**) and dialdehyde **bdta** (**11**) in a covered petri dish for 2 days in ambient conditions yields a highly reflective red film at the solution/air interface (Fig. 20) which can be picked up from the surface of the solution. Film thickness can be controlled by isolating films at different stages of growth; longer incubation times led to thicker films. This simple method for forming nanometer-thin, large area films enabled the use of this material as semiconductor active layer in thin-film FETs with average mobilities of 3.0 x 10^{-6} $cm^2V^{-1}s^{-1}$.

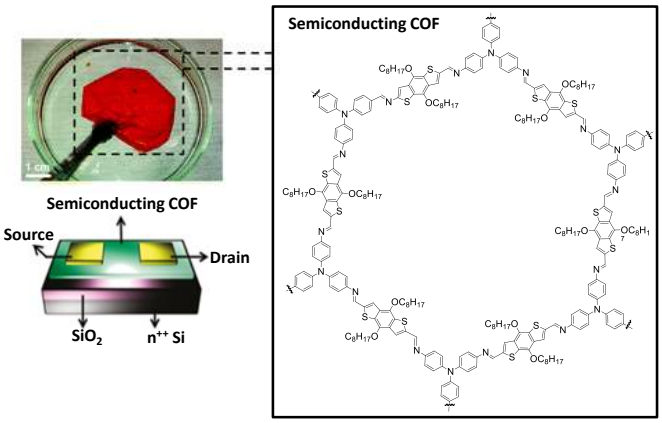

Fig. 20 Chemical structure of **PolyTB** and picture of the highly reflective red film formed at the solution/air interface which can be used as semiconductor active layer in thin-film FETs. Adapted from ref. [76].

The relatively low mobility of these COF-based transistors may be attributable to defects in the thin film, suggesting that improvements in both chemistry and film preparation are needed to yield higher mobility devices. The use of more planar branching monomers in place of **tapa** (**39**) will probably lead to larger crystalline domains with fewer electronic defects.

In 2013, Jiang *et al* reported the synthesis and study of a conjugated organic framework with three-dimensionally ordered stable structure and delocalized π-clouds (**CS-COF,** Scheme 7).[50] The pyrazine system consists of a six-membered D2h ring with two nitrogen atoms facing each other. The *tert*-butyl side groups in **PT** (**44**) were employed for enhancing the solubility of monomer. The crystalline structure determined for **CS-COF** corresponds to a slipped AA-stacking mode and remained intact in organic solvents, such as methanol, benzene, $CHCl_3$ and hexane, irrespective of their polarity, in addition to aqueous HCl and NaOH solutions (1 M). The preference for this AA-stacking mode is reasonable because the eclipsed stacking structure would cause the clash of *tert*-butyl groups between neighbouring layers.

In order to evaluate the potential electronic applications of this COF the energy of the HOMO and LUMO orbitals were calculated with the self-consistent charge DFTB method showing the following values -5.70 and -3.69 eV, respectively. On the other hand, the inherent charge carrier mobility of **CS-COF** was determined using the flash photolysis time-resolved microwave conductivity method showing that **CS-COF** is a high-rate hole-conducting framework with exceptional mobility of 4.2 $cm^2V^{-1}s^{-1}$, which is ranked among the top-class hole transporting organic semiconductors.[152, 164] Interestingly, CS-COF allows for complementary functionalization using the microporous space to crystallize counterpart fullerene molecules that can merge extended π conjugation with bi-continuous order into a donor–acceptor system (**CS-COF⊃C_{60}**, Fig. 21).[50] Because of the slipped AA stacking and the presence of bulky *tert*-butyl groups on the walls, the nanochannels accommodate only one C_{60} molecule in the cross-section. The presence of C_{60} in the pores of CS-COF is revealed by the drastic decrease in nitrogen gas sorption. Strong diffraction peaks in the XRD pattern assignable to C_{60} indicates that the C_{60}

molecules are crystallized in **CS-COF**. The C_{60} content in **CS-COF⊃C$_{60}$** is *ca*. 25 wt% as revealed by both elemental and thermal gravimetric, suggesting a peapod-like encapsulation of C_{60} molecules in the pores (Fig. 21). The possibility of using **CS-COF⊃C$_{60}$** as an active layer for photoenergy conversion was also investigated. The organic semiconductor [6,6]-phenyl-C_{61}-butyric acid methyl ester (PCBM) was used as a glue to fabricate 1 x 1 cm^2 indium tin oxide (ITO)/active layer/Al cells using spin-coated **CS-COF⊃C$_{60}$** films. The thickness of the active layer was adjusted to *ca*. 100 nm. On illumination under air mass 1.5 conditions, the thin film cells showed a power conversion efficiency of 0.9 %. The large open-circuit voltage of 0.98 V is remarkable and originates from the low HOMO level of **CS-COF**. Considering that the COF platelets are not unidirectionally oriented in the cell, resulting in boundaries between grains, which interfere with the carrier transport to the electrodes, there is still room for a significant improvement in the photoenergy conversion once these type of COFs can be obtained as large-area-oriented thin films.[165]

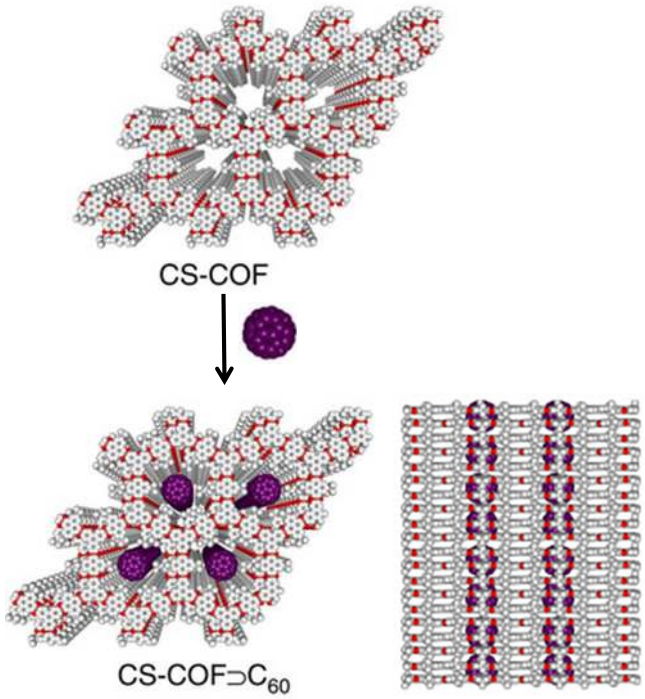

Fig. 21 Scheme of the synthesis of **CS-COF⊃C$_{60}$** by sublimed crystallization of fullerenes in the open one-dimensional channels (white: carbon; red: nitrogen; purple: fullerene). A side view of **CS-COF⊃C$_{60}$** is also shown. Reprinted by permission from Macmillan Publishers Ltd: *Nature Communications* 2013, 4, 2736, copyright (2013).

More recently, Oh *et al* have also used pyrazine linkers to obtain a layered network structure that possesses evenly distributed holes and nitrogen atoms and a C_2N stoichiometry in its basal plane (**C$_2$N-*h*2D**, Fig. 7).[57] This COF has uniform periodic holes in a fused aromatic network structure and resemble what can be called a "holey graphene" in which the benzene rings are bridged by pyrazine rings. The unique N-containing holey 2D crystal was simply synthesized by the reaction between hexaaminobenzene (**HAB**, **57**) trihydrochloride and hexaketocyclohexane (**HKH**, **58**) octahydrate in *N*-methyl-2-pyrrolidone (NMP) in the presence of a few drops of acid which are the classical conditions for the synthesis of the versatile hexaazatriphenylene (HAT) moiety.[166] The remarkable potential energy gain by aromatization (*ca*. 89.7 kcal $Umol^{-1}$, calculated using DFT) is responsible for the spontaneous polycondensation between the **HAB** and **HKH** and leads to the formation of a layered crystalline 2D network structure. First-principles DFT calculations were used to investigate the electronic structure of **C$_2$N-*h*2D**. The magnitude of the bandgap and the existence of flat bands near the Fermi levels suggest that the **C$_2$N-*h*2D** is completely different compared with other more widely studied 2D materials. Therefore, this material can offer complementary features to graphene, which has a vanishing bandgap (that is a conductor) and hexagonal boron nitride (h-BN), which has a wide bandgap (that is an insulator). To illustrate its electrical properties, FETs were fabricated using **C$_2$N-*h*2D** as the active layer showing ambipolar charge transport with an electron mobility of 13.5 $cm^2V^{-1}s^{-1}$ and a hole mobility of 20.6 $cm^2V^{-1}s^{-1}$. The semimetallic behaviour is attributed to the unintentional doping effects by the trapped impurities and/or adsorbed gases in the holey **C$_2$N-*h*2D** crystal structure, thereby suggesting that the electronic properties of the **C$_2$N-*h*2D** crystal are tuneable. Thus, it is worth pointing out that, in comparison with the many known difficulties involved in the synthesis of graphene and *h*-BN, the synthesis of **C$_2$N-*h*2D** provides a simple and highly efficient method for the formation of a fused aromatic 2D network structure. The combination of the successful synthesis using a simple and powerful conceptual wet-chemistry-based bottom-up together with the versatility of organic synthesis may open a new chapter in the cost-effective generation of other 2D materials with tuneable properties, which will be a flourishing new area of research.

3. 6 COFs for energy storage

The development of clean and renewable energy storage materials as well as their devices is a field of research of enormous current interest.[167] Among various energy storage devices, rechargeable batteries and electrochemical capacitors (ECs) are regarded typically as a suitable choice to store energy by transforming chemical energy into electrical energy. Electrochemical capacitors, also called supercapacitors, are promising candidates for alternative electrical energy storage devices due to their high power density, exceptional cycle life, and low maintenance cost.[168]

The unique ability of COFs to offer uniform nanometer scale pores and predictive design criteria to organize functional building blocks has been also used to access microporous electrodes for energy storage and conversion devices including electrochemical capacitors. For many years, the use of COFs in electrochemical devices was hampered by the poor hydrolytic and oxidative stability of boronate ester-linked frameworks that dominated the early COF literature. In 2013, Dichtel *et al* reported for the first time the use of a COF based on Schiff-base chemistry for pseudocapacitive energy storage.[169] With this aim, they incorporate redox-active 2,6-diaminoanthraquinone (**DAAQ**, **23**) moieties into a 2D-COF linked by β-ketoenamines,

which we have already mentioned that confer outstanding hydrolytic stability. Thus, **DAAQ-TFP COF** was synthesized by reaction between 1,3,5-triformylphloroglycinol (**28, TFP**) and 2,6-diaminoanthraquinone (**23, DAAQ**) under solvothermal conditions (Figure 10).

The anthraquinone moieties within the **DAAQ-TFP COF** exhibit a well-defined electrochemical response with two reversible redox processes. It exhibits a reversible Faradaic process with an E° of −0.058 V *vs* Ag/AgCl. The peak separation (ΔEp) between the oxidative and reductive waves is quite small (4 mV), indicatives of rapid electron transfer between the glassy carbon electrode and the COF anthraquinones.

The high surface area (BET of up to 1800 $m^2 g^{-1}$) and reversible redox processes of the **DAAQ-TFP COF** are of interest for pseudocapacitive energy storage devices, in which charge is stored both in the electrochemical double layer and through surface-bound Faradaic (pseudocapacitive) processes. The **DAAQ-TFP COF** exhibits enhanced capacitance relative to diaminoanthraquinone, and carbon black, as determined by galvanostatic charge−discharge experiments. Thus, **DAAQ-TFP COF** modified electrodes initially provided a capacitance of 48 ± 10 F g^{-1}, which stabilized at 40 ± 9 F g^{-1} after 10 charge/discharge cycles, after which no further significant decrease was observed after 5000 cycles. In principle, this low performance is due, at least in part, to poor electrical contact to the insoluble COF powder samples, so that only a small fraction (*ca*. 3%) of the redox-active groups is electrochemically accessible. Thus, in 2015 Dichtel *et al* have described the first oriented thin films of β-ketoenamine-linked 2D-COFs, which were formed through the slow introduction of the **TFP** monomer into a solution of **DAAQ** in the presence of Au substrates.[75] With this strategy, **DAAQ-TFP COF** thin films provide near-quantitative addressability of the anthraquinone moieties at thicknesses up to *ca*. 200 nm, with areal capacitances of 3.0 mF cm^{-2} (as compared to 0.40 mF cm^{-2} for powder-modified electrodes). These findings demonstrate a means to incorporate 2D-COFs into supercapacitors, particularly as lightweight thin-film electrodes on flexible substrates and show the potential of COFs based on Schiff-base chemistry for electrochemical energy storage devices thus paving the way for the incorporation of other redox-active groups.

Accordingly, Jiang *et al* has recently used a general strategy for converting conventional COFs into an outstanding platform for energy storage through post-synthetic functionalization with organic radicals.[29] Reaction of 2,5-bis(2-propynyloxy)terephthalaldehyde (**BPTA**, **7**) and 2,5-dimethoxyterephthalaldehyde (**DMTA**, **4**) at different molar ratios with nickel 5,10,15,20-tetrakis(4'-tetraphenylamino) porphyrin (**NiP**, **48**, **M = Ni**) under solvothermal conditions yielded **NiPCOF**, **$[HC{\equiv}C]_{50\%}$-NiP-COF**, and **$[HC{\equiv}C]_{100\%}$-NiPCOF** with 0, 50 and 100 % ethynyl units on the COF walls. The ethynyl groups undergo click reaction with 4-azido-2,2,6,6-tetramethyl-1-piperidinyloxy in a smooth and clean manner to yield **$[TEMPO]_{50\%}$-NiP-COF** and **$[TEMPO]_{100\%}$-NiP-COF** quantitatively (Scheme 9). TEMPO is a typical organic radical that not only holds all the unique properties of radicals but also features redox ability for energy storage by reversibly switching between the oxidation states of the neutral radical and the oxoammonium cation. Thus, the radical frameworks with openly accessible polyradicals immobilized on the pore walls undergo rapid and reversible redox reactions, leading to capacitive energy storage with high capacitance, high-rate kinetics, and robust cycle stability. For example, at a current density of 100 mAg^{-1}, **$[TEMPO]_{100\%}$-NiP-COF** and **$[TEMPO]_{50\%}$-NiP-COF** exhibit a capacitance of 167 and 124 Fg^{-1}, respectively. The results suggest that channel-wall functional engineering with redox-active species will be a facile and versatile strategy to explore COFs for energy storage.

A different approach has been used by Wang, Sun *et al* that have reported a simple method to fabricate COFs/graphene composites through the reaction of aldehyde group in 1,3,5-triformylbenzene (**27**) and the amine group in amine modified reduced graphene oxide (**NH_2-rGO**) and *p*-phenylenediamine (**17a**) in one step on the surface of amino functionalized graphene (Fig. 22).[170] The layered **NH_2-rGO** and the spherical COFs can be observed in the SEM images of synthesized **COFs/NH_2–rGO**. The spherical COFs was anchored tightly on the graphene sheets, which is ascribed to the reaction of aldehyde group in 1,3,5-triformylbenzene and amine group in **NH_2–rGO**. The anchored spherical COFs hinder the stacking or aggregation between graphene sheets, thus increasing the effective electrode surface area.

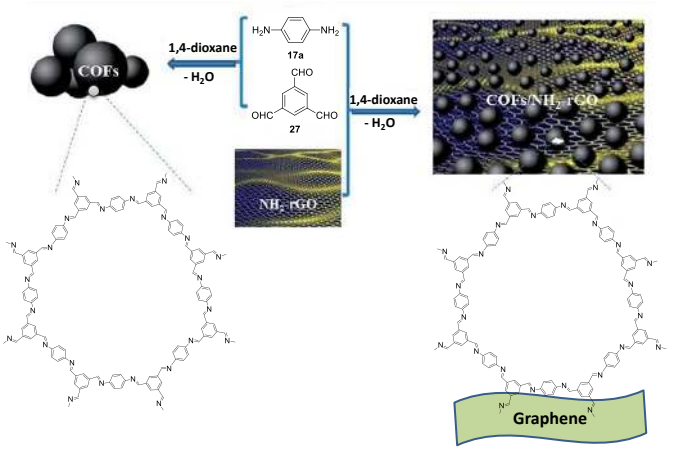

Fig. 22 Synthesis of the COF and **COFs/NH_2–rGO**. Adapted from ref. [170] with permission from the Royal Society of Chemistry.

It was found that **COFs/NH_2–rGO** possesses specific capacitance of 533 F g^{-1} at current density of 0.2 A g^{-1} which is higher than that of pristine COF (226 F g^{-1}) and **NH_2–rGO** (190 F g^{-1}). After 1000 consecutive cycles, the discharge capacitance remains at 79 % of its initial value which highlights the excellent high-rate capability and long cycle lifetime of the **COFs/NH_2–rGO** electrode material.

3.7 Miscellaneous applications of COFs

3.7.1 Proton conduction

The search for a high-performance proton-conducting material for use in fuel cells is central to the development of efficient

methods to convert energy from chemicals — such as hydrogen, methanol or small hydrocarbons — into electricity. In a hydrogen-fuelled cell, hydrogen is catalytically split at the anode into electrons and protons. Through an external circuit, the electrons are transferred to a cathode and produce direct current. On the other hand, the protons are transported across a proton-conducting membrane to the cathode, where they react with oxygen to produce water as a by-product. This proton-conducting membrane is key to the operation of the fuel cell.[171] With this aim, in 2014 Banerjee *et al* synthesized an azo (–N=N–)-functionalized COF (**Tp-Azo COF**) using the reversible Schiff base reaction between 1,3,5-triformylphloroglucinol (**Tp**, **28**) and 4,4'-azodianiline (Azo, **21**).[49] Stability towards acidic conditions is the first precondition for using such materials for proton conduction; however as **Tp-Azo COF** exhibits almost zero conductivity alone, the second precondition is the loading of a proton-conductive compound. To this end, a simple impregnation process loaded phosphoric acid inside the framework up to 5.4 wt %. The azo units of **Tp-Azo COF** were protonated and formed hydrogen-bonding interactions with the $H_2PO_4^-$ anion, which further interacted with free phosphoric acid molecules to form a hydrogen-bonding network in the one-dimensional channels. Proton conduction in both the hydrous ($\sigma = 9.9 \times 10^{-4}$ S cm^{-1}) and anhydrous state ($\sigma = 6.7 \times 10^{-5}$ S cm^{-1}) was determined. These contributions represented the first emergence of COF as proton conducting materials thus offering an appealing platform for construction of proton-conducting systems for applications in fuel cells, sensors and electronic devices.

3.7.2 Stationary phase for high resolution gas chromatography

Yan *et al* have recently reported an approach for the fabrication of a spherical COF **TpBD** (a COF synthesized from 1,3,5-triformylphloroglucinol (**Tp**, **28**) and benzidine (**BD**, **18a**) with good solvent and thermal stability for its application in high-resolution chromatographic application.[56] The spherical COF have large surface area, good solvent stability and high thermostability which make it a good candidate to be used for high resolution gas chromatography (GC). It is worth mentioning that only 0.3 mg of **TpBD** is enough to fabricate a 20 m long **TpBD** coated capillary column *via* a dynamic coating method.[172] Diverse important industrial analytes including alkanes, cyclohexane and benzene, α-pinene and β-pinene, and alcohols are baseline separated on the **TpBD** coated column with high column efficiency and good precision. The separation of these important industrial analytes not only relies on the van der Waals interaction, but also on the π–π interaction and the hydrogen bond between analytes and the TpBD frameworks. This contribution highlights the great potential of COFs for chromatographic separation thus opening a new field for the application of COFs in chromatography.

3.7.3 Colorimetric humidity-responsive behaviour

In 2013, Liu *et al* reported the synthesis of novel COF-based crystalline nanofibers which can epitaxially grow on the aramide microfiber surface thus providing a nanocomposite with interesting colourimetric humidity-responsive behaviour (Fig. 23).[173] This COF (**DHNDA-TAPP-COF**) can be obtained by reaction between 2,6-dihydroxynaphthalene-1,5-dicarbaldehyde (**DHNDA**, **10**) and 2,4,6-tris(4-aminophenyl)pyridine (**TAPP**, **38b**) under solvothermal conditions. A morphological transformation can be observed when tracing the morphology evolution process. The reaction between **DHDNA** (**10**) and **TAPP** (**38b**) quickly leads to precipitates of irregular nanoparticles with diameter about 40 nm. These nanoparticles gradually fused to microspheres with diameter about 350 nm, some short nanofibers can be found on the surface of microspheres. Unexpectedly, with increasing the solvothermal reaction time, the nanofibers grew longer and longer; meanwhile, the microspheres become smaller and smaller. After 24 h, the microspheres can be scarcely observed, only uniform nanofibers can be found. The formation of COF nanofibers can be rationalized in terms of an interesting dissolution recrystallization process[174] due to the reversible nature of dynamic imine bonds. Due to the good nucleation ability of aramid fabric for many kinds of polymers, the formation of COF hybrid structures was obtained through adding some aramic fabric as foreign nucleate agents during COF formation.

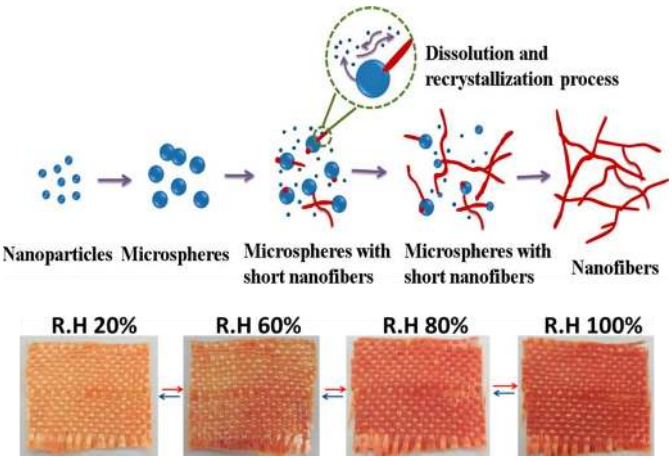

Fig. 23 Top: Formation of COF nanofibers through dynamic imine chemistry enabled by dissolution-recrystallization process. **Bottom:** Digital photographs of the reversible humidity-responsive color-changes of COF/aramid fabrics under different relative humidity. Adapted with permission from *ACS App. Mater. Interf.* 2013, 5, 8845-8849. Copyright (2013) American Chemical Society.

The transformation of isomers between enol form and keto form promoted by moisture[175] provides a humidity-responsive colour-changing property to the COF/aramid nanohybrid material obtained by this procedure. In a dry atmosphere (relative humidity (R.H) 20%), the fabric is light yellow, the colour of the fabric gradually changed from light red to dark red with increasing R.H from 20 to 100%. The colour-changing process (Fig. 23) is reversible and repeatable, which provides a simple naked-eye detection for the environmental humidity. Such a low-cost and scalable method for the fabrication of colorimetric moisture-sensitive fabrics will have great advantage for its further applications.

Conclusions and Perspectives

The promising features of COFs have stimulated the inventiveness of chemists in order to develop synthetic strategies for the preparation of novel COFs based on Schiff-base chemistry. The most extensively used ***synthetic reactions*** for the preparation of these COFs are the solvothermal conditions in a variety of solvent mixtures, using different reaction times and temperatures. However the use of microwave-assisted solvothermal reaction conditions have been also reported, thus decreasing significantly the reaction times. One important synthetic challenge at the moment is the development of novel synthetic procedures to be carried out at room temperature without solvothermal conditions. In this respect, the use of mechanochemical grinding and direct formation of COFs at room temperature represent some seminal steps in that direction. In the next coming year, we believe that novel synthetic methods will be implemented for the synthesis of COFs in order to enable their large scale production and their incorporation to other systems.[176] For instance, the use of techniques that have already demonstrated useful for MOFs preparation, such as chemical vapour deposition[176] and spray-drying,[177] will be tested.

Another important subject to consider for the ***COFs design*** is the study of the suitable modifications carried out in the monomers in order to fine tune the final structure of these COFs. Thus, the chemical stability and crystallinity in 2D-COFs enhance by introducing -OH functionalities adjacent to the Schiff-base centres (C=N) to form an intramolecular O-H----N=C hydrogen bond.[23, 24] On the other hand, the use of an irreversible enol to-keto tautomerization following the Schiff-base reaction is also an effective strategy toward the enhancement of chemical stability of the crystalline framework.[49] Research in these directions are required to enhance COF performances. Additionally, pores chemical functionalization is relevant from many perspectives. In this respect, an essential aspect that will deserve attention is the development of COFs with highly functionalized pore wall structures which are difficult to obtain *via* direct polycondensation reactions. The post-synthetic modification constitute an excellent tool for systematic functionalization of COFs with different purposes.[79] Despite several works have used different strategies for this purpose, the use of the Azide-Alkyne Huisgen Cycloaddition reaction, known as “click” reaction, have been demonstrated very efficient for pore-wall surface engineering, allowing the incorporation of organic radicals and chiral moieties for catalysis.[80] Another simple post-synthetic modification includes the preparation of metal doped COFs and of hybrids based on COFs and metal nanoparticles that provide new properties to the materials.

COFs have recently emerged as realistic alternative ***porous materials*** for gas adsorption, separation and storage applications. Despite this is a relatively new research topic, imine-based COFs with efficient adsorption uptake of H_2, CH_4, CO_2 or N_2 have been already obtained. In addition, high selectivity in the separation of CO_2 over N_2 and CH_4 have been also achieved. Furthermore, COFs based on Schiff-base chemistry have shown to be able to immobilize large molecules such as enzymes or lactic acid.

The use of COFs in ***catalysis*** is still in its infancy but we believe that novel post-synthetic transformations at the pore will provide opportunities for molecular recognition as well as incorporation of more specific active sites for catalysis. Imine-based COFs are especially suited for this application given that they are highly stable in water and most organic solvents, and the imine type (Schiff base) ligands are versatile in incorporating a variety of metal ions. Thus, in the last few years, COFs have revealed as excellent platforms to be used as catalyst, photocatalyst and electrocatalyst.

Other applications of COFs such as ***Chemo and Bio-sensing*** agents based on luminescent COFs in which nitrogen sites serve as docking sites to lock guest molecules have been reported and will be for sure a subject to development in the next coming years.

The possibility of having synthetic access to conducting organic materials with total control over their nanoscale structure and orientation is another important challenge in the area of organic (opto)electronics. By virtue of their three-dimensional orderings at the atomic scale, 2D-COFs have shown a great potential to perform core functions in organic electronics such as light emission, charge transfer and separation, and semiconduction. In this respect, COFs based on Schiff-base chemistry offer the possibility to develop fully conjugated 2D crystalline networks capable of in-plane charge transport. The possibility of using donor-acceptor COF derivatives as active layer for photoenergy conversion has been also investigated although the efficiencies obtained are still low. The current challenge in this area is to obtain these type of COFs as large-area-oriented thin films. The unique ability of COFs to offer uniform nanometer scale pores and predictive design criteria to organize functional building blocks has been also used to access microporous electrodes for energy storage and conversion devices including electrochemical capacitors. Other less explored applications already investigated for this type of COFs are their ability for proton conduction, their potential use as stationary phase for high resolution gas chromatography, their colorimetric humidity-responsive behaviour and their use as precursors of 2D-sheets nanomaterials. Indeed the production of ***single/few layers COFs*** integrated on different surfaces is currently receiving a great deal of interest given that it provides a unique opportunity of obtaining both atomic thick sheets or thin-films with covalently bonded organic building units with unique properties associated with reduced dimensionality, well-defined in-plane structure, and tuneable functionalities. In general the confinement of the building blocks at the solid-liquid interface, known as on-surface synthesis, has been used to produce layers of COFs but typically with small areas (nanometer range), leading to small coverage of the substrate. However, the opportunity to generate COFs at the liquid-liquid or liquid-air interfaces is still not well developed. Indeed the synthesis of a disordered ultra-large (millimetre range) two-dimensional covalent organic monolayer has been recently reported through dynamic imine chemistry at the air-water interface, highlighting its great potential.[178] Therefore, we

consider that these strategies will be further developed in a near future.

Although this general landscape foresees a broad number of future applications, the development of methods that enable their procesability will be required in order to accomplish the integration of COFs as useful materials. Therefore, we envision that novel techniques, such as ink-jet printing, wet-lithography or roll-to-roll, will be implemented. Additionally, we consider that aspects dealing with the morphology and size-reduction of the materials will be developed bringing new properties and opportunities for COF´s applications.

Finally, in addition to potential applications of this family of COFs in energy and catalysis, we believe that COFs based on Schiff-base chemistry will find opportunities for water decontamination.[37]

In summary, COFs based on Schiff-base chemistry are a type of materials whose interesting properties have challenged the creativity and inventiveness of chemists in areas such as organic, polymer, and materials chemistry as well as in nanoscience. The knowledge accumulated during this years of research based on this systems will certainly lead to novel applications for this unique materials.

Acknowledgements

Financial support from Spanish Government (Project MAT2014-52305-P and MAT2013-46753-C2-1-P) and a UCM-BSCH joint project (GR3/14) is acknowledged. The authors wish to give credit to the scientists who have participated in the development of this research field whose names are cited in the references.

References

1.A. P. Cote, A. I. Benin, N. W. Ockwig, M. O'Keeffe, A. J. Matzger and O. M. Yaghi, *Science*, 2005, **310**, 1166-1170.
2. S. Wan, J. Guo, J. Kim, H. Ihee and D. L. Jiang, *Angew. Chem. Int. Ed.*, 2008, **47**, 8826-8830.
3. R. W. Tilford, W. R. Gemmill, H. C. zur Loye and J. J. Lavigne, *Chem. Mater.*, 2006, **18**, 5296-5301.
4. E. L. Spitler and W. R. Dichtel, *Nat Chem*, 2010, **2**, 672-677.
5. R. W. Tilford, S. J. Mugavero, P. J. Pellechia and J. J. Lavigne, *Adv. Mater.*, 2008, **20**, 2741-2743.
6. H. M. El-Kaderi, J. R. Hunt, J. L. Mendoza-Cortes, A. P. Cote, R. E. Taylor, M. O'Keeffe and O. M. Yaghi, *Science*, 2007, **316**, 268-272.
7. J. X. Jiang and A. I. Cooper, *Top. Curr. Chem.*, 2010, **293**, 1-33.
8. A. P. Cote, H. M. El-Kaderi, H. Furukawa, J. R. Hunt and O. M. Yaghi, *J. Am. Chem. Soc.*, 2007, **129**, 12914-12915.
9. J. X. Jiang, F. Su, A. Trewin, C. D. Wood, H. Niu, J. T. A. Jones, Y. Z. Khimyak and A. I. Cooper, *J. Am. Chem. Soc.*, 2008, **130**, 7710-7720.
10. F. J. Uribe-Romo, J. R. Hunt, H. Furukawa, C. Klock, M. O'Keeffe and O. M. Yaghi, *J. Am. Chem. Soc.*, 2009, **131**, 4570-+.
11. H. Furukawa and O. M. Yaghi, *J. Am. Chem. Soc.*, 2009, **131**, 8875-8883.
12. C. J. Doonan, D. J. Tranchemontagne, T. G. Glover, J. R. Hunt and O. M. Yaghi, *Nat. Chem.*, 2010, **2**, 235-238.
13. P. Kuhn, M. Antonietti and A. Thomas, *Angew. Chem. Int. Ed.*, 2008, **47**, 3450-3453.
14. E. L. Spitler, M. R. Giovino, S. L. White and W. R. Dichtel, *Chem. Sci.*, 2011, **2**, 1588-1593.
15. S. Y. Ding, J. Gao, Q. Wang, Y. Zhang, W. G. Song, C. Y. Su and W. Wang, *J. Am. Chem. Soc.*, 2011, **133**, 19816-19822.
16. X. A. Feng, L. Chen, Y. P. Dong and D. L. Jiang, *Chem Commun*, 2011, **47**, 1979-1981.
17. R. Dawson, A. I. Cooper and D. J. Adams, *Progr. Poly. Sci.*, 2012, **37**, 530-563.
18. B. J. Smith, A. C. Overholts, N. Hwang and W. R. Dichtel, *Chem. Commun.*, 2016, **52**, 3690-3693.
19. P. J. Waller, F. Gandara and O. M. Yaghi, *Acc. Chem. Res.*, 2015, **48**, 3053-3063.
20. L. M. Lanni, R. W. Tilford, M. Bharathy and J. J. Lavigne, *J. Am. Chem. Soc.*, 2011, **133**, 13975-13983.
21. S. Y. Ding and W. Wang, *Chem. Soc. Rev.*, 2013, **42**, 548-568.
22. X. Feng, X. S. Ding and D. L. Jiang, *Chem. Soc. Rev.*, 2012, **41**, 6010-6022.
23. X. Chen, M. Addicoat, E. Jin, L. Zhai, H. Xu, N. Huang, Z. Guo, L. Liu, S. Irle and D. Jiang, *J. Am. Chem. Soc.*, 2015, **137**, 3241-3247.
24. D. B. Shinde, S. Kandambeth, P. Pachfule, R. R. Kumar and R. Banerjee, *Chem. Commun.*, 2015, **51**, 310-313.
25. S. Kandambeth, D. B. Shinde, M. K. Panda, B. Lukose, T. Heine and R. Banerjee, *Angew. Chem. Int. Ed.*, 2013, **52**, 13052-13056.
26. S. Kandambeth, V. Venkatesh, D. B. Shinde, S. Kumari, A. Halder, S. Verma and R. Banerjee, *Nat. Commun.*, 2015, **6**, Art. Num. 6786.
27. Z. Kahveci, T. Islamoglu, G. A. Shar, R. Ding and H. M. El-Kaderi, *CrystEngComm*, 2013, **15**, 1524-1527.
28. X. Chen, M. Addicoat, S. Irle, A. Nagai and D. Jiang, *J. Am. Chem. Soc.*, 2013, **135**, 546-549.
29. H. Xu, J. Gao and D. L. Jiang, *Nat Chem*, 2015, **7**, 905-912.
30. B. Lukose, A. Kuc and T. Heine, *Chem. Eur. J.*, 2011, **17**, 2388-2392.
31. J. R. Song, J. Sun, J. Liu, Z. T. Huang and Q. Y. Zheng, *Chem. Commun.*, 2014, **50**, 788-791.
32. E. L. Spitler, B. T. Koo, J. L. Novotney, J. W. Colson, F. J. Uribe-Romo, G. D. Gutierrez, P. Clancy and W. R. Dichtel, *J. Am. Chem. Soc.*, 2011, **133**, 19416-19421.
33. S. Dalapati, M. Addicoat, S. Jin, T. Sakurai, J. Gao, H. Xu, S. Irle, S. Seki and D. Jiang, *Nat. Commun.*, 2015, **6**, Art. Num. 7786.
34. T. Y. Zhou, S. Q. Xu, Q. Wen, Z. F. Pang and X. Zhao, *J. Am. Chem. Soc.*, 2014, **136**, 15885-15888.
35. Y. B. Zhang, J. Su, H. Furukawa, Y. Yun, F. Gandara, A. Duong, X. Zou and O. M. Yaghi, *J. Am. Chem. Soc.*, 2013, **135**, 16336-16339.
36. Q. Fang, Z. Zhuang, S. Gu, R. B. Kaspar, J. Zheng, J. Wang, S. Qiu and Y. Yan, *Nat. Commun.*, 2014, **5**, Art. Num. 4503.
37. Y. Z. Liu, Y. H. Ma, Y. B. Zhao, X. X. Sun, F. Gandara, H. Furukawa, Z. Liu, H. Y. Zhu, C. H. Zhu, K. Suenaga, P. Oleynikov, A. S. Alshammari, X. Zhang, O. Terasaki and O. M. Yaghi, *Science*, 2016, **351**, 365-369.
38. F. J. Uribe-Romo, C. J. Doonan, H. Furukawa, K. Oisaki and O. M. Yaghi, *J. Am. Chem. Soc.*, 2011, **133**, 11478-11481.
39. S. J. Rowan, S. J. Cantrill, G. R. L. Cousins, J. K. M. Sanders and J. F. Stoddart, *Angew. Chem. Int. Ed.*, 2002, **41**, 898-952.
40. L. Stegbauer, K. Schwinghammer and B. V. Lotsch, *Chem. Sci.*, 2014, **5**, 2789-2793.
41. S. Dalapati, S. Jin, J. Gao, Y. Xu, A. Nagai and D. Jiang, *J. Am. Chem. Soc.*, 2013, **135**, 17310-17313.
42. Z. Li, Y. Zhi, X. Feng, X. Ding, Y. Zou, X. Liu and Y. Mu, *Chem. Eur. J.*, 2015, **21**, 12079-12084.
43. Z. Li, X. Feng, Y. Zou, Y. Zhang, H. Xia, X. Liu and Y. Mu, *Chem. Commun.*, 2014, **50**, 13825-13828.
44. V. S. Vyas, F. Haase, L. Stegbauer, G. Savasci, F. Podjaski, C. Ochsenfeld and B. V. Lotsch, *Nat. Commun.*, 2015, **6**, Art. Num. 8508.
45. P. Pachfule, S. Kandmabeth, A. Mallick and R. Banerjee, *Chem. Commun.*, 2015, **51**, 11717-11720.

46. S. Kandambeth, A. Mallick, B. Lukose, M. V. Mane, T. Heine and R. Banerjee, *J. Am. Chem. Soc.*, 2012, **134**, 19524-19527.
47. B. P. Biswal, S. Chandra, S. Kandambeth, B. Lukose, T. Heine and R. Banerjee, *J. Am. Chem. Soc.*, 2013, **135**, 5328-5331.
48. S. Chandra, S. Kandambeth, B. P. Biswal, B. Lukose, S. M. Kunjir, M. Chaudhary, R. Babarao, T. Heine and R. Banerjee, *J. Am. Chem. Soc.*, 2013, **135**, 17853-17861.
49. S. Chandra, T. Kundu, S. Kandambeth, R. Babarao, Y. Marathe, S. M. Kunjir and R. Banerjee, *J. Am. Chem. Soc.*, 2014, **136**, 6570-6573.
50. J. Guo, Y. Xu, S. Jin, L. Chen, T. Kaji, Y. Honsho, M. A. Addicoat, J. Kim, A. Saeki, H. Ihee, S. Seki, S. Irle, M. Hiramoto, J. Gao and D. Jiang, *Nat. Commun.*, 2013, **4**, Art. Num. 2736.
51. Y. Zeng, R. Zou, Z. Luo, H. Zhang, X. Yao, X. Ma, R. Zou and Y. Zhao, *J. Am. Chem. Soc.*, 2015, **137**, 1020-1023.
52. A. de la Hoz, A. Diaz-Ortiz and A. Moreno, *Chem. Soc. Rev.*, 2005, **34**, 164-178.
53. H. Wei, S. Chai, N. Hu, Z. Yang, L. Wei and L. Wang, *Chem. Commun.*, 2015, **51**, 12178-12181.
54. T. Friščić, *Chem. Soc. Rev.*, 2012, **41**, 3493-3510.
55. A. de la Peña Ruigómez, D. Rodríguez-San-Miguel, K. C. Stylianou, M. Cavallini, D. Gentili, F. Liscio, S. Milita, O. M. Roscioni , M. L. Ruiz-González, C. Carbonell, D. Maspoch, R. Mas-Ballesté, J. L. Segura and F. Zamora, *Chem. Eur. J.*, 2015, **21**, 10666-10670.
56. C. X. Yang, C. Liu, Y. M. Cao and X. P. Yan, *Chem. Commun.*, 2015, **51**, 12254-12257.
57. J. Mahmood, E. K. Lee, M. Jung, D. Shin, I. Y. Jeon, S. M. Jung, H. J. Choi, J. M. Seo, S. Y. Bae, S. D. Sohn, N. Park, J. H. Oh, H. J. Shin and J. B. Baek, *Nat. Commun.*, 2015, **6**, Art. Num. 6486.
58. T. Shiraki, G. Kim and N. Nakashima, *Chem. Lett.*, 2015, **44**, 1488-1490.
59. R. Mas-Balleste, C. Gomez-Navarro, J. Gomez-Herrero and F. Zamora, *Nanoscale*, 2011, **3**, 20-30.
60. H. Zhang, *ACS Nano*, 2015, **9**, 9451-9469.
61. P. Payamyar, B. T. King, H. C. Ottinger and A. D. Schluter, *Chem. Commun.*, 2016, **52**, 18-34.
62. D. Rodriguez-San-Miguel, P. Amo-Ochoa and F. Zamora, *Chem. Commun.*, 2016, **52**, 4113-4127.
63. I. Berlanga, M. L. Ruiz-Gonzalez, J. M. Gonzalez-Calbet, J. L. G. Fierro, R. Mas-Balleste and F. Zamora, *Small*, 2011, **7**, 1207-1211.
64. I. Berlanga, R. Mas-Balleste and F. Zamora, *Chem. Commun.*, 2012, **48**, 7976-7978.
65. D. N. Bunck and W. R. Dichtel, *J. Am. Chem. Soc.*, 2013, **135**, 14952-14955.
66. A. Gourdon, *Angew. Chem. Int. Ed.*, 2008, **47**, 6950-6953.
67. H. Liang, Y. He, Y. Ye, X. Xu, F. Cheng, W. Sun, X. Shao, Y. Wang, J. Li and K. Wu, *Coord. Chem. Rev.*, 2009, **253**, 2959-2979.
68. J. Greenwood and C. J. Baddeley, *Langmuir*, 2013, **29**, 653-657.
69. R. Tanoue, R. Higuchi, K. Ikebe, S. Uemura, N. Kimizuka, A. Z. Stieg, J. K. Gimzewski and M. Kunitake, *J. Nanosci. Nanotech.* 2014, **14**.
70. L. R. Xu, X. Zhou, Y. X. Yu, W. Q. Tian, J. Ma and S. B. Lei, *ACS Nano*, 2013, **7**, 8066-8073.
71. X. H. Liu, C. Z. Guan, S. Y. Ding, W. Wang, H. J. Yan, D. Wang and L. J. Wan, *J. Am. Chem. Soc.*, 2013, **135**, 10470-10474.
72. J. Y. Yue, X. H. Liu, B. Sun and D. Wang, *Chem. Commun.*, 2015, **51**, 14318-14321.
73. L. Xu, X. Zhou, W. Q. Tian, T. Gao, Y. F. Zhang, S. Lei and Z. F. Liu, *Angew. Chem. Int. Ed.*, 2014, **53**, 9564-9568.
74. Z. Zha, L. Xu, Z. Wang, X. Li, Q. Pan, P. Hu and S. Lei, *ACS App. Mater. Int.*, 2015, **7**, 17837-17843.
75. C. R. DeBlase, K. Hernandez-Burgos, K. E. Silberstein, G. G. Rodriguez-Calero, R. P. Bisbey, H. D. Abruna and W. R. Dichtel, *ACS Nano*, 2015, **9**, 3178-3183.
76. J. I. Feldblyum, C. H. McCreery, S. C. Andrews, T. Kurosawa, E. J. Santos, V. Duong, L. Fang, A. L. Ayzner and Z. Bao, *Chem. Commun.*, 2015, **51**, 13894-13897.
77. P. Wang, M. Kang, S. Sun, Q. Liu, Z. Zhang and S. Fang, *Chin. J. Chem.*, 2014, **32**, 838-843.
78. S. L. Cai, Y. B. Zhang, A. B. Pun, B. He, J. H. Yang, F. M. Toma, I. D. Sharp, O. M. Yaghi, J. Fan, S. R. Zheng, W. G. Zhang and Y. Liu, *Chem. Sci.*, 2014, **5**, 4693-4700.
79. X. Chen, N. Huang, J. Gao, H. Xu, F. Xu and D. Jiang, *Chem. Commun.*, 2014, **50**, 6161-6163.
80. N. Huang, R. Krishna and D. L. Jiang, *J. Am. Chem. Soc.*, 2015, **137**, 7079-7082.
81. M. S. Lohse, T. Stassin, G. Naudin, S. Wuttke, R. Ameloot, D. De Vos, D. D. Medina and T. Bein, *Chem. Mater.*, 2015.
82. W. Zhang, P. Jiang, Y. Wang, J. Zhang, Y. Gao and P. Zhang, *RSC Adv.*, 2014, **4**, 51544-51547.
83. J. Thote, H. B. Aiyappa, A. Deshpande, D. Diaz Diaz, S. Kurungot and R. Banerjee, *Chem. Eur. J.*, 2014, **20**, 15961-15965.
84. P. Pachfule, S. Kandambeth, D. Diaz Diaz and R. Banerjee, *Chem. Commun.*, 2014, **50**, 3169-3172.
85. H. Hoppe and N. S. Sariciftci, *J. Mater. Res.*, 2004, **19**, 1924-1945.
86. G. Li, R. Zhu and Y. Yang, *Nat. Photon.*, 2012, **6**, 153-161.
87. T. A. Makal, J.-R. Li, W. Lu and H.-C. Zhou, *Chem. Soc. Rev.*, 2012, **41**, 7761-7779.
88. A. G. Slater and A. I. Cooper, *Science*, 2015, **348**, 988-990
89. M. P. Suh, H. J. Park, T. K. Prasad and D.-W. Lim, *Chem. Rev.*, 2012, **112**, 782-835.
90. R. B. Getman, Y.-S. Bae, C. E. Wilmer and R. Q. Snurr, *Chem. Rev.*, 2012, **112**, 703-723.
91. F. Li, J. J. Zhao and L. X. Sun, *Abs. Papers ACS*, 2012, **244**.
92. K. Sumida, D. L. Rogow, J. A. Mason, T. M. McDonald, E. D. Bloch, Z. R. Herm, T. H. Bae and J. R. Long, *Chem. Rev.*, 2012, **112**, 724-781.
93. Z. R. Herm, B. M. Wiers, J. A. Mason, J. M. van Baten, M. R. Hudson, P. Zajdel, C. M. Brown, N. Masciocchi, R. Krishna and J. R. Long, *Science*, 2013, **340**, 960-964.
94. K. A. Cychosz, R. Ahmad and A. J. Matzger, *Chem. Sci.*, 2010, **1**, 293-302.
95. O. M. Yaghi, M. O'Keeffe, N. W. Ockwig, H. K. Chae, M. Eddaoudi and J. Kim, *Nature*, 2003, **423**, 705-714.
96. J. L. Mendoza-Cortes, S. S. Han and W. A. Goddard, *J. Phys. Chem. A*, 2012, **116**, 1621-1631.
97. R. Babarao, R. Custelcean, B. P. Hay and D. E. Jiang, *Cryst. Grow. Des.*, 2012, **12**, 5349-5356.
98. D. J. Martin, K. Qiu, S. A. Shevlin, A. D. Handoko, X. Chen, Z. Guo and J. Tang, *Angew. Chem. Int. Ed.*, 2014, **53**, 9240-9245.
99. W. Li, Y. Pang and J. Zhang, *J. Mol. Mod.*, 2014, **20**, 2346.
100. B. Ashourirad, A. K. Sekizkardes, S. Altarawneh and H. M. El-Kaderi, *Chem. Mater.*, 2015, **27**, 1349-1358.
101. H. A. Patel, S. Hyun Je, J. Park, D. P. Chen, Y. Jung, C. T. Yavuz and A. Coskun, *Nat. Commun.*, 2013, **4**, Art. Num. 1357.
102. M. G. Rabbani, A. K. Sekizkardes, Z. Kahveci, T. E. Reich, R. S. Ding and H. M. El-Kaderi, *Chem. Eur. J.*, 2013, **19**, 3324-3328.
103. Y. H. Jin, Y. L. Zhu and W. Zhang, *CrystEngComm*, 2013, **15**, 1484-1499.
104. T. Burchell and M. Rogers, *SAE Techn. Papers Ser.*, 2000, 2001.
105. S. Amirjalayer, R. Q. Snurr and R. Schmid, *J. Phys. Chem. C*, 2012, **116**, 4921-4929.
106. D. Kaleeswaran, P. Vishnoi and R. Murugavel, *J. Mater. Chem. C*, 2015, **3**, 7159-7171.
107. Q. Gao, L. Bai, X. Zhang, P. Wang, P. Li, Y. Zeng, R. Zou and Y. Zhao, *Chin. J. Chem.*, 2015, **33**, 90-94.
108. Y. Zhu, H. Long and W. Zhang, *Chem. Mater.*, 2013, **25**, 1630-1635.
109. P. Mohanty, L. D. Kull and K. Landskron, *Nat. Commun.*, 2011, **2**, Art. Num. 401.

110. S. Cavenati, C. A. Grande and A. E. Rodrigues, *J. Chem. Eng. Data*, 2004, **49**, 1095-1101.
111. C. Shen, H. Yu and Z. Wang, *Chem. Commun.*, 2014, **50**, 11238-11241.
112. N. Huang, X. Chen, R. Krishna and D. Jiang, *Angew. Chem. Int. Ed.*, 2015, **54**, 2986-2990.
113. S. Jin, K. Furukawa, M. Addicoat, L. Chen, S. Takahashi, S. Irle, T. Nakamura and D. Jiang, *Chem. Sci.*, 2013, **4**, 4505-4511.
114. Y. Du, K. M. Mao, P. Kamakoti, P. Ravikovitch, C. Paur, S. Cundy, Q. C. Li and D. Calabro, *Chem. Commun.*, 2012, **48**, 4606-4608.
115. G. Das, B. P. Biswal, S. Kandambeth, V. Venkatesh, G. Kaur, M. Addicoat, T. Heine, S. Verma and R. Banerjee, *Chem. Sci.*, 2015, **6**, 3931-3939.
116. Y.-F. Xie, S.-Y. Ding, J.-M. Liu, W. Wang and Q.-Y. Zheng, *J. Mater. Chem. C*, 2015, **3**, 10066-10069.
117. A. Thomas, *Angew. Chem. Int. Ed.*, 2010, **49**, 8328-8344.
118. A. Corma, *Chem. Rev.*, 1997, **97**, 2373-2420.
119. A. Corma, H. García and F. X. Llabrés i Xamena, *Chem. Rev.*, 2010, **110**, 4606-4655.
120. G. Singh, P. A. Singh, A. K. Sen, K. Singha, S. N. Dubeya, R. N. Handa and J. Choi, *Synth. React. Inorg. Met. Org. Chem.*, 2002, **32**, 171-187.
121. N. Miyaura and A. Suzuki, *Chem. Rev.*, 1995, **95**, 2457-2483.
122. F. X. Llabrés i Xamena, A. Abad, A. Corma and H. Garcia, *J. Catal.*, 2007, **250**, 294-298.
123. Y. Hou, X. Zhang, J. Sun, S. Lin, D. Qi, R. Hong, D. Li, X. Xiao and J. Jiang, *Microp. Mesop. Mater.*, 2015, **214**, 108-114.
124. P. Pachfule, M. K. Panda, S. Kandambeth, S. M. Shivaprasad, D. D. Diaz and R. Banerjee, *J. Mater. Chem. A*, 2014, **2**, 7944-7952.
125. S. Lin, C. S. Diercks, Y.-B. Zhang, N. Kornienko, E. M. Nichols, Y. Zhao, A. R. Paris, D. Kim, P. Yang, O. M. Yaghi and C. J. Chang, *Science*, 2015, **349**, 1208-1213.
126. Q. Fang, S. Gu, J. Zheng, Z. Zhuang, S. Qiu and Y. Yan, *Angew. Chem. Int. Ed.*, 2014, **53**, 2878-2882.
127. H. Xu, X. Chen, J. Gao, J. Lin, M. Addicoat, S. Irle and D. Jiang, *Chem. Commun.*, 2014, **50**, 1292-1294.
128. Y. Wu, H. Xu, X. Chen, J. Gao and D. Jiang, *Chem. Commun.*, 2015, **51**, 10096-10098.
129. W. Gao, X. Sun, H. Niu, X. Song, K. Li, H. Gao, W. Zhang, J. Yu and M. Jia, *Microp. Mesop. Mater.*, 2015, **213**, 59-67.
130. Y. Nakao and T. Hiyama, *Chem. Soc. Rev.*, 2011, **40**, 4893-4901.
131. R. Ishimoto, K. Kamata and N. Mizuno *Angew. Chem. Int. Ed.*, 2009, **48**, 8900-8904.
132. S. Lin, Y. Hou, X. Deng, H. Wang, S. Sun and X. Zhang, *RSC Adv.*, 2015, **5**, 41017-41024.
133. E. Merino, E. Verde-Sesto, E. M. Maya, M. Iglesias, F. Sánchez and A. Corma, *Chem. Mater.*, 2013, **25**, 981-988.
134. W. Notz, F. Tanaka and C. F. Barbas, *Acc. Chem. Res.*, 2004, **37**, 580-591.
135. D. W. C. MacMillan, *Nature*, 2008, **455**, 304-308.
136. M. Juhl and D. Tanner, *Chem. Soc. Rev.*, 2009, **38**, 2983-2992.
137. C. Janiak, *Dalton Trans.*, 2000, 3885-3896.
138. A. Fateeva, P. A. Chater, C. P. Ireland, A. A. Tahir, Y. Z. Khimyak, P. V. Wiper, J. R. Darwent and M. J. Rosseinsky, *Angew. Chem. Int. Ed.*, 2012, **51**, 7440-7444.
139. K. Schwinghammer, B. Tuffy, M. B. Mesch, E. Wirnhier, C. Martineau, F. Taulelle, W. Schnick, J. Senker and B. V. Lotsch, *Angew. Chem. Int. Ed.*, 2013, **52**, 2435-2439.
140. A. Nagai, X. Chen, X. Feng, X. Ding, Z. Guo and D. Jiang, *Angew. Chem. Int. Ed.*, 2013, **52**, 3770-3774.
141. H. Zhong, H. Lai and Q. Fang, *J. Phys. Chem. C*, 2011, **115**, 2423-2427.
142. J. Kiwi and M. Gratzel, *Nature*, 1979, **281**, 657-658.
143. J. Zhang, X. Chen , K. Takanabe, K. Maeda, K. Domen, J. D. Epping, X. Fu, M. Antonietti and X. Wang *Angew. Chem. Int. Ed.*, 2010, **49**, 441-444.
144. M. C. DeRosa and R. J. Crutchley, *Coord. Chem. Rev.*, 2002, **233–234**, 351-371.
145. W. Spiller, H. Kliesch, D. Wöhrle, S. Hackbarth, B. Röder and G. Schnurpfeil, *J. Porph. Phthalocy.*, 1998, **02**, 145-158.
146. W. Ma, P. Yu, T. Ohsaka and L. Mao, *Electrochem. Comm.*, 2015, **52**, 53-57.
147. C. Costentin, M. Robert and J.-M. Saveant, *Chem. Soc. Rev.*, 2013, **42**, 2423-2436.
148. H. Deng, C. J. Doonan, H. Furukawa, R. B. Ferreira, J. Towne, C. B. Knobler, B. Wang and O. M. Yaghi, *Science*, 2010, **327**, 846-850.
149. M. Dogru and T. Bein, *Chem. Commun.*, 2014, **50**, 5531-5546.
150. J. L. Segura, F. Giacalone, R. Gomez, N. Martin, D. M. Guldi, C. P. Luo, A. Swartz, I. Riedel, D. Chirvase, J. Parisi, V. Dyakonov, N. S. Sariciftci and F. Padinger, *Mater. Sci. Eng. C Biomim. Supramol. Syst.*, 2005, **25**, 835-842.
151. M. Dogru, M. Handloser, F. Auras, T. Kunz, D. Medina, A. Hartschuh, P. Knochel and T. Bein, *Angew. Chem. Int. Ed.*, 2013, **52**, 2920-2924.
152. S. Wan, F. Gándara, A. Asano, H. Furukawa, A. Saeki, S. K. Dey, L. Liao, M. W. Ambrogio, Y. Y. Botros, X. Duan, S. Seki, J. F. Stoddart and O. M. Yaghi, *Chem. Mater.*, 2011, **23**, 4094-4097.
153. N. S. Sariciftci, L. Smilowitz, A. J. Heeger and F. Wudl, *Science*, 1992, **258**, 1474-1476.
154. G. Yu, J. Gao, J. C. Hummelen, F. Wudl and A. J. Heeger, *Science*, 1995, **270**, 1789-1791.
155. D. Braga and G. Horowitz, *Adv. Mater.*, 2009, **21**, 1473-1486.
156. R. P. Ortiz, H. Herrera, R. Blanco, H. Huang, A. Facchetti, T. J. Marks, Y. Zheng and J. L. Segura, *J. Am. Chem. Soc.*, 2010, **132**, 8440-8452.
157. L. Chen, K. Furukawa, J. Gao, A. Nagai, T. Nakamura, Y. Dong and D. Jiang, *J. Am. Chem. Soc.*, 2014, **136**, 9806-9809.
158. J. L. Segura and N. Martin, *Angew. Chem. Int. Ed.*, 2001, **40**, 1372-1409.
159. S.-L. Cai, Y.-B. Zhang, A. B. Pun, B. He, J. Yang, F. M. Toma, I. D. Sharp, O. M. Yaghi, J. Fan, S.-R. Zheng, W.-G. Zhang and Y. Liu, *Chem. Sci.*, 2014, **5**, 4693-4700.
160. G. H. V. Bertrand, V. K. Michaelis, T.-C. Ong, R. G. Griffin and M. Dincă, *Proc. Nat. Ac. Sci. USA*, 2013, **110**, 4923-4928.
161. H. Ding, Y. Li, H. Hu, Y. Sun, J. Wang, C. Wang, C. Wang, G. Zhang, B. Wang, W. Xu and D. Zhang, *Chem. Eur. J.*, 2014, **20**, 14614-14618.
162. S. B. Jin, T. Sakurai, T. Kowalczyk, S. Dalapati, F. Xu, H. Wei, X. Chen, J. Gao, S. Seki, S. Irle and D. L. Jiang, *Chem. Eur. J.*, 2014, **20**, 14608-14613.
163. V. Coropceanu, J. Cornil, D. A. da Silva Filho, Y. Olivier, R. Silbey and J.-L. Brédas, *Chem. Rev.*, 2007, **107**, 926-952.
164. X. Feng, L. L. Liu, Y. Honsho, A. Saeki, S. Seki, S. Irle, Y. P. Dong, A. Nagai and D. L. Jiang, *Angew. Chem. Int. Ed.*, 2012, **51**, 2618-2622.
165. J. W. Colson, A. R. Woll, A. Mukherjee, M. P. Levendorf, E. L. Spitler, V. B. Shields, M. G. Spencer, J. Park and W. R. Dichtel, *Science*, 2011, **332**, 228-231.
166. J. L. Segura, R. Juarez, M. Ramos and C. Seoane, *Chem. Soc. Rev.*, 2015, **44**, 6850-6885.
167. L. Mai, X. Tian, X. Xu, L. Chang and L. Xu, *Chem. Rev.*, 2014, **114**, 11828-11862.
168. F. Beguin and E. Frackowiak, *Supercapacitors: Materials, Systems and Applications*, John Wiley & Sons, 2013.
169. C. R. DeBlase, K. E. Silberstein, T. T. Truong, H. D. Abruna and W. R. Dichtel, *J. Am. Chem. Soc.*, 2013, **135**, 16821-16824.
170. P. Wang, Q. Wu, L. Han, S. Wang, S. Fang, Z. Zhang and S. Sun, *RSC Adv.*, 2015, **5**, 27290-27294.

171. H. Xu and D. Jiang, *Nat. Chem.*, 2014, **6**, 564-566.
172. Z.-Y. Gu and X.-P. Yan, *Angew. Chem. Int. Ed.*, 2010, **49**, 1477-1480.
173. W. Huang, Y. Jiang, X. Li, X. Li, J. Wang, Q. Wu and X. Liu, *ACS App. Interf.*, 2013, **5**, 8845-8849.
174. Z. Wang, J. Liu, X. Chen, J. Wan and Y. Qian, *Chem. Eur. J.*, 2005, **11**, 160-163.
175. M. Ziółek, J. Kubicki, A. Maciejewski, R. Naskręcki and A. Grabowska, *J. Chem. Phys.*, 2006, **124**, 124518.
176. I. Stassen, M. Styles, G. Grenci, H. V. Gorp, W. Vanderlinden, S. Feyter, P. Falcaro, D. Vos, P. Vereecken and R. Ameloot, *Nat. Mat.*, 2015, 304-310.
177. A. Carne-Sanchez, I. Imaz, M. Cano-Sarabia and D. Maspoch, *Nat. Chem.*, 2013, **5**, 203-211.
178. W. Y. Dai, F. Shao, J. Szczerbinski, R. McCaffrey, R. Zenobi, Y. H. Jin, A. D. Schluter and W. Zhang, *Angew. Chem. Int. Ed.*, 2016, **55**, 213-217.